NUREG/CR-0631
PNL-2891
RE

Quantitative Assessment of Aquatic Impacts of Power Plants

July 1979

Prepared for:
the U.S. Nuclear Regulatory Commission

Pacific Northwest Laboratory
Operated for the U.S. Department of Energy
by Battelle Memorial Institute

Battelle

PNL-2891

Available from
National Technical Information Service
Springfield, Virginia 22161

NUREG/CR-0631
PNL-2891
RE

QUANTITATIVE ASSESSMENT OF AQUATIC IMPACTS OF POWER PLANTS

D. H. McKenzie
E. M. Arnold
J. R. Skalski
D. H. Fickeisen
K. S. Baker

Manuscript Completed: July 1979
Date Published: August 1979

Prepared for the Office of Nuclear Regulatory Research
U.S. Nuclear Regulatory Commission
Washington, D. C. 20555 under a Related Services Agreement
with the U. S. Department of Energy
Contract EY-76-C-06-1830
FIN No. B2072

Pacific Northwest Laboratory
Richland, Washington 99352

ABSTRACT

This report is part of a continuing study of the design and analysis of aquatic environmental monitoring programs for assessing the impacts caused by nuclear power plants. The efforts of this year's study were divided into ecological monitoring, simulation model evaluation and hydrologic modeling.

Analysis of ecological monitoring data from three nuclear power plants confirmed the generic applicability of a control-treatment pairing (CTP) design suggested by McKenzie et al. (1977). Simulation models of aquatic ecosystems were reviewed and evaluated. A process notebook was compiled and each model equation was translated into a standarized notation. Individual model testing and evaluation was started. The Aquatic Generalized Environmental Impact Simulator (AGEIS) was also developed at the University of Washington. A compendium of models commonly applied to nuclear power plants was assembled and two well-received hydrodynamic models were applied to data from the Surry Nuclear Power Plant. Conclusions indicated that slight inaccuracies of boundary data have little effect on mass conservation, but for model calculations, accurate bathymetry data are necessary for conservation of mass. The results of this year's work should provide valuable reference information for model users and monitoring program designers.

SUMMARY

This report is part of a continuing study of the design and analysis of aquatic environmental monitoring programs for assessing the impacts of nuclear power plants. Analysis of data from Calvert Cliffs, Pilgrim and San Onofre nuclear power plants confirmed the generic applicability of the control-treatment pairing design suggested by McKenzie et al. (1977).

Substantial progress was made on the simulation model evaluation task. A process notebook was compiled in which each model equation was translated into a standardized notation. Individual model testing and evaluating was started. The Aquatic Generalized Environmental Impact Simulator (AGEIS) was developed at the University of Washington and will initially be tested using data from Lake Keowee, South Carolina. Further work is required to test the various models and perfect AGEIS for impact analyses at actual power plant sites.

Efforts on the hydrologic modeling task resulted in a compendium of models commonly applied to nuclear power plants and the application of two well-received hydrodynamic models to data from the Surry Nuclear Power Plant in Virginia. Conclusions from the study of these models indicate that slight inaccuracies of boundary data have little influence on mass conservation and accurate bathymetry data are necessary for conservation of mass through the model calculations. The hydrologic modeling task provides valuable reference information for model users and monitoring program designers.

CONTENTS

FIGURES

TABLES

GENERAL INTRODUCTION

This study, sponsored by the U.S. Nuclear Regulatory Commission (NRC), is part of Pacific Northwest Laboratory's (PNL) review of analysis and design of environmental monitoring programs for nuclear power plants. Studies on this subject have been conducted at the Argonne National Laboratory (ANL), Oak Ridge National Laboratory (ORNL) and PNL.

The environmental monitoring data for Zion, Prairie Island and Nine Mile Point Nuclear Power Plants have been previously evaluated (Murarka et al., 1976a, 1976b; Murarka, 1976, respectively). Adams et al. (1977a, 1977b and 1977c) evaluated the monitoring data for Surry, Peach Bottom and San Onofre Nuclear Power Plant sites duing the ORNL studies. The nonradiological monitoring data for the Monticello, Haddam Neck and Millstone Nuclear Power Plants were evaluated by Gore et al. (1976a, 1976b and 1977) at PNL. To synthesize these studies, McKenzie et al. (1977) examined the techniques used at these nine nuclear power plant sites to develop a specific monitoring design and analysis approach for both aquatic communities and thermal effluents.

Discussion of further investigations on the design and analysis of aquatic monitoring programs at nuclear power plants (NPP) for this year's annual report is divided into three major chapters:

1) Ecological monitoring
2) Simulation model evaluation
3) Hydrologic modeling.

The ecological monitoring chapter addresses the analysis of aquatic data from three NPP using statistical procedures to estimate the experimental error associated with monitoring programs of the control-treatment pairing (CTP) design (McKenzie et al., 1977). The CTP design is intended to quantify possible changes in organism density resulting from impacts of NPP operations. The design matches potentially impacted treatment stations (located within the plant's potential influence) with nonimpacted control stations (outside the plant's influence). As in classical experimentation, a control is used to measure the effects of experimental conditions. The treatment measures environmental conditions plus an added stimulus, the impact due to power plant operation. Therefore, CTP design requires selection of station pairs in which organism abundance responds similarly to changes in environmental parameters.

In the CTP design, control-treatment pairs are established during the preoperational phase of the NPP and sampling stations are maintained and sampled into the operational period. Sampling during the preoperational period serves two functions. First, it can be used to evaluate the success of the pairing scheme before plant operation. Second, and more importantly, preoperational sampling establishes relationships between organism densities at control and treatment stations. These relationships can later be compared with those observed during the operational period to determine possible impacts.

The nature and extent of a monitoring program depends on a number of constraints:

1) site-specific habitat characteristics of an NPP
2) quantitative objectives of the monitoring program
3) experimental error
4) limitations on time and effort.

In this document we examine how these constraints might affect implementation of the CTP design and make recommendations for the establishment of monitoring programs using the CTP design.

This year's emphasis in evaluating simulation models was on models of fish population dynamics and their representations of controlling processes (e.g. consumption, respiration, metabolism, growth, fecundity and mortality). In collaboration with Dr. Gordon Swartzman of the University of Washington, state-of-the-art mathematical models of the dynamics of aquatic ecosystem components were evaluated to establish guidelines for their application to impact analysis.

Models were selected for review based on their potential applicability to impact analysis and the availability of clear documentation supporting them. A model notebook was developed classifying the objectives of each model, the components and processes it includes, its equation forms and its parameter values. A standardized notation was defined and the equations in each of the models were translated into a standard terminology to facilitate their comparison. A process notebook organized by major process includes all of the representations in standard notation, critical evaluation of supporting rationale, notes on historical development, parametric values, a subjective rating of their "variance," recommendations regarding the range of applicability of each representation and other notes for the user. Compatibility schemes define allowable combinations of representations and computation order which will be useful in developing hybrid models. The Aquatic Generalized Environmental Impact Simulator (AGEIS), developed at the University of Washington, will be used to test and evaluate the models with parameters fitted to available data (initially from Lake Keowee, South Carolina). Model sensitivity to parameter values will be investigated. The Simulation Model Evaluation chapter in this report presents an overview of the process representations.

The hydrologic modeling research effort included preparation of a compendium of models representing the mathematical class commonly applied to NPP sites. A finite difference hydrodynamic model (Leendertse, 1967) and the Research Management Associates' finite element hydrodynamic models RMA-I and II (Norton et al., 1973) were applied to Surry Nuclear Power Plant data to determine whether the Surry monitoring program supports the models and how the quality, abundance and spatial arrangement of data effect the performance of the models.

Model information was compiled to provide a reference for input and verification data for model users and designers of monitoring programs. This

compilation describes the basic physical phenomena simulated and the numerical techniques used in calculating the values desired. The mathematical models are discussed in four groups:

1) General hydrodynamic and hydrothermal models
2) Hydrodynamic/water quality models
3) Integral thermal plume models
4) Constituent/sediment transport models.

Data required to operate each model are listed where possible. These should be useful to monitoring program designers for determining the spatial layout of the sampling stations and selecting the appropriate model for particular application.

ECOLOGICAL MONITORING

ANALYSIS OF AQUATIC DATA FROM MONITORING PROGRAMS AT NUCLEAR POWER PLANTS

INTRODUCTION

This section presents an analysis of aquatic data from three nuclear power plants (NPP) using statistical procedures suggested by McKenzie et al. (1977). The aquatic data used in this report were collected at Calvert Cliffs NPP on upper Chesapeake Bay, Maryland between January 1974 and December 1977, Pilgrim NPP at Cape Cod Bay, Massachusetts between August 1971 and May 1977 and San Onofre NPP, California between January 1976 and November 1977.

The objective of this analysis is to estimate the experimental error (mean square for error, MSE) associated with monitoring programs employing the control-treatment pairing (CTP) design (McKenzie et al., 1977). Experimental error can be defined as a measure of the extraneous variation in an experiment resulting from the inherent variability among replications and inconsistencies of the sampling procedures. Knowledge of the expected size of experimental error for a monitoring program is essential if the study is to be properly designed. Estimates of the experimental error computed for plankton and benthic communities are presented.

This report provides estimates of MSE for plankton and benthic communities computed by analysis of variance methods using an a posteriori application of CTP designs. The results of this analysis will help establish whether the experimental error for plankton and benthic communities is independent of site specifications. Consistency among the MSE permits the design of future monitoring programs without extensive preliminary sampling at each new site to estimate the MSE.

Sampling intensity within a monitoring program is dependent on five criteria:

1) the size of change, Δ, considered important to detect
2) the significance level, α, or the probability of declaring a significant impact when none has occurred
3) the desired probability of detecting a change of size Δ when such a change has occurred, $1-\beta$, often called the power of the test
4) the experimental design of the monitoring program
5) the magnitude of the MSE.

The first three of these parameters needed for determining the sample size for a study are subjective and can be considered the quantitative objectives of a monitoring program. These quantitative objectives express the biological and statistical significance of an impact. The choice of experimental

design is also subjective. However, designs which yield the smallest experimental error per unit of effort expended are preferred. Unlike the other parameters, the size of the experimental error must be objectively determined. The magnitude of the MSE is, in part, a function of the environment and the trophic level of the organisms studied. The value of MSE is also a function of the variability in the field procedures and deviation of the model equation describing organism abundance from that of reality.

Once the subjective criteria are established, an estimate of the needed sample size for a monitoring program is computed as a function of the MSE. Whether the objectives (criteria 1-3) of the monitoring program can be fulfilled depends on how closely the expected MSE approximates the MSE calculated from data collected during the monitoring program. When the value of the expected MSE is chosen too low, the number of samples needed will be underestimated. An underestimation of the needed program size will result in a monitoring program not capable of detecting the size of change in abundance proposed. When the expected value of MSE is chosen too high, the sampling program will be excessive. The monitoring program objectives will be fulfilled in this case, but at an unnecessary expense to the sponsor.

Discrepancies between the expected and observed MSE may result from variability in the spatial distribution of organisms between sites or differences in field techniques and their application in monitoring programs. The uniqueness of monitoring sites tends to produce values of MSE which only approximate values observed in other monitoring programs. Thus, there may exist a discrepancy between the proposed objectives of a monitoring program and their realization because of the choice of the sampling intensity.

The consequences of inaccurately estimating the needed sampling intensity should be considered in the design of monitoring programs. Higher values of MSE may be used to estimate the needed sample size to assure adequate sampling intensity. After data has been collected, however, the size of the monitoring program could be adjusted to correspond to the observed value of MSE. By this adjustment process, the objectives of the study may be maintained at a reasonable cost to the program.

STATISTICAL METHODS

Analysis of variance procedures employing the CTP design were used to compute the MSE. In the pairing of control and treatment stations, density levels of organisms at station pairs are assumed to respond similarly to changes in environmental conditions. Without this assumption, under hypothesis testing situations, changes at treatment stations could not be assigned to stresses induced by the operation of the nuclear power plant. Since pairing was *a posteriori*, the validity of the pairing schemes and hence the analyses were undetermined.

Three methods used to determine the paired differences between control and treatment stations in the analysis were arithmetic, square root and

logarithmic. Choice of the proper transformation requires knowledge of the functional relationship between densities of organisms at the control and treatment stations. McKenzie et al. (1977) discusses which data transformation to use when various functional relationships for the densities between control and treatment sites exist. Transformations also serve to convert data to a form more accordant with the assumptions of the analysis of variance. These assumptions include factors affecting density having an additive response, and individual observations being independent, normally distributed and with common variance. Since the design and analysis of aquatic data was a posteriori, verification of the assumptions for the different transformations is difficult.

The treatments are considered to be in a factorial array and conceptualized as being in a completely randomized design for the analysis of variance. No interaction term of order three or greater is included in the model equations. This assumes that the higher order interaction terms are nonsignificant and can be included in the error term. The factors affecting density at the control and treatment stations are also assumed to be fixed. Treating these factors as fixed effects, inference can be made only to the factors and their levels observed during the monitoring program.

McKenzie et al. (1977) discuss the assumptions of the analysis of variance and their relationship to the CTP design. Repeated observations at sampling stations through time tend to be serially correlated and, hence, not independent. The spacing of sampling periods one or two months apart is suggested to reduce the correlation. Imperical evidence presented by McKenzie et al. (1977) suggests that taking the difference in the log of the densities of zooplankton between control and treatment stations can result in approximately independent, and normally distributed observations. All data analyzed in this report were collected monthly or bimonthly, decreasing the chance for serial correlation. For count data, McKenzie et al. (1977) also suggest that samples of organisms should be large enough to avoid zero counts, and thereby increase the chances for normally distributed data.

When good CTP is observed, the variance of the difference in densities between the control and treatment stations should be reduced. The variance of the difference between two random variables, X_1 and X_2, can be expressed as

$$\text{Var}\ (X_1 - X_2) = \text{Var}\ (X_1) + \text{Var}\ (X_2) - 2\ \text{Cov}\ (X_1, X_2).$$

With favorable pairing, the covariance between density values at control and treatment stations should be positive, thus decreasing the observed variance (McKenzie et al., 1977).

Computing the sample correlation coefficient among repeated observations of a control-treatment pair should provide a measure of the success of pairing. The correlation coefficient, ρ, can be expressed as

$$\rho_{X_1X_2} = \frac{\text{Cov}(X_1,X_2)}{\sqrt{\text{Var}\ (X_1)\ \ \text{Var}\ (X_2)}}$$

The variance of the difference $X_1 - X_2$ can, therefore, be written in terms of the correlation coefficient as

$$\text{Var}\ (X_1 - X_2) = \text{Var}\ (X_1) + \text{Var}\ (X_2) - 2\rho_{X_1X_2}\sqrt{\text{Var}\ (X_1)\ \ \text{Var}\ (X_2)}$$

Assuming Var (X_1) = Var (X_2), which is reasonable if the control and treatment stations are in similar environments, then

$$\text{Var}\ (X_1 - X_2) = 2\ \text{Var}\ (X_1) - 2\rho_{X_1X_2}\ \text{Var}\ (X_1).$$

Thus, as $\rho_{X_1X_2}$ approaches 1, Var $(X_1 - X_2)$ decreases.

As the variance of the difference in densities between control and treatment stations decreases, the power of the statistical analysis increases. A positive correlation coefficient, ρ, can therefore be associated with an increased ability to test for a change in abundance, Δ. The absence of correlation ($\rho = 0$) between control-treatment pairs will usually produce a slight loss of power ($1-\beta$) when CTP designs are employed. Use of CTP designs on data exhibiting a negative correlation ($\rho < 0$), however, may substantially reduce the power to detect changes in organism abundance. For a particular transformation of the data, the sample correlation coefficient, r, should indicate whether the CTP design was a suitable method of analysis.

DATA FROM MONITORING PROGRAMS AT NUCLEAR POWER PLANTS

San Onofre

Data on zooplankton and phytoplankton abundance collected during the period of January 1976 to November 1977 at San Onofre NPP (Southern California Edison Company, 1977, 1978) were analyzed. Measurements were collected bimonthly at six sampling stations located on the 9 m depth contour (Figure 1.1). Abundance measurements used in the analysis were:

1) total numbers of zooplankton per m^3
2) mg chlorophyll *a* per m^3
3) mg pheopigments per m^3.

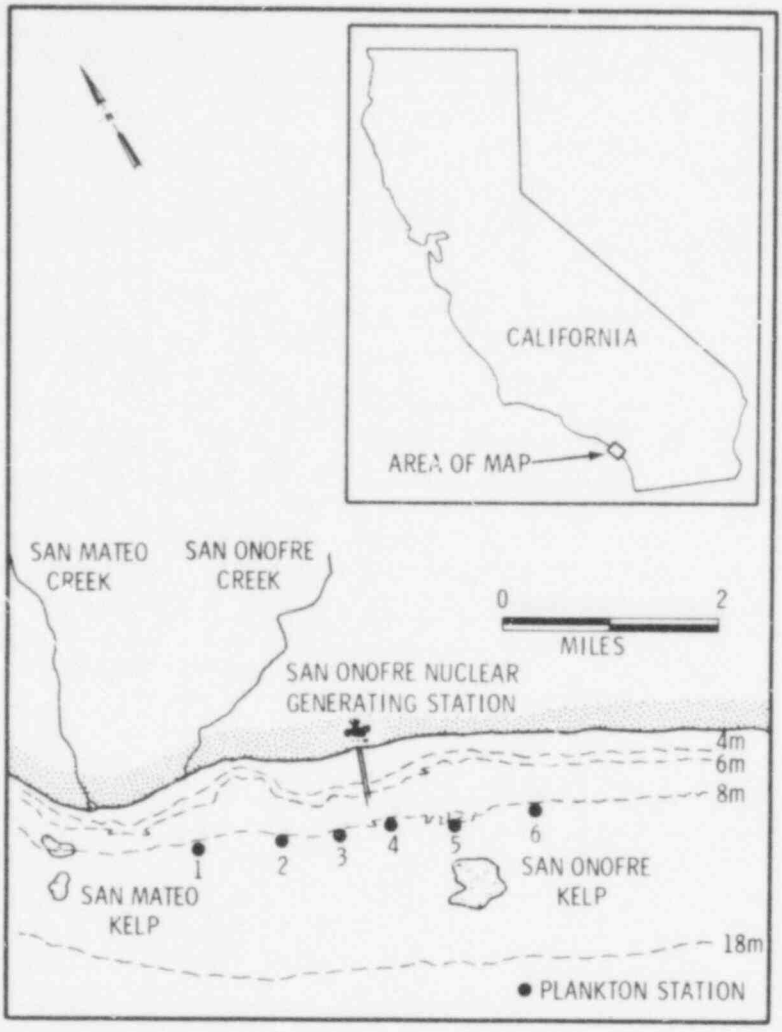

FIGURE 1.1. Sampling Stations for Plankton near San Onofre NPP (From Southern California Edison Company, 1977)

Samples of zooplankton were taken at two depth intervals, 0-5 m and 5-9 m. Sampling for chlorophyll *a* and pheopigments was conducted at 1 m and 8 m.

When multiple samples were collected simultaneously at a station, the mean value of the replicates was used for the analysis. Taking the mean of the multiple grab samples at a station was suggested by McKenzie et al. (1977) for CTP designs. The rationale for this suggestion was based on Eberhardt's observation (1978) that the variance from subsampling plots was not a suitable basis for comparing treatments.

Total zooplankton counts used in the analysis were reconstructed from reported information on counts and percent occurrences of individual species by the formula:

$$\text{estimated total zooplankton counts} = \frac{\text{reported \#/m}^3 \text{ for a dominant species}}{\text{reported fractional occurrence of species in total count}}$$

Two a posteriori schemes were employed in the analysis of the plankton data. In one pairing scheme, stations 1 and 6 were assumed to represent control stations and paired with treatment stations 3 and 4, respectively (Figure 1.1). The other pairing scheme used stations 2 and 5 as controls, with stations 3 and 4 as treatment sites, respectively. The two pairing schemes were analyzed to provide information on the effects of spatial separation between control and treatment stations on the error variance observed. The distance between the control and treatment sites in the first pairing scheme was approximately twice that of the second scheme. However, the analyses of the two pairing schemes were not independent. Agreement in the analysis of the two schemes would depend, in part, on the homogeneity of the monitoring site and the extent of an impact away from the NPP.

To facilitate comparison of monitoring programs of various NPP, factors considered for inclusion in the treatment design are listed below. Factors indicated as having a single level were not included in the data analysis for the particular NPP or data set. For the San Onofre NPP, factors included in the analysis were:

1) depth sample, $j = 1, 2$ or $j = 1$
2) bimonthly sampling, $k = 1, \ldots, 6$
3) depth contour, $\ell = 1$
4) relative position of station pair, east or west of NPP, $m = 1, 2$.

Calvert Cliffs NPP

Abundance and productivity data on phytoplankton collected from January 1974 to December 1977 (Baltimore Gas and Electric Company, 1975a,b,c,d, 1976a,b,c,d, 1977a,b, 1978a,b) at Calvert Cliffs NPP were analyzed. Taxonomic groups and dates of the data used in the analysis included:

1) total numbers of phytoplankton per m^3, 1974-1977
2) numbers of diatoms (Bacillareophyta) per m^3, 1974-1977
3) numbers of dinoflagellates (Pyrrophyta) per m^3, 1974-1977
4) numbers of blue-green algae (Cyanophyta) per m^3, 1974-1976
5) numbers of golden-brown, and yellow-green algae (Chrysophyta) per m^3, 1974, 1976-1977
6) mg chlorophyll a per m^3, 1975-1976.

Phytoplankton counts were taken from samples collected at Kenwood Beach and at the plant site, as shown in Figure 1.2. Samples of phytoplankton were taken at the water surface and approximately 1 m above the bottom. All stations were located on the 9 m depth contour. Kenwood Beach was considered a control site while the sampling station at the Plant Site, potentially within the influences of the thermal plume, was considered the treatment station.

In the productivity study, chlorophyll a measurements were taken at Kenwood Beach, Plant Site, Rocky Point and Cove Point. Rocky Point was considered a treatment station, and Cove Point was a control site south of the Calvert Cliffs NPP. Only surface samples were taken for the chlorophyll a analysis.

FIGURE 1.2. Sampling Stations for Plankton near Calvert Cliffs NPP (From Baltimore Gas and Electric Company, 1978a)

If zero counts were included in a data set, the transformation $\log_{10}(x)$ could not be used, so the transformation $\log_{10}(x+1)$ was employed. Factors included in the factorial treatment design were:

1) depth sample, $j = 1, 2$ or $j = 1$
2) bimonthly sampling, $k = 1, \ldots, 6$
3) depth contour, $\ell = 1$
4) relative position of station pair, north or south of NPP, $m = 1$ or $m = 1, 2$.

Pilgrim NPP

Data on benthic fauna and flora colonization in the intertidal and subtidal zones near Pilgrim NPP were analyzed. Data collected at Pilgrim NPP from August 1971 to May 1977 (Boston Edison Company, 1973a,b, 1974a,b, 1975a,b, 1976a,b, 1977a,b) were used in the analysis. Sampling was conducted seasonally for fauna and flora in intertidal and subtidal environments with rocky and sandy substrates. The taxonomic groupings and dates of data sets used in the analysis include:

1) fauna, intertidal zone, rock substrate
   a) total biomass, gm/m^2, 1971-1977
   b) total numbers of organisms per m^2, 1971-1977
   c) numbers of mussel (Mytilus edulis) per m^2, 1971-1977
   d) numbers of periwinkles (Littorina spp.) per m^2, 1971-1977

2) fauna subtotal zone, rocky substrate
   a) total biomass, gm/m^2, 1972-1977
   b) total numbers of organisms per m^2, 1972-1977
   c) numbers of mussel (Modiolus modiolus) per m^2, 1972-1975
   d) numbers of snail (Lacuna vincta) per m^2, 1976-1977

3) fauna, subtidal zone, sandy substrate
   a) total biomass, gm/m^2, 1971-1977
   b) total numbers of organism per m^2, 1971-1977
   c) numbers of tellen (Tellina agiles) per m^2, 1971-1977
   d) numbers of sand dollar (Echinarochinius parma) per m^2, 1971-1977

4) flora, intertidal zone, rocky substrate
   a) total biomass, gm/m^2 dry weight, 1971-1974
   b) biomass of rockweed (Fuscus vesiculosus) gm dry weight/m^2, 1971-1977
   c) biomass of rockweed (Ascoplyllum nodosum) gm dry weight/m^2, 1971-1977

5) flora, subtidal zone, rocky substrate
   a) biomass of Irish moss (Chondrus crispus), gm dry weight/m^2
   b) biomass of red algae (Phyllophora spp.), gm dry weight/m^2
   c) biomass of kelp (Laminaria spp. and Aquarum), gm dry weight/m^2.

Sampling stations located at or near Rocky Point and Effluent were considered treatment sites, while sampling stations at White Horse Beach and

Manomet Point were used as control sites (Figure 1.3). To analyze the fauna and flora at subtidal stations with rocky substrate, sites at 3.0 m and 9.1 m depth contours at Rocky Point were paired with stations at the 3.0 m and 9.1 m depth contours at Manomet Point. Intertidal fauna and flora on rocky substrate were investigated by pairing the Rocky Point and Manomet Point intertidal stations. Subtidal fauna on sandy substrates were studied by pairing the Effluent and White Horse Beach sites at the 9.1 m depth contours. When replicate samples were taken at a sampling site, the mean of the replicates was used for analysis. The logarithmic transformation $\log_{10}(x + 1)$ was used instead of $\log_{10}(x)$ for those data sets containing zero counts.

Factors included in the factorial treatment design used in the analysis were:

1) depth at which sample was taken, $j = i$
2) season of sampling, $k = 1, \ldots, 4$
3) depth contour, $\ell = 1, 2$ or $\ell = 1$
4) relative position of station pair, $m = 1$.

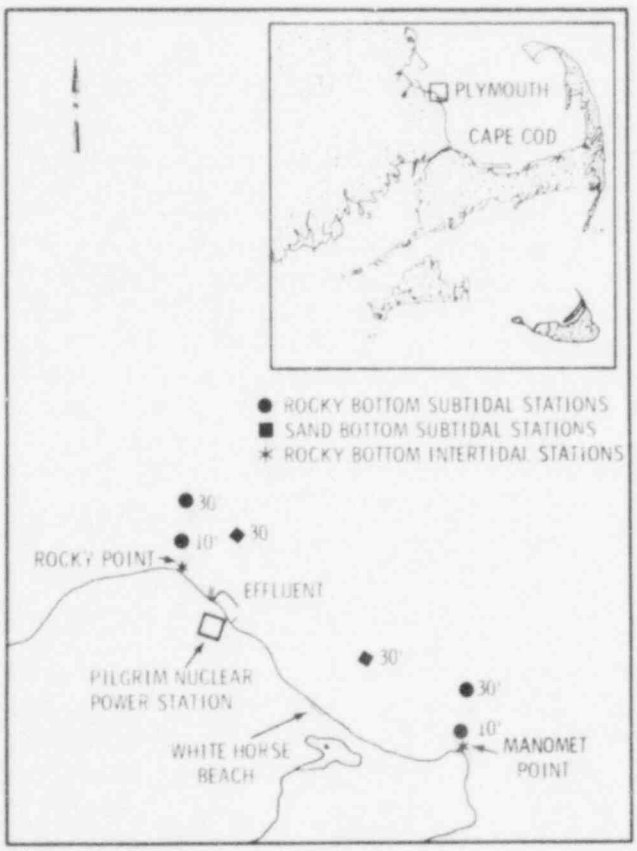

FIGURE 1.3. Sampling Stations for Plankton and Benthic Organisms near Pilgrim NPP (From Boston Edison Company, 1977)

RESULTS

Estimates of the experimental error (MSE) from the phytoplankton and zooplankton data from San Onofre, Calvert Cliffs and Pilgrim NPP are summarized in Table 1.1. The range of values for the estimates of experimental error in Table 1.1 generally agrees with values reported by the McKenzie et al. (1977). Table 1.2 summarizes the values of MSE observed for $\log_{10}$ transformations of plankton and benthic data reported here and by McKenzie et al. (1977).

Among the data sets analyzed, the values of MSE based on the $\log_{10}$ scale for total plankton counts and concentrations of chlorophyll a were of similar magnitude with a range of values from 0.026 to 0.093. Values of MSE for total counts of benthic organisms showed a much wider range, however, with values from 0.036 to 0.823.

Similarity in the magnitude of the MSE among monitoring programs for plankton abundance and productivity suggests that the variance might be site-independent within the range of environmental conditions studied. This stability in MSE may permit the design of future monitoring programs using the CTP design without the need for extensive preliminary sampling to estimate the expected experimental error.

However, in benthic communities there is up to a sevenfold difference in the value of MSE between power plant sites and up to a 23-fold difference between tidal zones within a monitoring site. Because of this wide range in values of MSE, estimates of the sample size needed for future monitoring programs in benthic communities will be computed with a higher degree of uncertainty. Thus, there is a greater chance of either overestimating or underestimating the sample sizes needed for proposed programs. It is suggested that an estimate of variance in the upper range of the observed values for benthic data be used to establish sampling intensities for future monitoring programs. After data from the preoperational period have been collected, the number of station pairs could then be reduced to correspond to any reduction in the observed variance at the NPP site.

Values of MSE computed from benthic data are generally larger than those from plankton data, with mean values of 0.295 and 0.056, respectively. The larger values of MSE for benthic data indicate a greater sampling effort is needed to investigate impact in these communities than in plankton communities.

Comparison of the sample correlation coefficients among the control-treatment pairs (Table 1.1) indicates that generally favorable pairing conditions existed in the data analyzed. The one major exception to the significant correlation coefficients observed is the data from intertidal zones at Pilgrim NPP. Few of the data pairings under any of the transformations resulted in significant ($\alpha < 0.10$) correlation between control and treatment sites in the intertidal zone. This apparent unfavorable pairing may reflect the a posteriori process of pairing used in the analysis. The low correlation coefficients may, however, indicate a relatively greater heterogeneity within

TABLE 1.1. Size of the Mean Square for Error (MSE), Degrees of Freedom (D.F.) Associated with MSE, Number of Pairs of Control-Treatment Observations (n) Used in the Analysis and the Correlation Coefficient (r) Computed Between the Control and Treatment Pairs for Abundance Data on Plants. Analysis of variance was performed using the CTP design with arithmetic (AR), logarithmic (LOG) and square root (SQRT) transformations.

Location	Data Set	Transformation	MSE	D.F.	n	r
San Onofre NPP						
Station pairs (1-3, 6-4)	Zooplankton counts #/m^3 (No. 1)†	AR	6.03×10^6	28	47	0.76**
		LOG	0.07			0.74**
		SQRT	289.06			0.74**
Station pairs (2-3, 5-4)	Zooplankton counts #/m^3 (1)†	AR	5.45×10^6	29	48	0.78**
		LOG	0.08			0.70**
		SQRT	296.37			0.74**
Station pairs (1-3, 6-4)	Chlorophyll *a* mg/m^3 (2)†	AR	1.43	29	48	0.63**
		LOG	0.09			0.76**
		SQRT	0.18			0.70**
Station pairs (2-3, 5-4)	Chlorophyll *a* mg/m^3 (2)†	AR	0.68	29	48	0.75**
		LOG	0.04			0.85**
		SQRT	0.09			0.82**
Station pairs (1-3, 6-4)	Pheopigments mg/m^3 (3)†	AR	0.65	29	48	0.16**
		LOG	0.09			0.58**
		SQRT	0.11			0.38**
Station pairs (2-3, 5-4)	Pheopigments mg/m^3†	AR	0.70	29	48	0.17**
		LOG	0.11			0.52**
		SQRT	0.12			0.39**
Calvert Cliffs NPP						
Station pairs (Kenwood Beach - Plant Site)	Phytoplankton total counts #/mℓ (1)†	AR	2.41×10^7	70	94	0.81**
		LOG	0.03			0.84**
		SQRT	388.61			0.84**
	Diatom counts #/mℓ (2)†	AR	9.60×10^6	68	92	0.77**
		LOG	0.07			0.87**
		SQRT	233.31			0.86**
	Dinoflagellate counts #/mℓ (3)†	AR	1.80×10^6	70	94	0.73**
		LOG (x+1)	0.22			0.80**
		SQRT	151.17			0.83**
	Blue-green algae counts #/mℓ (5)†	AR	63.27	48	72	0.68**
		LOG (x+1)	0.51			0.74**
		SQRT	1.19×10^5			0.61**
	Yellow-green algae counts #/mℓ (5)†	AR	2.29×10^6	46	70	0.96**
		LOG (x+1)	0.13			0.89**
		SQRT	149.87			0.93**
Station pairs (Kenwood Beach - Plant Site, Cove Point - Rocky Point)	Chlorophyll *a* µg/ℓ (6)†	AR	136.41	22	46	0.58**
		LOG	0.05			0.79**
		SQRT	1.04			0.74**
Pilgrim NPP Intertidal, rocky substrate						
Station pairs (Manomet Point - Rocky Point)	Fauna, total biomass gm/m^2 (1a)†	AR	71822.28	20	24	0.66**
		LOG	0.30			0.70**
		SQRT	45.87			0.75**
	Fauna, total counts #/m^2 (1b)†	AR	3.32×10^9	20	24	-0.02
		LOG	0.31			0.31*
		SQRT	13357.98			0.10

TABLE 1.1 (Contd)

	Mytilus edulus counts #/m² (1c)†	AR	2.76 x 10^9	17	21	0.00
		LOG	0.49			0.35*
		SQRT	12213.54			0.15
	Littorina spp. counts #/m² (1d)†	AR	2.03 x 10^6	17	21	0.03
		LOG	0.24			0.29
		SQRT	225.62			0.16
Pilgrim NPP Subtidal rocky substrate						
Station pairs (Manomet Point - Rocky Point	Fauna, total biomass gm/m² (2a)†	AR	11761.45	30	38	0.14
		LOG	0.46			0.24*
		SQRT	28.82			0.20
	Fauna, total counts #/m² (2b)†	AR	1.21 x 10^{11}	30	38	0.78**
		LOG (x+1)	0.82			0.68**
		SQRT	28124.07			0.88**
	Modiolus modiolus counts #/m² (2c)†	AR	1.58 x 10^{11}	22	30	0.77**
		LOG (x+1)	0.68			0.92**
		SQRT	35266.05			0.90**
	Lacuna vincta counts #/m² (2d)†	AR	4.45 x 10^6	22	30	0.75**
		LOG (x+1)	0.34			0.77**
		SQRT	331.17			0.78**
Pilgrim NPP Subtidal, sandy substrate						
Station pairs (White Horse Beach - Effluent)	Fauna, total biomass gm/m² (3a)†	AR	27861.22	19	23	0.35**
		LOG	0.33			0.57**
		SQRT	35.59			0.47**
	Fauna, total counts #/m² (3b)†	AR	2.21 x 10^6	19	23	0.84**
		LOG	0.04			0.82**
		SQRT	144.64			0.83**
	Tellina agiles counts #/m² (3c)†	AR	1.97 x 10^5	16	20	0.79**
		LOG	0.20			0.68**
		SQRT	69.62			0.79**
	Echinarachnius parma counts #/m² (3d)†	AR	17888.65	15	19	0.69**
		LOG	0.23			0.60**
		SQRT	28.80			0.63**
Pilgrim NPP Intertidal, rocky substrate						
Station pairs (Manomet Point - Rocky Point)	Flora, total biomass gm/m² dry weight (4a)†	AR	2.73 x 10^7	8	12	0.15
		LOG	0.06			0.13
		SQRT	657.29			0.15
	Fuscus vesiculosus gm/m² dry weight (4b)†	AR	2.95 x 10^5	18	22	0.16
		LOG	1.85			0.21
		SQRT	715.00			0.10
	Ascophyllum nodosum gm/m² dry weight (4c)†	AR	1.59 x 10^7	18	22	0.53**
		LOG	0.10			0.52**
		SQRT	581.70			0.56**
Pilgrim NPP Subtidal, rocky substrate						
Station pairs (Manomet Point - Rocky Point)	Chondrus crispus gm/m² dry weight (5a)†	AR	58786.48	35	43	0.68**
		LOG	0.48			0.56**
		SQRT	40.62			0.72**
	Phyllophora spp. gm/m² dry weight (5b)†	AR	16287.62	35	43	0.22*
		LOG	0.66			0.11
		SQRT	34.34			0.25*
	Laminaria and Agarum gm/m² dry weight (5c)†	AR	18957.99	14	22	0.42**
		LOG	0.14			0.67**
		SQRT	20.46			0.59**

† McKenzie et al., 1977
* significant at $\alpha = 0.10$
** significant at $\alpha = 0.05$
See text for complete description of data set.

TABLE 1.2. Comparison of Values of MSE from Benthic and Plankton Studies Using a LOG_{10} Transformation of the Data and Computed by Analysis of Variance Employing CTP Designs

Data Set	Location	MS	D.F.
Total Zooplankton Counts #/m^3	†Zion NPP	0.048	283
	San Onofre NPP	0.073	28
	San Onofre NPP	0.089	29
Total Phytoplankton Counts #/mℓ	†Haddem Neck NPP	0.042	44
	†Prairie Island NPP	0.036	8
	†Zion NPP	0.075	286
	Calvert Cliffs NPP	0.026	70
Total Benthic Counts #/m^2	†Haddem Neck NPP	0.192	166
	†Zion NPP	0.112	173
	Pilgrim NPP		
	intertidal, rocky	0.311	20
	subtidal, rocky	0.823	30
	subtidal, sandy	0.036	19
Chlorophyll a mg/m^3	San Onofre NPP	0.093	29
	San Onofre NPP	0.086	29
	Calvert Cliffs NPP	0.051	22

† McKenzie et al., 1977

the intertidal environment compared to subtidal zones and open water environments. If larger heterogeneity is the case, greater care will be needed in site selection of control-treatment station pairs in benthic communities. Since the use of CTP design is based on the assumption of proper station pairing, this is an important consideration.

Differences in the degree of correlation existed between control and treatment sites depending upon the type of data analyzed. Significant correlation ($\alpha < 0.01$) was observed between control and treatment sites for total faunal biomass in the intertidal benthic community at Pilgrim NPP, but not when total faunal counts are analyzed. In the subtidal zones, the opposite relationship tended to occur. Higher correlations were observed between control and treatment sites for total faunal counts than faunal biomass. These relationships between the correlation coefficient and the type of data analyzed suggest collection of either biomass or count data alone may not always be sufficient for monitoring benthic communities. Different cause-and-effect mechanisms may exist with biomass and count data in benthic communities, indicating that perhaps both types of data should be monitored.

In communities such as plankton, where there is a high correlation between biomass and numbers of individuals, either biomass or count data may be sufficient. For benthic communities, where the size range of the organisms is large, collection and analysis of both numerical and biomass data is suggested. If discrepancies in the analysis occur when both biomass and count data are used, the individual taxa composing the observations should be investigated.

Comparison of the MSE's for data from San Onofre NPP by the two pairing schemes analyzed show very little difference in value. The sample correlation coefficients for the two pairing schemes are also comparable. Similarity in the results for the two schemes may be due either to their lack of independence or the homogeneity of the different control sites. Correlation coefficients for data at corresponding control sites on either side of the thermal discharge (1 and 2, 5 and 6) from San Onofre NPP are generally significant ($\alpha < 0.10$). The magnitude of the correlation between densities at the control sites indicates a degree of homogeneity in the aquatic environment at the NPP, but not to the extent that nonindependence can be disregarded as the cause for similar MSE values for the different pairing schemes.

DESIGN OF AQUATIC MONITORING PROGRAMS

INTRODUCTION

This section presents recommendations for the establishment of monitoring programs using a CTP design (McKenzie et al., 1977). The nature and extent of a program to monitor plankton or benthic communities depends on a number of constraints:

1) site-specific habitat characteristics of a nuclear power plant
2) quantitative objectives of the monitoring program
3) experimental error
4) limitations on time and effort.

The objective of this section is to discuss how these constraints may affect the implementation of CTP designs for monitoring programs.

The purpose of the CTP design is to quantify changes in organism density that might result from impacts caused by operation of NPP. The CTP design matches potentially impacted treatment stations with nonimpacted control stations. Treatment stations are located within the potential influence of the power plant while control sites are established outside the influence. As in classical experimentation, a control is used to measure the effects of experimental conditions and the treatment measures environmental conditions plus an added stimulus, the impact due to power plant operation. A critical requirement of CTP design, therefore, is to select station pairs where organism abundance responds similarly to changes in environmental parameters.

In the CTP design, control-treatment pairs are established during the preoperational phase of the NPP and sampling stations are maintained and sampled into the operational period. Sampling during the preoperational period serves two functions. First, it can be used to evaluate the success of the pairing scheme prior to the operation of the NPP. More importantly, preoperational sampling establishes the relationship of organism densities between control and treatment stations which can later be compared with that observed during the operational period.

The critical assumption in any CTP design is that control and treatment stations "track" each other. This tracking assures that organism abundance at control and treatment stations respond similarily to changes in environmental conditions. Unless this assumption is valid, there is no way to determine if changes in density at the treatment stations are the result of environmental conditions or the impact due to operation of the NPP.

There are also assumptions inherent in the analysis of data from a CTP design. The nature of CTP design allows differences in density between control and treatment stations to be used in the analysis to determine the existence of an impact. There are two assumptions associated with the analysis of density differences. First, use of the differences is assumed to remove

annual and seasonal density changes that occur in plankton and benthic communities. Removal of annual variation allows repeated observations of a treatment combination between years to be considered as replications. Secondly, use of the differences reduces the serial correlation that can exist among successive observations of density at sampling stations. Serial correlation within data has been found to seriously hamper analysis of variance procedures (Scheffe, 1959).

For the assumptions in the analysis of CTP data to be valid, the numerical relationship between densities at control and treatment stations must be known. Analytically, observations on density can be handled in three common manners: as untransformed count and biomass data, as square roots of the data and as logarithmic transformations. Proper transformation of the data depends on the nature of the response being studied and distributional characteristics of the random variables (densities) observed. McKenzie et al. (1977) reviewed the assumptions and merits of various data transformations used on monitoring data and recommended the logarithmic transformation. In this report, only logarithmic transformations of the data will be considered. In using logarithmic transformations, a constant proportional relationship is assumed to exist between organism densities at control and treatment stations.

Considerable interdependence may exist between constraints influencing the design of a monitoring program. Changes in any one constraint may directly affect the fulfillment of the remaining considerations for monitoring program design.

Each of the four constraints mentioned as important in the implementation of CTP designs are discussed here. Examples of CTP designs are then used to illustrate the interrelationships among constraints which influence the design of monitoring programs.

SITE-SPECIFIC HABITAT CHARACTERISTICS OF A NPP

Station pairs should be selected which possess the particular combination of environmental factors considered important in the analysis of the aquatic systems. Factors to include in the design depend in large part on site-specific habitat characteristics of the nuclear power plant and the organisms to be studied. For each environmental factor determined to be important, two or more levels of treatment, reflecting differences in potential influence on organism densities, are identified. A factorial treatment design is then constructed by forming all possible combinations among the different factors at their various levels.

Since the objective of a monitoring program is to determine whether the operation of NPP has affected organism abundance, station pairs are sampled during both preoperational and operational phases. The first factor in the treatment design is, therefore, the operational status of the NPP. Additional factors which may affect organism abundance must also be included in the design.

In plankton communities, the depth at which a water sample is collected directly influences the observed density of organisms. Thus, the depth at which a plankton sample is collected is considered a factor in monitoring design. A distinction is made between samples collected at the surface and those collected deeper in the water. The abundance and species composition of plankton is seasonal in nature, so time of sampling is also included as a factor in the design. If sampling is conducted monthly, 12 levels of treatment for the time of sampling are considered. Six levels are considered if sampling is bimonthly, and four levels if seasonal samples are taken. Other factors, such as distance from the shoreline, the depth contour at which sampling stations are located and the position of station pairs relative to the NPP, may also be considered.

In a study of benthic communities, the depth at which a sample is collected is not considered a factor since all organisms are located on the bottom. However, the type of substrate at sampling stations and whether the stations are located in the intertidal or subtidal zone must be considered. The various substrate types and tidal zones may be considered either as factors in the analysis or separated into individual monitoring programs. When appreciable differences in species composition or density exist between tidal zones, separate monitoring designs are indicated. In this case, separate designs simplify interpretation of the results and increase the likelihood that the statistical assumptions of the analysis are valid.

To help illustrate the nature of a factorial treatment design, consider the plankton study at Zion Nuclear Power Plant shown in Figure 1.4 (McKenzie et al., 1977). The factors and their levels of treatment can be summarized as

1) Status: two levels--preoperational and operational
2) Depth at which sample was collected: one level--surface of water
3) Time of sampling: 12 levels--monthly samples were collected
4) Location of station pairs at depth contours: three levels--located at 3 (10 ft), 9 (30 ft), and 18 (60 ft) m contours
5) Relative position of the station pairs: two levels--north and south of the NPP.

For the Zion example, the different factors at their various levels define 144 (2 x 1 x 12 x 3 x 2) distinct treatment combinations in the factorial treatment design.

Assuming suitable station pairs can be found and established, a number of design problems still need to be considered. The properties of orthogonality and balance must be addressed in the design of a monitoring program. An orthogonal design requires that a level of a factor appear an equal number of times with all levels of another factor. For factor status, each treatment combination in the preopertional period must also be present in the operational period for the design to be orthogonal. In order for a design to be balanced, each unique treatment combination must be replicated an equal number of times. In CTP design, for example, this requires equal duration for the preoperational and operational phases of the monitoring program.

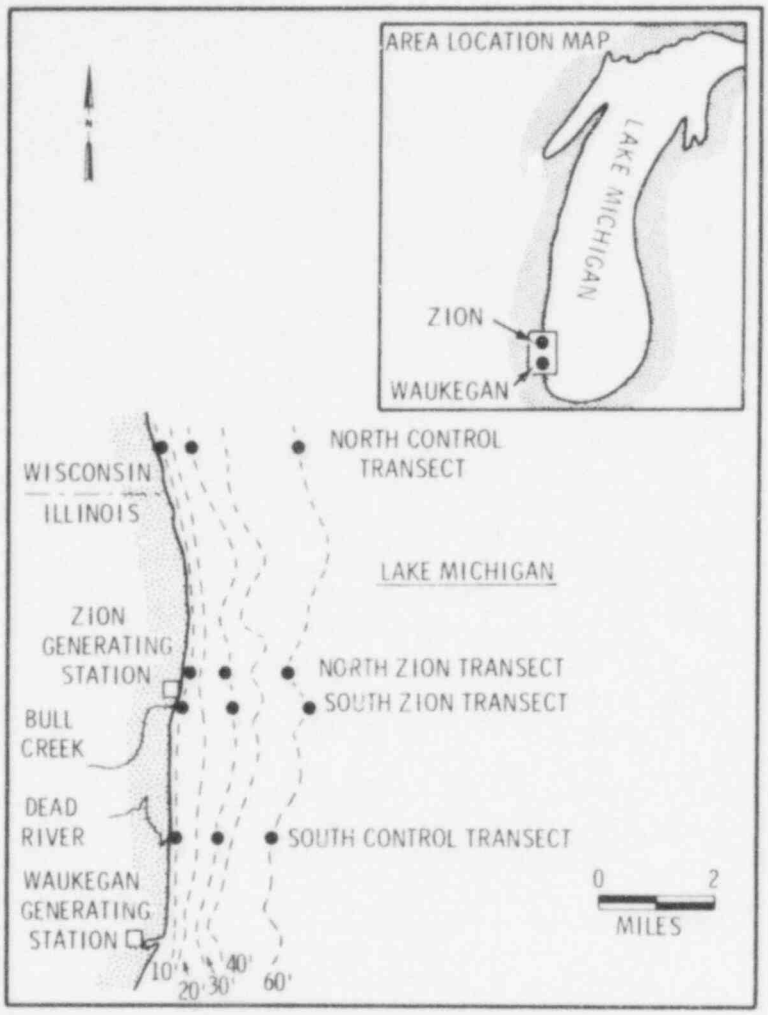

FIGURE 1.4. Location of Control-Treatment Stations for Plankton Sampling near Zion NPP

Orthogonal and balanced monitoring designs greatly simplify analysis of the data collected. Data sets that are not balanced or not orthogonal often arise as the result of sampling periods or stations being missed during data collection. For large factorial treatment designs characteristic of monitoring programs, lack of balance and/or orthogonality can produce results that cannot be interpreted.

QUANTITATIVE OBJECTIVES OF THE MONITORING PROGRAM

Objectives of a monitoring program must be explicitly stated before the field design of a monitoring program can be determined. These objectives must include the

1) size of change in density, Δ, considered important to detect
2) probability, α, of declaring a significant impact when none has occurred
3) probability, $(1-\beta)$, of detecting a change in density of size Δ or greater when such a change has occurred.

Define Δ as the difference in the log of the ratios of densities at control (C) and treatment (T) sites between preoperational (1) and operational (2) periods, such that

$$\Delta = \log \frac{T_2}{C_2} - \log \frac{T_1}{C_2}$$

Further, let ρ = the proportionality constant for densities between years and let γ = the fractional change in density at the treatment site due to the impact of the NPP. Then

$$C_2 = \rho C_1 \text{ and } T_2 = (1 + \gamma)\, \rho T_1$$

so
$$\Delta = \log \frac{(1+\gamma)\rho T_1}{\rho C_1} - \log \frac{T_1}{C_1}$$

$$\Delta = \log (1+\gamma).$$

This derivation of Δ assumes that a constant proportional relationship exists between densities at the control and treatment stations, and indicates the importance of proper station pairing. To illustrate the relationship between a change in density at the treatment station and Δ, a 30% decrease (γ = -0.30) in density at the treatment site is equivalent to $\Delta = \log_{10} (1-0.30) = -0.1549$. A 30% increase ($\gamma$ = 0.30) in density is equivalent to $\Delta = \log_{10} (1 + 0.30) = 0.1139$. The fact that

$$|\log (1-C)| > |\log (1+C)| \quad \text{for } 0 < C < 1$$

indicates that CTP designs more readily detect a decrease than an increase in density at the treatment site. Since monitoring projects are usually more concerned with the detection of decreases in organism abundance, this unequal detectability will generally not be a disadvantage.

For the multiplicative model describing organism density, which uses logarithmetric transformations, as the absolute value of Δ (or γ) decreases, the size of the monitoring program must increase for a given α and β. Monitoring

programs can be expanded either by extending the length of preoperational and operational periods or by increasing the number of factorial treatment combinations. In this report, only monitoring programs with two- or three-year preoperational and operational periods are considered. The size of the monitoring program instead is enlarged by increasing the number of sampling periods or stations.

The values chosen for α and β also influence the size of the monitoring program. The higher the desired probability $(1-\beta)$ of detecting a change in density of size Δ, the larger the monitoring program must be for a given Δ and α. In addition, the smaller the chance (α) one is willing to take in declaring for a significant impact of size Δ, when in actuality it has not occurred, the larger the monitoring program must be for a given Δ and β.

Hence, it is evident that the size of the monitoring program is closely related to quantitative objectives of the program as expressed in terms of values for Δ, α and β. McKenzie et al. (1977) suggest using values of $\alpha = 0.10$ and $\beta = 0.20$ for the analysis of monitoring data, and in this report, all design considerations incorporate these values. The value of Δ is allowed to "float" so that each monitoring design can be evaluated on the basis of its sensitivity to changes in organism density. By this procedure, values of Δ can be selected which may be of biological significance to specific populations or communities being studied.

EXPERIMENTAL ERROR

Natural variability in organism abundance between sampling pairs and sampling periods has a direct effect on the design of a monitoring program. The greater the temporal and spatial heterogeneity in organism abundance at the monitoring site, the greater the sampling effort must be. For specified values of Δ, α and β, as variability increases, so must the sampling effort. This increase in effort can be accomplished by either increasing the number of treatment combinations or by increasing the number of years of monitoring.

Variability in organism abundance is expressed as the MSE or the experimental error associated with the monitoring program. The value of MSE is an unbiased estimate of σ^2, the actual value for the variance of the difference in densities between replicates of a control-treatment pair. An estimate of σ^2 is required to compute the number of treatment combinations and duration of the proposed monitoring program.

How close the initial estimate of MSE is to the MSE observed during the monitoring program determines if the quantitative objectives of the program can be achieved. If the initial estimate of MSE is below the value observed in the monitoring program, the number of treatment combinations or duration of the study is underestimated. Underestimation of the size of the monitoring program will result in reduced sensitivity (increase in Δ) and/or power $(1-\beta)$ for detecting changes in abundance resulting from NPP operation. When the initial value of MSE is larger than the value observed for the monitoring

program, the size of the required study is overestimated. Greater sensitivity and power results from overestimation, but at an additional cost to the sponsor.

In the previous section on the analysis of aquatic data, values of MSE were given for monitoring programs using CTP designs to study plankton benthic communities. The relative stability among estimates of experimental error for monitoring programs of plankton communities suggests that these values of MSE can be used to estimate the size of future monitoring programs satisfactorily. For benthic communities, much greater variability among values of MSE were reported. Values of MSE presented can be used to design monitoring programs for benthic organisms, but have a greater risk of either underestimating or overestimating the size of the proposed monitoring program associated with their use.

LIMITATIONS ON TIME AND EFFORT

It is essential that the limitations of time, cost and effort required also be considered in the design of any monitoring program. After the quantitative objectives of the study have been stated and the site-specific requirements of the study, including the MSE, have been considered, practical problems of implementation remain.

Objectives of the study and the value of MSE are chosen primarily to determine the number of treatment combinations and duration of the monitoring program needed. Within the limitations of the chosen values of α, β and Δ, and the value of MSE, several field study designs may be acceptable. The field design is defined by the factorial treatment design used in the monitoring program.

Certain flexibility can exist in the choice of possible factors and levels of treatment to include in a monitoring design. This flexibility can be used to design monitoring programs which best fit limitations of time and effort. If limitations exist on the number of sampling stations that can be established and maintained, the number of sampling periods per year and the duration of the study can be adjusted to accommodate such restrictions. When the duration of a monitoring study is a limiting factor, the number of sampling stations or the intensity of the sampling may be increased to adjust for the shorter time period.

Adjustment of factors and treatment levels to accommodate limitations in manpower and time must be tempered by several considerations. Additional station pairs should be established only in those areas where treatment sites are within the zone of potential impact by the NPP. Extending station pairs along depth contours outside the influence of the thermal plume can introduce significant status by location interactions in the analysis. The presence of significant interaction terms among the factors can greatly complicate interpretation of results.

Problems can arise if numerous station pairs are placed in close proximity for the sole purpose of increasing sample size. Station pairs in this case serve only as additional subsamples of an area and may erroneously decrease the observed experimental error. Experimental error based on subsampling, rather than within treatment variance normally used in analysis of variance procedures, may produce faulty hypotheses testing results.

Care should also be taken when increasing sampling frequency. Sampling too often may produce observations with a high serial correlation and should be avoided if analysis of variance procedures are to be employed. At most, monthly and bimonthly samples of plankton and benthic organisms, respectively, should be taken if high serial correlation is to be avoided (McKenzie et al., 1977).

DESIGN OF MONITORING PROGRAMS

Consideration will be given to monitoring programs which can be defined by any subset of the following factors and treatment levels:

1) Status: 2 levels
2) Depth at which sample was collected: 1 or 2 levels
3) Times of sampling: 4, 6 or 12 times per year (levels)
4) Depth contours: 1, 2, 3, 4 or 5 levels
5) Relative position of station pairs: 1 or 2 levels.

A majority of the monitoring programs using CTP designs to study benthos or plankton communities can probably be defined by the parameters given above. All monitoring programs are also assumed to use the values $\alpha = 0.01$ and $\beta = 0.20$.

Let a, b, c, d and e, respectively, define the number of treatment levels for factors given above. Factor status always has preoperational and operational levels in a monitoring design, so $a = 2$. With this notation, the number of station pairs for a proposed design will equal (d x e), so the number of control and treatment stations needed for a monitoring program will be (2de). Similarly, the number of benthos or plankton samples collected during any one sampling period will be equal to (2bde) where b defines the number of depths at which samples are collected per station. The total number of samples collected each year of the monitoring program will therefore be (2bcde).

Using the power function of the F distribution (Tiku, 1972), the size of change Δ detectable by a proposed monitoring program at $\alpha = 0.10$ and $\beta = 0.20$ can be determined. The level of detectability depends on values of α, β and MSE, as well as the degrees of freedom (d.f.) associated with the test of the hypothesis. The hypothesis of interest is whether the main effect for status equals zero. In other words, the null hypothesis to be tested states that the relationship between densities at control and treatment stations is the same

during preoperational and operational phases of the NPP. Degrees of freedom associated with the F-test for status main effects are

$$d.f._1 = 1$$

$$d.f._2 = nabcde - \sum_{v=a}^{e} (v - 1) - 1/2 \sum_{v=a}^{e} \sum_{\substack{w=a \\ v \neq w}}^{e} (v - 1)(w - 1) - 1$$

where

n = number of replications, either two or three years.

Degrees of freedom for the denominator of the F-test depend on the design of the monitoring program and method of analysis. Monitoring programs are conceptualized in this report as completely randomized designs where second-order or higher interactions are considered to be relatively small.

Figures 1.5a through 1.5d present graphs of the power function for the F-test of the main effects for status. Figures 1.5a and 1.5b indicate the size of change in the density of plankton organisms detectable for various monitoring designs with two- and three-year preoperational and operational phases, respectively. Similarly, Figures 1.5c and 1.5d indicate the size of change in density detectable in studies of benthic organisms with two and three years per phase, respectively. The values of MSE used for the figures were the minimum, maximum and average values observed in the analysis of plankton and benthic communities reported earlier.

In Figures 1.5a through 1.5d, various monitoring designs are represented by the value of (bcde), the number of control-treatment samples collected during one year of monitoring. However, different values of b, c, d and e can result in the same value of (bcde). For example, (bcde) = 2 x 4 x 3 x 2 = 1 x 6 x 4 x 2 = 48. The degrees of freedom for the F-test of status main effects for these two designs differ. The first has 1 and 159 d.f. while the second has 1 and 149 d.f. for a two-year-per-phase study. For a given value of MSE, the detectability associated with these two designs differs since the d.f. differ, but not enough to be distinguishable on the figures.

Example: Zion NPP

In the example of the plankton study at Zion NPP, the value of bcde = 1 x 12 x 3 x 2 = 72. If the value of MSE from the analysis of plankton data at Zion NPP was 0.089, the monitoring design would be capable of detecting a change as small as a 22.3% increase in abundance, or an 18.2% decrease in

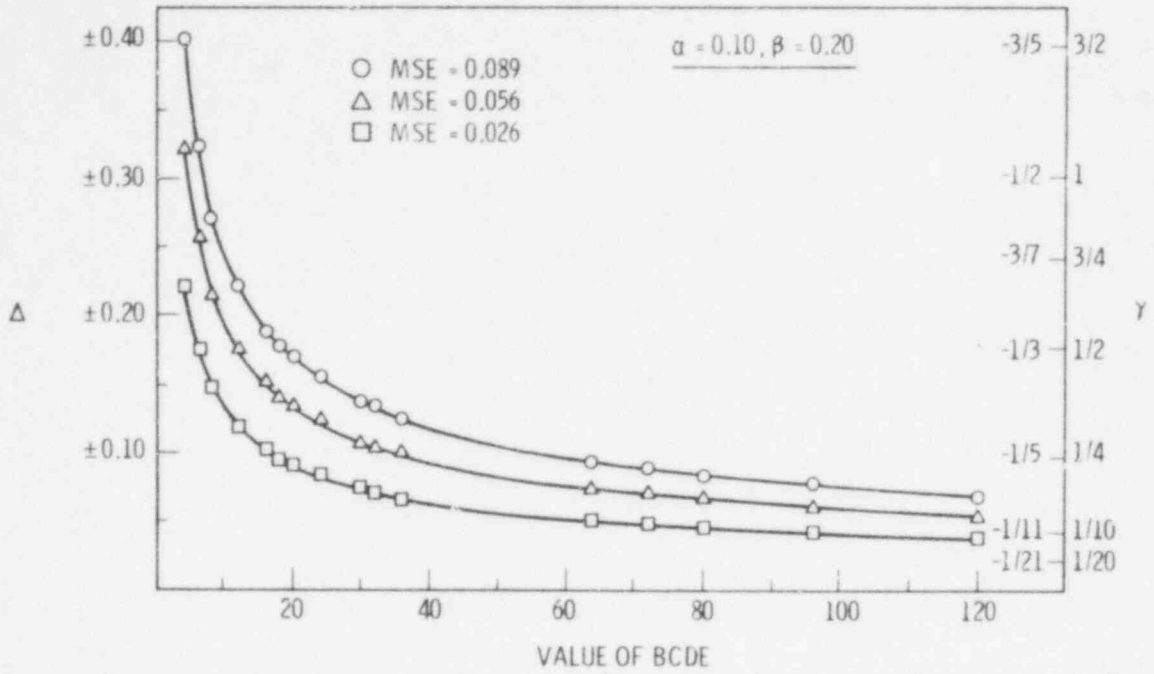

a. Plankton Studies with Two-Year Preoperational and Operational Phases

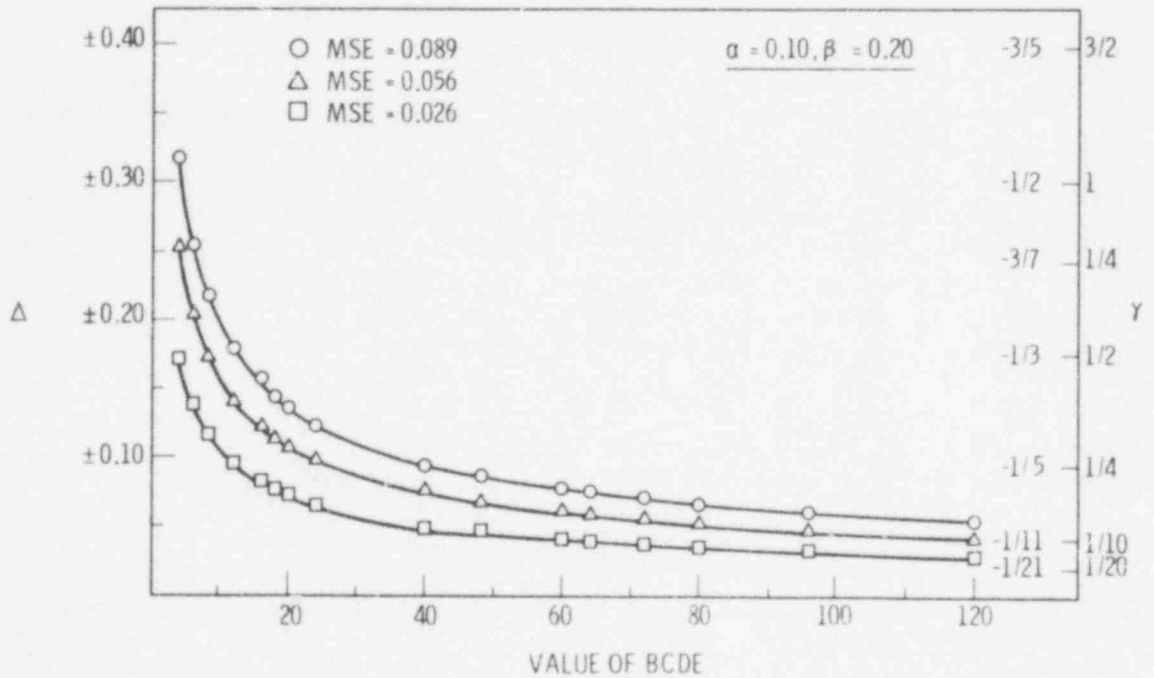

b. Plankton Studies with Three-Year Preoperational and Operational Phases

FIGURE 1.5. Power Curves for the F-Test ($\alpha = 0.10$, $\beta = 0.20$) for No-Status Main Effects Using CTP Designs. The value of bcde is the total number of control-treatment samples collected during one year of monitoring. Values of MSE are the minimum, maximum and average values observed in analysis of data for plankton and benthic communities (Table 2).

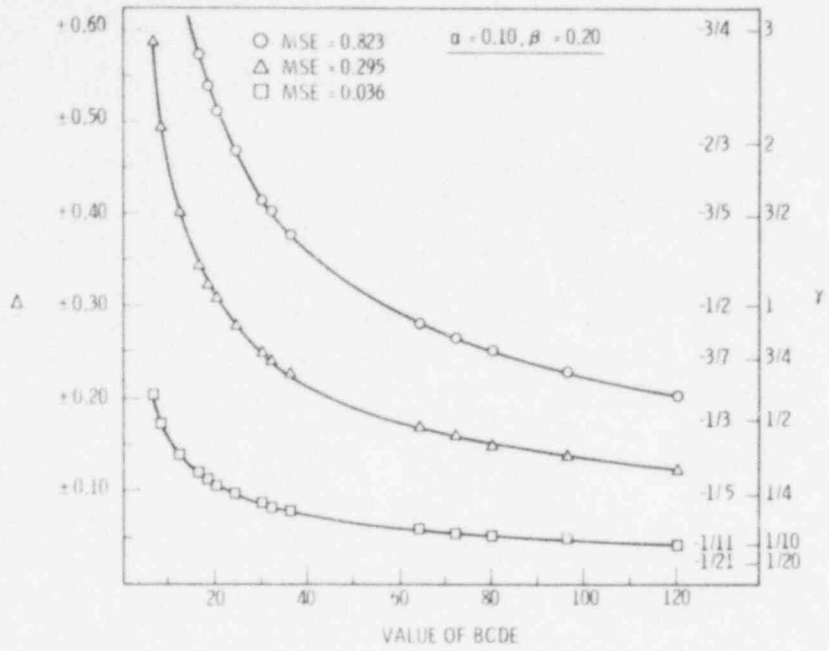

c. Benthic Studies with Two-Year Preoperational and Operational Phases

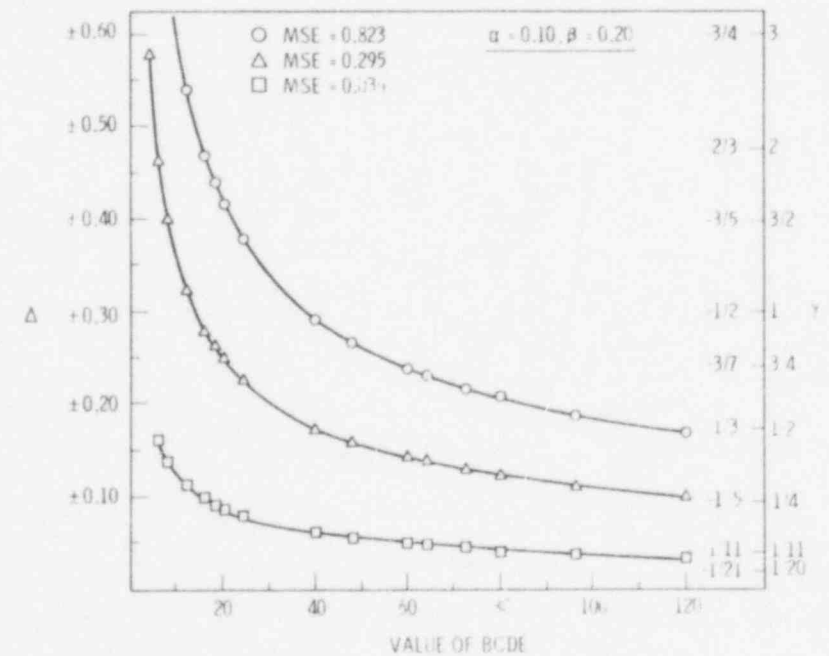

d. Benthic Studies with Three-Year Preoperational and Operational Phases

abundance between preoperational and operational phases if monitored two years each (Figure 1.5a). In a three-year preoperational and three-year operational study, a 17.5% increase or 14.9% decrease in abundance could be detected (Figure 1.5b).

Another question that could be asked is, what size monitoring program is needed to detect a 50% increase (or 33% decrease) in plankton abundance? Considering the maximum observed value for MSE of 0.089, a value of bcde = 19 for a two-year-per-phase study, or a bcde = 12 for a three-year-per-phase study is indicated. One design for a monitoring program giving a value of bcde $\geq$ 19 would be 1 x 6 x 2 x 2 = 24. This design would require bimonthly sampling of two station pairs at two locations near the NPP for two years preoperational and two years operational.

In order to detect a 50% decrease (100% increase) in abundance at the treatment stations when MSE = 0.089, a value of bcde = 7 for a two-year-per-phase study, or bcde = 4 for a three-year-per-phase study is indicated by Tables 1.2 and 1.3. The difference in the values of bcde between this case and the example above indicates the relative efficiency of the CTP design to detect opposite trends in density.

Numerous monitoring designs can produce equal values of bcde. The choice of proper design should depend on site-specific characteristics of the NPP and the limitations of time and effort. More levels of treatment should be given to those factors which may most likely be affected by an impact due to the NPP. For example, if impact is suspected to occur only during certain seasons of the year, frequent sampling is desirable to assure that such a response is monitored. Thus, flexibility in potential field designs permits the design of monitoring programs which best fit limitations of time and effort.

Example: A Benthic Monitoring Design

Suppose a monitoring program to study a benthic community in a marine environment is to be designed, but the size of the MSE is unknown and must be guessed. It is decided that tidal and subtidal zones should be investigated separately since species compositions are very different, and comparisons between zones would be difficult. Assume also that previous analysis indicates the tidal zone to exhibit greater variability in species composition and density than subtidal areas, again suggesting separate designs and analysis.

Let MSE take on the maximum observed value (0.823) for the tidal zone, and assume an average value of MSE (0.295) for the subtidal area. If a three-year-per-phase study is to be designed to detect a 33% reduction in species abundance, bcde must be 40 and 110 for the subtidal and tidal zones, respectively (Figure 1.5d).

For the subtidal zone study, one possible design would be (bcde) = 1 x 6 x 4 x 2 = 40. This design requires bimonthly sampling of four station pairs in

two relative positions around the NPP. Another possible design would be bcde = 1 x 4 x 5 x 2 = 40 which would require seasonal sampling of five station pairs in two relative positions near the NPP site. The choice of the proper design should depend on the limitations of the study and the proposed effects of the impact. If the impact may occur only during certain times of the year, designs with more frequent sampling should be chosen. When there may be a spatial pattern to the impact, more sampling stations are desirable.

These limitations include the facts that benthic samples are taken, at most, bimonthly to reduce serial correlation, and that all samples are taken at only one depth--the bottom. Referring to Figure 1.5d, the size of a detectable difference which a monitoring program with MSE = 0.823 can achieve when bcde = 60 is a 43% reduction in density. Therefore, either the quantitative objectives of the monitoring program have to be reconsidered in view of the large experimental error expected or an alternative design must be devised.

Increasing the sampling frequency to monthly provides the level of detectability desired with bcde = 1 x 12 x 5 x 2 = 120, but increases the chance of large serial correlation among successive observations. An alternative solution is to increase the number of depth contours beyond the suggested value of d = 5. A problem might exist, however, if the additional samples behave as subsamples. When spatial problems are not encountered, additional station pairs can be established and their performance evaluated. After the preoperational phase is complete, the value of MSE can be calculated and the number of station pairs adjusted. If the observed MSE is below the value of 0.823 initially used to estimate the size of the necessary monitoring program, the number of station pairs can be reduced accordingly. Those station pairs which "track" each other least should be eliminated. When elimination of station pairs is indicated, reductions should be made such that the properties of orthogonality and balance in the monitoring design are maintained. For example, if a station pair at the 20 m depth contour is to be eliminated, the corresponding station pair on the other side of the NPP at the same depth contour should be removed to maintain orthogonality. Balance is maintained by omitting all data from the discontinued station pairs in the analysis.

SITE SELECTION

The next objective in developing the previously described quantitative monitoring program design is to demonstrate its validity. This may be accomplished by implementing a CTP field test. The treatment site may be selected from sites that are either under construction or have filed for a construction permit. Currently, approximately 80 commercial nuclear power plants are undergoing some stage of the licensing process (Table 1.3). These sites may be characterized according to

1) type of aquatic environment
2) mode of cooling
3) number of units
4) projected completion date.

A desirable test site for the design is one most likely to show an impact. Therefore, the optimum condition within each characteristic is described below and an ideal combination may be used to choose a treatment/power plant site. A control site that is physically, geographically and biologically comparable may be selected to complete the pair.

Each of the four categories must be considered in the treatment site selection. Potential power plant effects are probably more apparent in closed aquatic ecosystems than in semi-closed or open-water systems. Also, while well-established water bodies are relatively stable, large fluctuations associated with the aging process in newly created reservoirs or cooling impoundments complicate quantifying power plant effects. Thus, an aquatic environment best suited for testing the design of an impact assessment monitoring program appears to be one with a well-established, closed ecosystem.

The volume and velocity of water withdrawn and circulated through a power plant makes the mode of cooling important in detecting impacts, and therefore important in examining the applicability of a monitoring design. Nuclear power plants may be cooled by once-through systems (open-cycle) or cooling towers with mechanical or natural draft withdraw and return. The more water that is withdrawn from the source water body, the higher the water velocity and the higher the risk for entrainment and impingement. Since a once-through cooling system uses quantities of cooling water an order of magnitude greater than cooling towers, it offers the best opportunity for effect detection and quantification and for design verification.

The ability of a monitoring program to detect and assess impacts of a nuclear power plant is affected by the number of units planned for the site. A plant may be designed for multiple power units or for a single unit. Multiple units generally become operational in series, about two years apart. If preoperational and operational data have been collected, the addition of supplemental units could perturb the aquatic environment and confound the problem of effect identification. This problem does not exist for a single unit power

TABLE 1.3. Nuclear Power Plants Under Construction or Planned
(Data taken from NUS Corporation, 1978)

Nuclear Plant	Location	Reactor Type	Capacity MWe	Construction Permit	Scheduled Completion	Environment	Mode of Cooling
Atlantic-1	11 mi N.E. Atlantic City, NJ	PWR	1150		1985	Atlantic Ocean	OTCNSW[a]
Atlantic-2	11 mi N.E. Atlantic City, NJ	PWR	1150		1986	Atlantic Ocean	OTCNSW
Cook-2	10 mi S. St. Joseph, MI	PWR	1060	03-25-6[illegible]	1978	Lake Michigan	OTCNSW
Diablo Canyon-1	12 mi W. San Luis Obispo, CA	PWR	1084	04-23-68	1978	Pacific Ocean	OTCNSW
Diablo Canyon-2	12 mi W. San Luis Obispo, CA	PWR	1106	12-09-70	1978	Pacific Ocean	OTCNSW
Ft. Calhoun-2	19 mi N. Omaha, NB	PWR	1150		1983	Missouri River	OTCNSW
Jamesport-1	6 mi N.E. Riverhead, NY	PWR	1150	01-04-79	1984	Estuary-Long Is. Sound	OTCNSW
Jamesport-2	6 mi N.E. Riverhead, NY	PWR	1150	01-04-79	1986	Estuary-Long Is. Sound	OTCNSW
Millstone Point-3	5 mi S.W. New London, CT	PWR	1156	08-09-74	1982	Estuary-Long Is. Sound	OTCNSW
New England Power-1	Washington Co., RI	PWR	1150		1984	Atlantic Ocean	OTCNSW
New England Power-2	Washington Co., RI	PWR	1150		1986	Atlantic Ocean	OTCNSW
NORCO-NP-1	Arecibo, Puerto Rico	PWR	583			Atlantic Ocean	OTCNSW
Pilgrim-2	35 mi N.E. Boston, MA	PWR	1180		1984	Ocean-Cape Cod Bay	OTCNSW
St. Lucie-2	12 mi S.E. Ft. Pierce, FL	PWR	810	05-02-77	1983	Atlantic Ocean	OTCNSW
Salem-2	8 mi S.W. Salem, JN	PWR	1115	09-25-68	1979	Delaware River	OTCNSW
San Onofre-2	5 mi S. San Clemente, CA	PWR	1100	10-18-73	1980	Pacific Ocean	OTCNSW
San Onofre-3	5 mi S. San Clemente, CA	PWR	1100	10-18-73	1982	Pacific Ocean	OTCNSW
Seabrook-1	Seabrook, NH	PWR	1200	03-30-73	1982	Atlantic Ocean	OTCNSW
Seabrook-2	Seabrook, NH	PWR	1200	03-30-73	1984	Atlantic Ocean	OTCNSW
Shoreham	12 mi N.W. Riverhead, NY	BWR	819	04-15-73	1980	Estuary-Long Is. Sound	OTCNSW
Sterling-1	60 mi N.E. Rochester, NY	PWR	1150	09-01-77	1984	Lake Ontario	OTCNSW
Waterford-3	Taft, LA	PWR	1113	11-14-74	1981	Mississippi River	OTCNSW
Nine Mile Point-2	8 mi N.E. Oswego, NY	BWR	1100	06-24-74	1982	Lake Ontario	OTCNSW
Allens Creek-1	Austin Co., TX	BWR	1150		1985	Reservoir	OTCR[b]
Allens Creek-2	Austin Co., TX	BWR	1150		1982	Reservoir	OTCR
Braidwood-1	2 mi S. Braidwood, IL	PWR	1120	12-31-75	1981	Reservoir	OTCR
Braidwood-2	2 mi S. Braidwood, IL	PWR	1120	12-31-75	1982	Reservoir	OTCR
Clinton-1	Hart Township, IL	BWR	933	02-24-76	1981	Reservoir	OTCR
Clinton-2	Hart Township, IL	BWR	933	02-24-76	1988	Reservoir	OTCR
Comanche Peak-1	40 mi S.W. Ft. Worth, TX	PWR	1150	12-19-74	1981	Reservoir	OTCR
Comanche Peak-2	40 mi S.W. Ft. Worth, TX	PWR	1150	12-19-74	1983	Reservoir	OTCR
La Salle-1	12 mi W. Morris, IL	BWR	1078	09-10-73	1979	Reservoir	OTCR
La Salle-2	12 mi W. Morris, IL	BWR	1078	09-10-73	1980	Reservoir	OTCR
McGuire-1	17 mi N.W. Charlotte, NC	PWR	1180	02-28-73	1979	Reservoir	OTCR
McGuire-2	17 mi N.W. Charlotte, NC	PWR	1180	02-28-73	1981	Reservoir	OTCR
Pebble Springs-1	145 mi E. Portland, OR	PWR	1260		1985	Reservoir	OTCR
Pebble Springs-2	145 mi E. Portland, OR	PWR	1260		1988	Reservoir	OTCR
South Texas-1	Matagorda Co., TX	PWR	1250	12-22-75	1980	Reservoir	OTCR
South Texas-2	Matagorda Co., TX	PWR	1250	12-22-75	1982	Reservoir	OTCR
Summer-1	26 mi N.W. Columbia, SC	PWR	900	03-21-73	1980	Reservoir	OTCR
Wolf Creek	4 mi N.E. Burlington, KS	PWR	1150	05-17-70	1982	Reservoir	OTCR
North Anna-1	40 mi N.W. Richmond, VA	PWR	898	02-19-71	1978	Reservoir	OTCR
North Anna-2	40 mi N.W. Richmond, VA	PWR	898	02-19-71	1979	Reservoir	OTCR
North Anna-3	40 mi N.W. Richmond, VA	PWR	907	07-26-74	1983	Reservoir	OTCR
North Anna-4	40 mi N.W. Richmond, VA	PWR	907	07-26-74	1983	Reservoir	OTCR

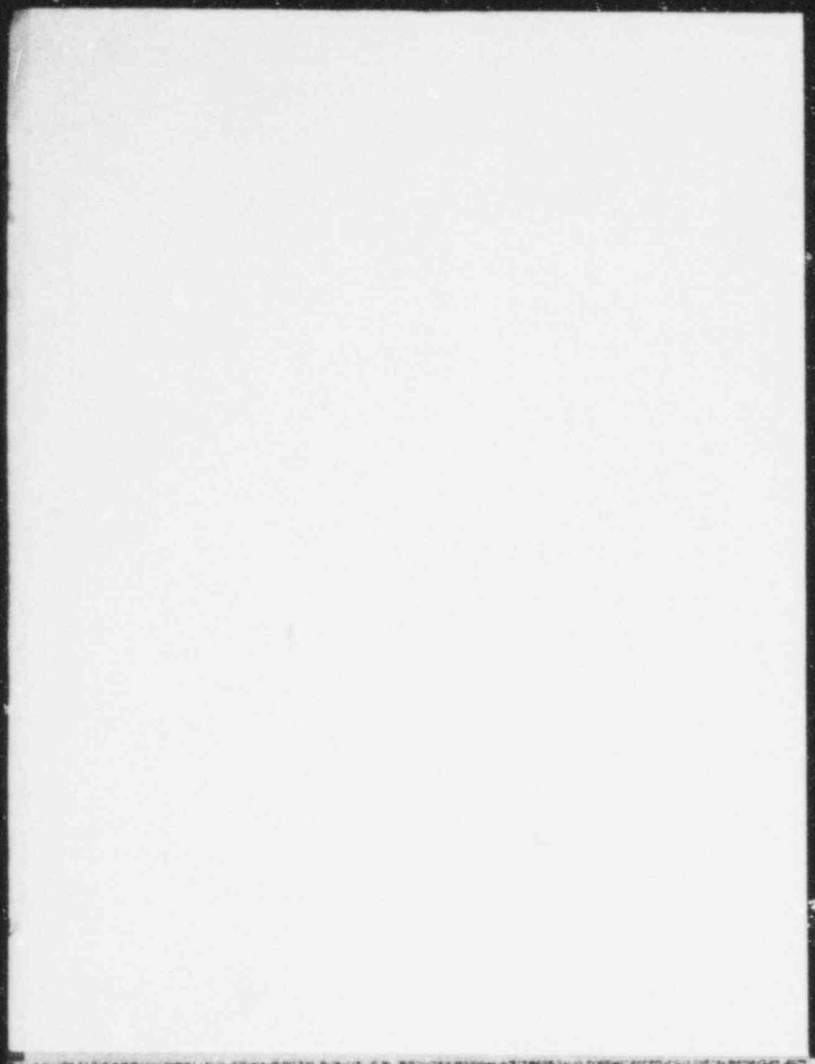
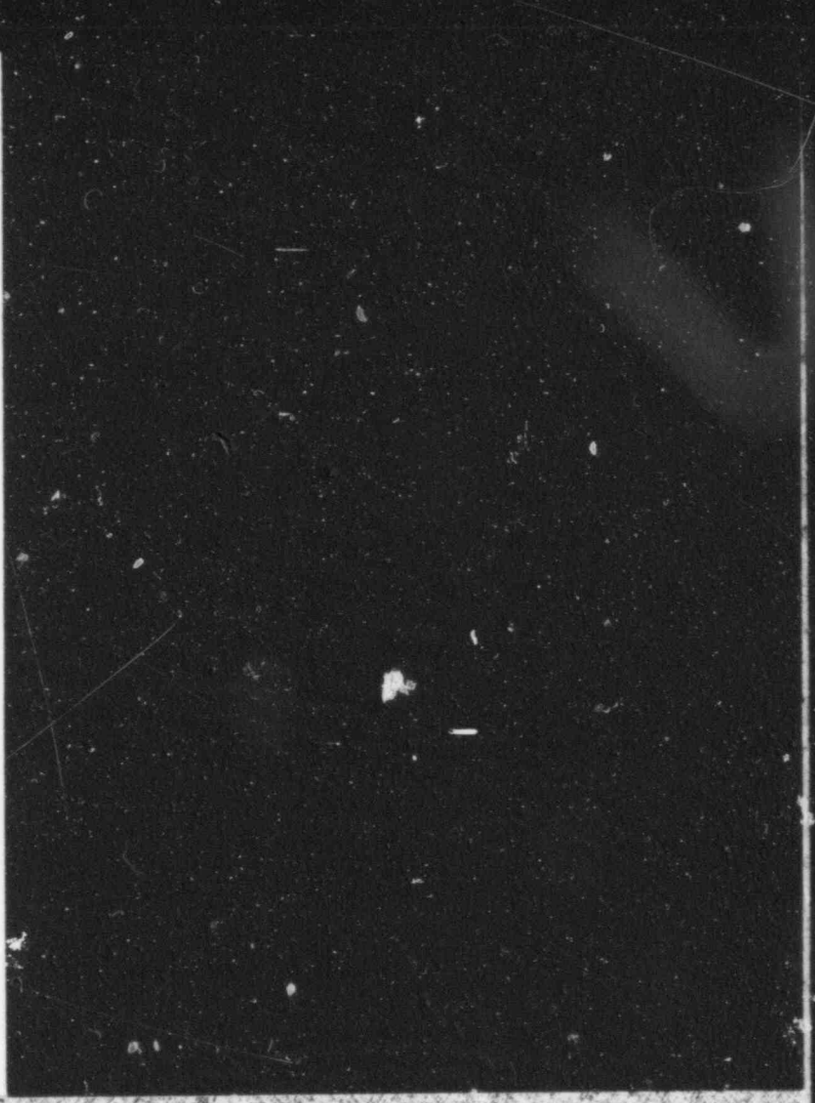
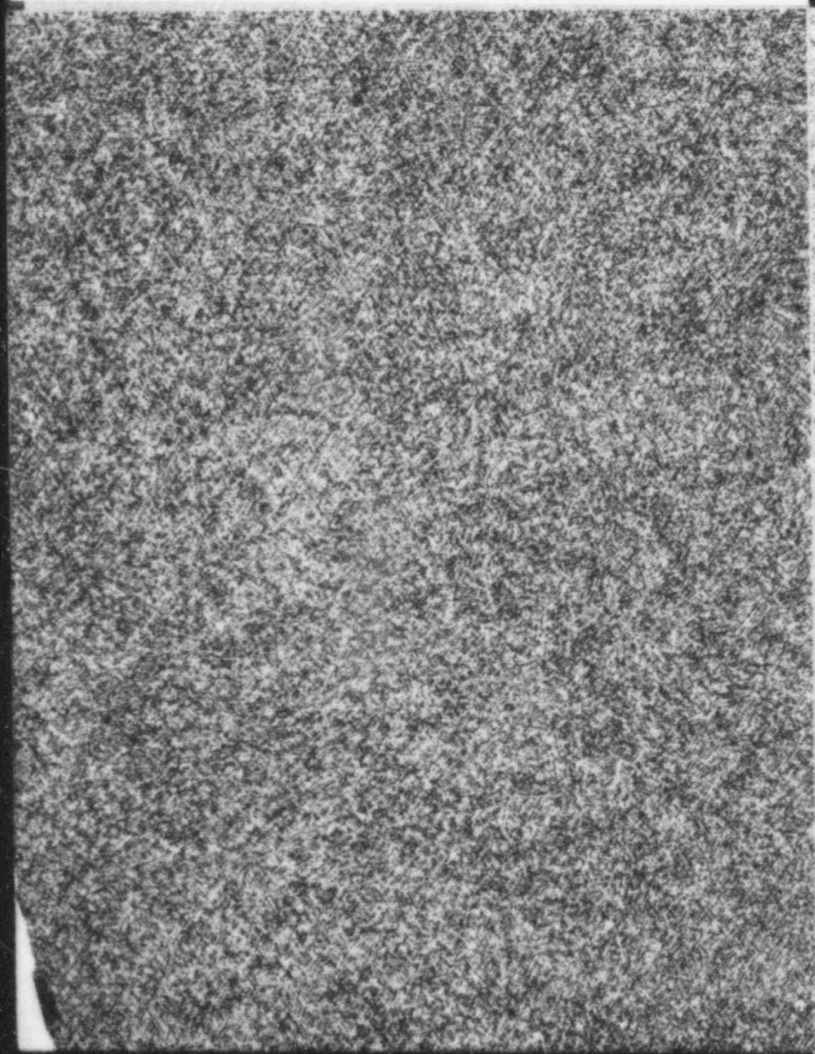
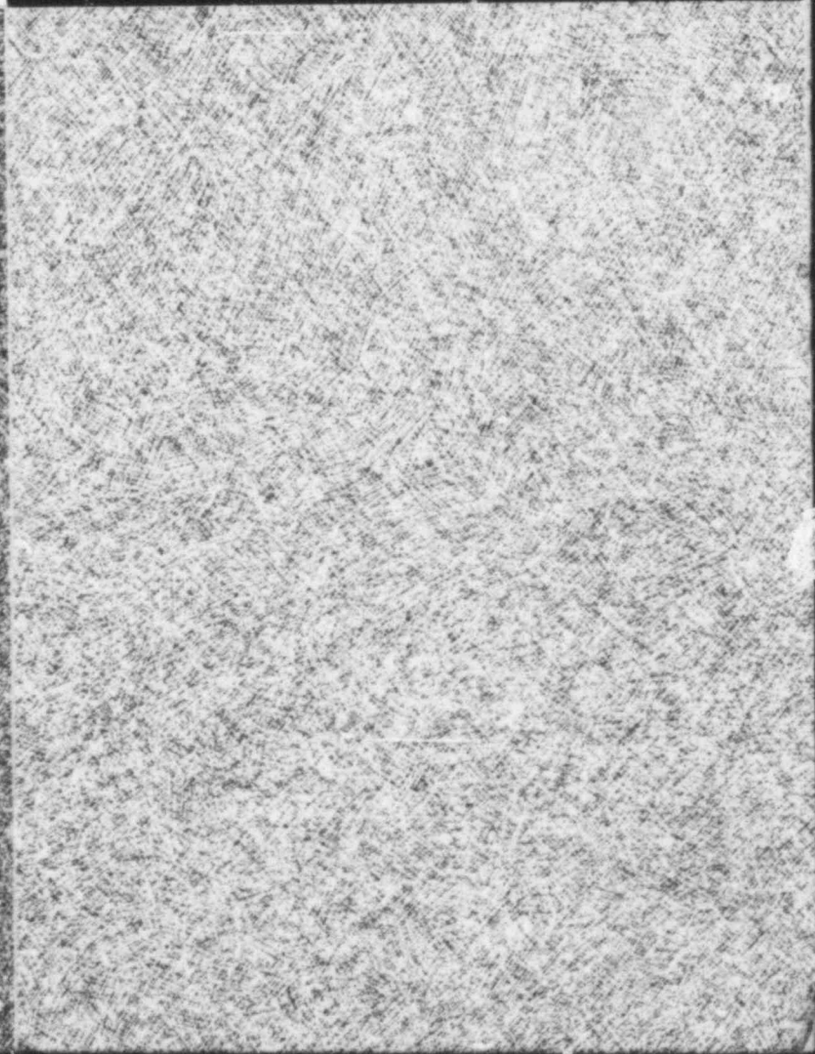

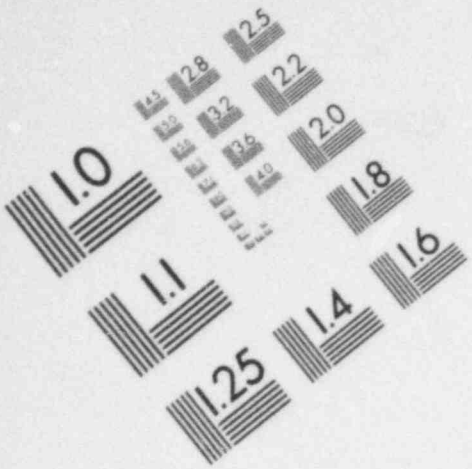

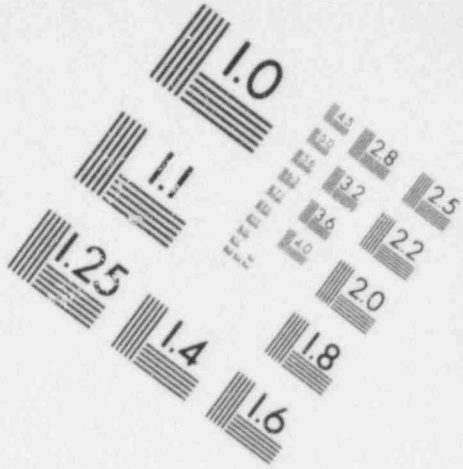

IMAGE EVALUATION TEST TARGET (MT-3)

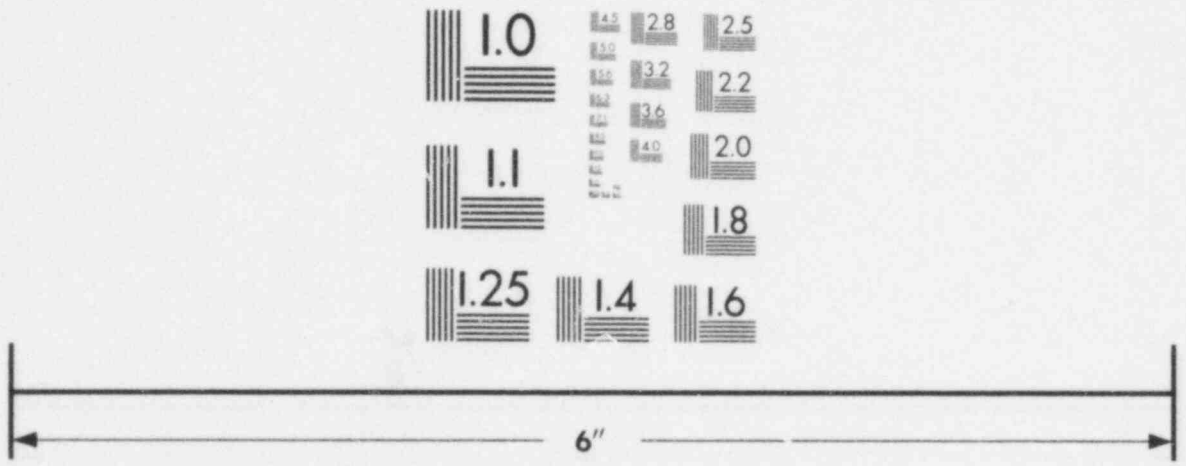

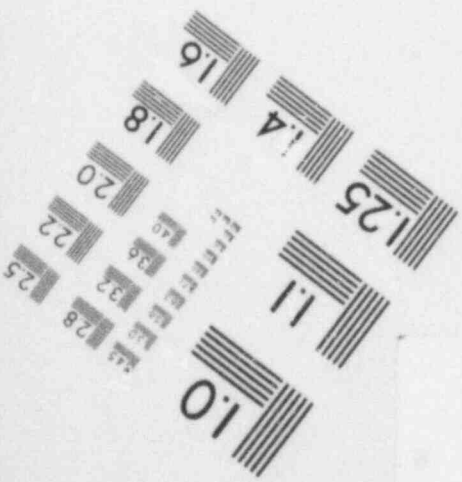

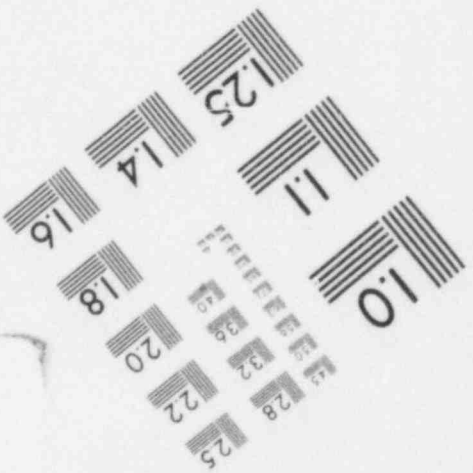

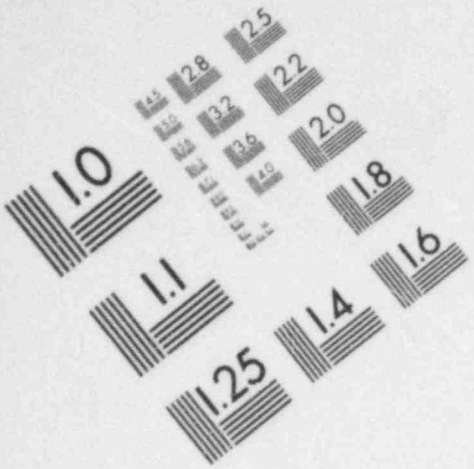

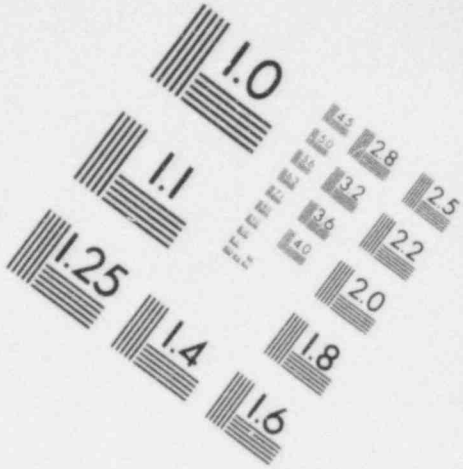

IMAGE EVALUATION TEST TARGET (MT-3)

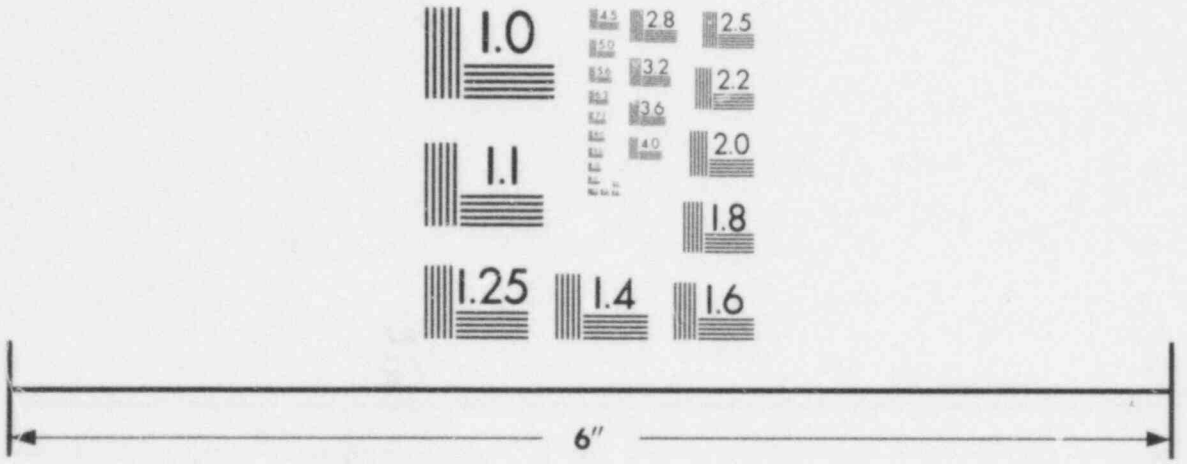

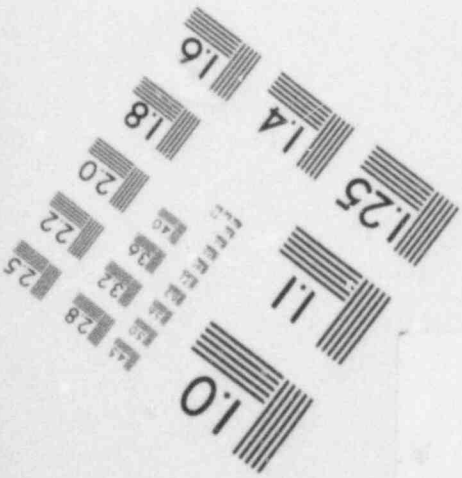

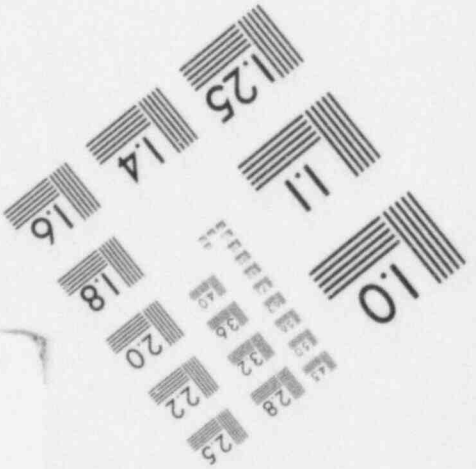

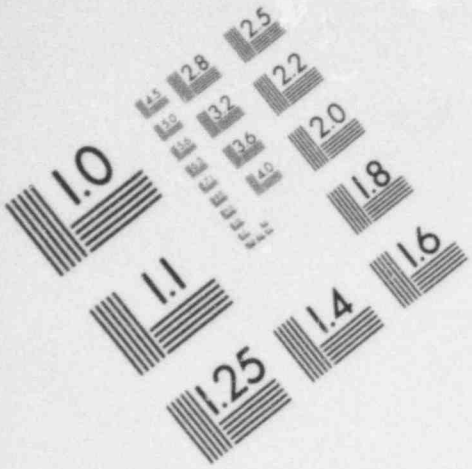

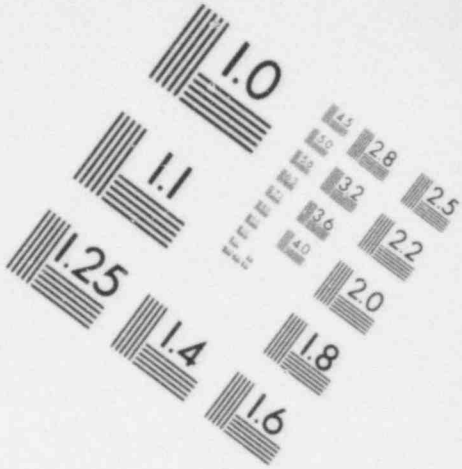

IMAGE EVALUATION TEST TARGET (MT-3)

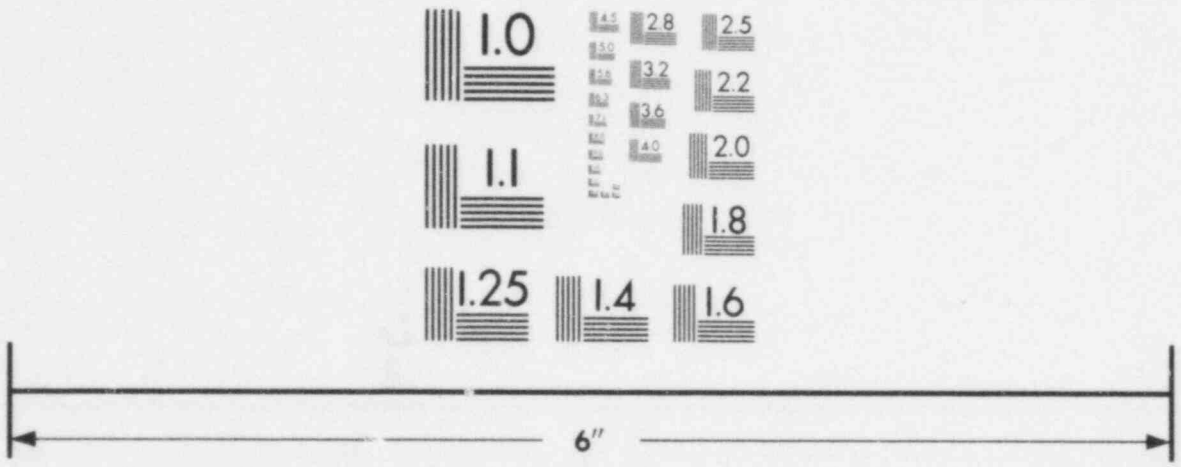

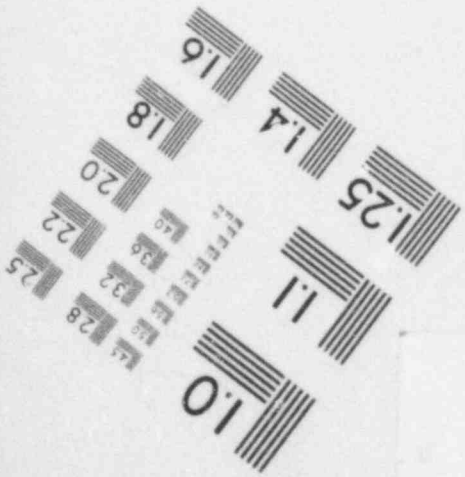

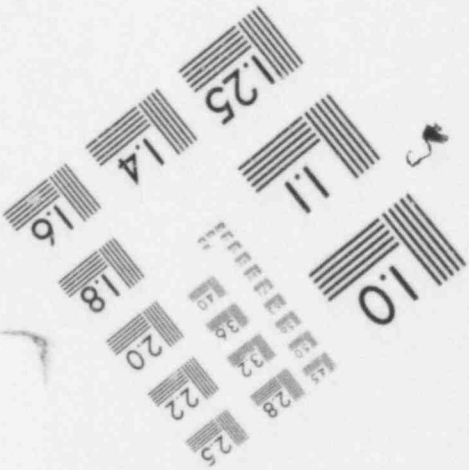

TABLE 1.3. (Contd)

Nuclear Plant	Location	Reactor Type	Capacity MWe	Construction Permit	Scheduled Completion	Environment	Mode of Cooling
Greenwood-2	50 mi N.N.E. Detroit, MI	PWR	1200		1987	Spray Canal	SC[c]
Greenwood-3	50 mi N.N.E. Detroit, MI	PWR	1200		1981	Spray Canal	SC
Surry-3	8 mi S. Williamsburg, VA	PWR	859	12-20-74	1983	Spray Canal	SC
Surry-4	8 mi S. Williamsburg, VA	PWR	859	12-20-74	1984	Spray Canal	SC
Arkansas Nuclear-2	Russelville, AK	PWR	912	12-06-72	1978	Arkansas River	NDT[d]
Bailly-1	12 mi N.E. Gary, IN	BWR	645	05-02-74	1982		NDT
Beaver Valley-2	25 mi N.W. Pittsburg, PA	PWR	852	05-03-74	1982		NDT
Bellefonte-1	7 mi E.N.E. Scottsboro, AL	PWR	1213	12-24-74	1980		NDT
Bellefonte-2	7 mi E.N.E. Scottsboro, AL	PWR	1213	12-24-74	1981		NDT
Byron-1	4 mi S. Byron, IL	PWR	1120	12-31-75	1981		NDT
Byron-2	4 mi S. Byron, IL	PWR	1120	12-31-75	1982		NDT
Callaway-1	10 mi S.E. Fulton, MO	PWR	1120	04-16-76	1982		NDT
Callaway-2	10 mi S.E. Fulton, MO	PWR	1120	04-16-76	1987		NDT
Davis-Besse-2	Toledo, OH	PWR	906	12-81-75 (limited)	1985		NDT
Davis-Besse-3	Toledo, OH	PWR	906	12-31-75	1987		NDT
Fermi-2	30 mi S.W. Detroit, MI	BWR	1093	09-26-72	1980		NDT
Grand Gulf-1	25 mi S. Vicksburg, MS	BWR	1250	09-04-74	1981		NDT
Grand Gulf-2	25 mi S. Vicksburg, MS	BWR	1250	09-04-74	1984		NDT
Harris-1	20 mi S.W. Raleigh, NC	PWR	900	11-14-74 (limited)	1984		NDT
Harris-2	20 mi S.W. Raleigh, NC	PWR	900	11-14-74 (limited)	1986		NDT
Harris-3	20 mi S.W. Raleigh, NC	PWR	900	11-14-74 (limited)	1990		NDT
Harris-4	20 mi S.W. Raleigh, NC	PWR	900	11-14-74 (limited)	1988		NDT
Hartsville-1	5 mi S.E. Hartsville, TN	BWR	1233	05-09-77	1983		NDT
Hartsville-2	5 mi S.E. Hartsville, TN	BWR	1233	05-09-77	1984		NDT
Hartsville-3	5 mi S.E. Hartsville, TN	BWR	1233	05-09-77	1983		NDT
Hartsville-4	5 mi S.E. Hartsville, TN	BWR	1233	05-09-77	1984		NDT
Hope Creek-1	8 mi S.W. Salem, NJ	BWR	1067	11-04-74	1984		NDT
Hope Creek-2	8 mi S.W. Salem, NJ	BWR	1067	11-04-74	1986		NDT
Koshkonong-1	4.2 mi S.W. Ft. Atkinson, WI	PWR	900		1982		NDT
Koshkonong-2	4.2 mi S.W. Ft. Atkinson, WI	PWR	900		1984		NDT
Limerick-1	30 mi N.W. Philadelphia, PA	BWR	1065	06-19-74	1983		NDT
Limerick-2	30 mi N.W. Philadelphia, PA	BWR	1065	06-19-74	1985		NDT
Montague-1	5 mi S.E. Greenfield, MA	BWR	1150		1986 or later		NDT
Montague-2	5 mi S.E. Greenfield, MA	BWR	1150		1988 or later		NDT
Perry-1	7 mi E. Painesville, OH	BWR	1205	05-03-77	1981		NDT
Perry-2	7 mi E. Painesville, OH	BWR	1205	05-03-77	1983		NDT
Phipps Bend-1	12 mi N.E. Rogersville, TN	BWR	1233		1984		NDT
Phipps Bend-2	12 mi N.E. Rogersville, TN	BWR	1233		1985		NDT
Sequoyah-1	18 mi N.E. Chattanooga, TN	PWR	1148	05-27-70	1978		NDT
Sequoyah-2	18 mi N.E. Chattanooga, TN	PWR	1148	05-27-70	1979		NDT
Skagit-1	Sedro Wooley, WA	BWR	1277	08-06-74	1984		NDT
Skagit-2	Sedro Wooley, WA	BWR	1277	08-06-74	1986		NDT

TABLE 1.3. (Contd)

Nuclear Plant	Location	Reactor Type	Capacity MWe	Construction Permit	Scheduled Completion	Environment	Mode of Cooling
Susquehanna-1	7 mi N.E. Berwick, PA	BWR	1050	11-03-73	1980		NDT
Susquehanna-2	7 mi N.E. Berwick, PA	BWR	1050	11-03-73	1982		NDT
Vogtle-1	25 mi S.E. Augusta, GA	PWR	1113	06-28-74	1984		
Vogtle-1	25 mi S.E. Augusta, GA	PWR	1113	06-28-74	1985		NDT
WPPSS Nuclear Proj-3	Satsop, WA	PWR	1242		1983	Columbia River	NDT
WPPSS Nuclear Proj-5	Satsop, WA	PWR	1242		1985	Columbia River	NDT
Watts Barr-1	8 mi S.W. Spring City, TN	PWR	1177	01-23-73	1979		NDT
Watts Barr-2	8 mi S.W. Spring City, TN	PWR	1177	01-23-73	1980		NDT
Zimmer	24 mi S.E. Cincinnati, OH	BWR	810	10-27-72	1979		NDT
Haven-1	5 mi N. Sheboygan, WS	PWR	900		1987		NDT
Haven-2	5 mi N. Sheboygan, WS	PWR	900		1989		NDT
Erie Nuclear-1	1 mi N. Berlin Heights, OH	PWR	1260		1985		NDT
Erie Nuclear-2	1 mi N. Berlin Heights, OH	PWR	1260		1986		NDT
Black Fox Station-1	3 mi S.W. Inola, OK	BWR	1150		1983		MDT[e]
Black Fox Station-2	3 mi S.W. Inola, OK	BWR	1150		1985		MDT
Blue Hills Station-1	18 mi N. Newton, TX	PWR	918		1989		MDT
Blue Hills Station-2	18 mi N. Newton, TX	PWR	918		1991		MDT
Catawba-1	19 mi S.W. Charlotte, SC	PWR	1153	08-07-75	1981		MDT
Catawba-2	19 mi S.W. Charlotte, SC	PWR	1153	08-07-75	1983		
Cherokee-1	Cherokee Co., SC	PWR	1280	05-28-76 (limited)	1984		MDT
Cherokee-2	Cherokee Co., SC	PWR	1280	05-28-76 (limited)	1986		MDT
Cherokee-3	Cherokee Co., SC	PWR	1280	05-28-76 (limited)	1989		MDT
Farley-2	16 mi E. Dothan, AL	PWR	829	08-16-72	1980		MDT
Hatch-2	11 mi N. Baxely, GA	BWR	795	12-27-72	1978		MDT
Marble Hill-1	10 mi S. Madison, IN	PWR	1130	08-24-77 (limited)	1982		MDT
Marble Hill-2	10 mi S. Madison, IN	PWR	1130	08-24-77 (limited)	1984		MDT
Palo Verde-1	2 mi S. Wintersburg, AZ	PWR	1238	05-25-76	1982		MDT
Palo Verde-2	2 mi S. Wintersburg, AZ	PWR	1238	05-25-76	1984		
Palo Verde-3	2 mi S. Wintersburg, AZ	PWR	1238	05-25-76	1986		MDT
Perkins-1	Davie Co., NC	PWR	1280		1985		MDT
Perkins-2	Davie Co., NC	PWR	1280		1987		MDT
Perkins-3	Davie Co., NC	PWR	1280		1990		MDT
River Bend-1	25 mi N. Baton Rouge, LA	BWR	934	03-25-77	1983		MDT
River Bend-2	25 mi N. Baton Rouge, LA	BWR	934	03-25-77	1985		MDT
Sundesert-1	16 mi S.W. Blythe, CA	PWR	950		1984		MDT
Sundesert-2	16 mi S.W. Blythe, CA	PWR	950		1988		MDT
Tyrone-1	19 mi W.S.W. Eau Claire, WI	PWR	1150		1984		MDT
WPPSS Nuclear Proj-1	Hanford, WA	PWR	1218	12-24-75	1982	Columbia River	MDT
WPPSS Nuclear Proj-4	Hanford, WA	PWR	1218	08-01-75 (limited)	1984	Columbia River	MDT
WPPSS Nuclear Proj-2	Hanford, WA	BWR	1103	03-19-73	1980	Columbia River	MDT
Yellow Creek-1	15 mi E. Corinth, MS	PWR	1300		1985		MDT
Yellow Creek-2	15 mi E. Corinth, MS	PWR	1300		1986		MDT

TABLE 1.3. (Contd)

Nuclear Plant	Location	Reactor Type	Capacity MWe	Construction Permit	Scheduled Completion	Environment	Mode of Cooling
Clinch River	Oak Ridge, TN	LMFBR	350		1982	Clinch River	OUC[f]
Forked River-1	9 mi S. Toms River, NJ	PWR	1070	07-12-[illegible]	1982		Tower
Midland-1	1 mi S. Midlands, MI	PWR	460	12-15-72	1980		OUC
Midland-2	1 mi S. Midlands, MI	PWR	811	12-15-72	19[illegible]		OUC
San Joaquin-1	33 mi N.W. Bakersfield, CA		1300		1987		OUC
San Joaquin-2	33 mi N.W. Bakersfield, CA		1300		1989		OUC
San Joaquin-3	33 mi N.W. Bakersfield, CA		1300		1989		OUC
San Joaquin-4	33 mi N.W. Bakersfield, CA		1300		1991		OUC
Three Mile Island-2	10 mi S.E. Harrisburg, PA	PWR	906	11-04-69	1978		NDT & MDT
Richmond	Richmond, ME	PWR	1150		1991		Tower
Carroll County-1	4 mi S.E. Savanna, IL		1100				OUC
Carroll County-2	4 mi S.E. Savanna, IL		1100				OUC
Vandalia Project	Near Prairie City, IA	PWR	1270				Closed cycle
NYSE&G-1		PWR	1250		1988		OUC
NYSE&G-2		PWR	1250		1990		OUC
Unnamed Unit-1		PWR			1990		OUC
Unnamed Unit-2		PWR			1992		OUC

[a]Once-through cooled -- natural surface water
[b]Once-through cooled -- reservoirs
[c]Spray canals
[d]Natural draft towers
[e]Mechanical draft towers
[f]Other and unspecified cooling

plant because data are collected without interruption. An ideal field site selection for testing the proposed monitoring design, therefore, appears to be a single unit plant.

Projected completion dates are important in field test site evaluation because of the time frame proposed for adequate monitoring. Two or three years each of preoperational and operational monitoring are necessary to quantify potential effects. Preoperational monitoring data are needed to determine the abundance and seasonality of relatively important species, observe natural variation and provide a data base sufficient for comparison. Monitoring after plant operation allows time for possible effects to become manifest. A monitoring program initiated in calendar year 1979 or 1980 at a nuclear power plant with a 1982 completion date seems optimal for expedient field verification.

Of the 80 sites reviewed, the Sterling Nuclear Power Plant is the only site that meets all of the criteria for favorable field testing and, therefore, provides a unique opportunity to validate the proposed monitoring design. It is located about 60 miles (97 km) NE of Rochester, New York and is operated by the Rochester Gas and Electric Corporation. A once-through pressurized water reactor using water resources of Lake Ontario, the Sterling plant is designed for a total MWe rating of 1150 and has a scheduled completion date of 1982. Thus, the Sterling Nuclear Power Plant appears to be the most desirable site for the field test of the proposed monitoring design program.

REFERENCES

Adams, S. M., Cunningham, P. A., Gray, D. D., and Kumar, K. D. 1977a. A critical evaluation of the nonradiological environmental technical specifications, Vol. 2, Surry Power Plants Units 1 and 2. ORNL/NUREG/TM-70. Oak Ridge, TN: Oak Ridge National Laboratory.

Adams, S. M., Cunningham, P. A., Gray, D. D., Kumar, K. D., and Witten, A. J. 1977b. A critical evaluation of the nonradiological environmental technical specifications, Vol. 3, Peach Bottom Atomic Power Station Units 2 and 3. ORNL/NUREG/TM-71. Oak Ridge, TN: Oak Ridge National Laboratory.

Adams, S. M., Cunningham, P. A., Gray, D. D., and Kumar, K. D. 1977c. A critical evaluation of the nonradiological environmental technical specifications, Vol. 4, San Onofre Nuclear Generating Station Unit 1. ORNL/NUREG/TM-72. Oak Ridge, TN: Oak Ridge National Laboratory.

Baltimore Gas and Electric Company. 1975a. Productivity studies, pp. 91-106. In Semi-annual report 1974, Biological and chemical baseline investigations in the vicinity of Calvert Cliffs Nuclear Power Plant. Baltimore.

Baltimore Gas and Electric Company. 1975b. Phytoplankton studies, pp. 107-136. In Semi-annual report 1974, Biological and chemical baseline investigations in the vicinity of Calvert Cliffs Nuclear Power Plant. Baltimore.

Baltimore Gas and Electric Company. 1975c. Phytoplankton productivity and biomass, pp. 5-107. In Semi-annual environmental monitoring report, Calvert Cliffs Nuclear Power Plant. Baltimore.

Baltimore Gas and Electric Company. 1975d. Phytoplankton, pp. 108-135. In Semi-annual report 1974, Biological and chemical baseline investigations in the vicinity of Calvert Cliffs Nuclear Power Plant. Baltimore.

Baltimore Gas and Electric Company. 1976a. Phytoplankton: productivity and biomass, pp. 1-39. In Semi-annual environmental monitoring report, Calvert Cliffs Nuclear Power Plant. Baltimore.

Baltimore Gas and Electric Company. 1976b. Phytoplankton. In Semi-annual environmental monitoring report, Calvert Cliffs Nuclear Power Plant. Baltimore.

Baltimore Gas and Electric Company. 1976c. Phytoplankton: productivity and biomass, pp. 1-31. In Semi-annual environmental monitoring report, Calvert Cliffs Nuclear Power Plant. Baltimore.

Baltimore Gas and Electric Company. 1976d. Phytoplankton, pp. 1-90. In Semi-annual environmental monitoring report, Calvert Cliffs Nuclear Power Plant. Baltimore.

Baltimore Gas and Electric Company. 1977a. Phytoplankton: productivity and biomass, pp. 1-50. In Non-radiological environmental monitoring report, Calvert Cliffs Nuclear Power Plant, July - December 1976. Baltimore.

Baltimore Gas and Electric Company. 1977b. Phytoplankton, pp. 1-33. In Non-radiological environmental monitoring report, Calvert Cliffs Nuclear Power Plant, July - December 1977. Baltimore.

Baltimore Gas and Electric Company. 1978a. Phytoplankton: productivity and biomass, pp. 1-49. In Non-radiological environmental monitoring report, Calvert Cliffs Nuclear Power Plant, January - December 1977. Baltimore.

Baltimore Gas and Electric Company. 1978b. Phytoplankton, pp. 1-39. In Non-radiological environmental monitoring report, Calvert Cliffs Nuclear Power Plant, July - December 1977. Baltimore.

Boston Edison Company. 1973a. Pre-operational report of Pilgrim nuclear studies: benthic survey. In Semi-annual report 3, Marine ecological studies related to operation of Pilgrim Station, July - December 1973. Boston.

Boston Edison Company. 1973b. Semi-annual report on Pilgrim nuclear studies: benthic survey. In Semi-annual report 3, Marine ecological studies related to operation of Pilgrim Station, July - December 1973. Boston.

Boston Edison Company. 1974a. Semi-annual report on Pilgrim nuclear studies: benthic survey. In Semi-annual report 4, Marine ecological studies related to operation of Pilgrim Station, January - June 1974. Boston.

Boston Edison Company. 1974b. Annual report on Pilgrim nuclear studies: benthic survey. In Semi-annual report 4, Marine ecological studies related to operation of Pilgrim Station, January - June 1974. Boston.

Boston Edison Company. 1975a. Interim report on benthic ecological studies in vicinity of Pilgrim Station. In Semi-annual report 5, Marine ecological studies related to operation of Pilgrim Station, July - December 1974. Boston.

Boston Edison Company. 1975b. Report on benthic ecological studies, September 1974 - May 1975. In Semi-annual report 6, Marine ecological studies related to operation of Pilgrim Station, January - June 1975. Boston.

Boston Edison Compan 1976a. Benthic faunal and floral studies in the vicinity of Pilgrim Station, report no. 3. In Marine ecological studies related to operation of Pilgrim Station, Semi-annual report 7, July - December 1975. Boston.

Boston Edison Company. 1976b. Benthic faunal and floral studies in the vicinity of Pilgrim Station, report no. 4. In Marine ecological studies related to operation of Pilgrim Station, Semi-annual report 8, January - June 1976. Boston.

Boston Edison Company. 1977a. Benthic faunal and floral studies in the vicinity of Pilgrim Station, report no. 5. In Marine ecological studies related to operation of Pilgrim Station, Semi-annual report 9, July - December 1976. Boston.

Boston Edison Company. 1977b. Benthic faunal and floral studies in the vicinity of Pilgrim Station, report no. 6. In Marine ecological studies related to operation of Pilgrim Station, Semi-annual report 10, January - July 1977. Boston.

Eberhardt, L. L. 1978. Appraising variability in population studies. J. Wildl. Manage. 42(2): 207-238.

Gore, K. L., Thomas, J. M., Kannberg, L. D., and Watson, D. G. 1976a Evaluation of Monticello Nuclear Power Plant, environmental impact prediction, based on monitoring programs. BNWL-2150/NRC-1. Richland, WA: Battelle, Pacific Northwest Laboratories.

Gore, K. L., Thomas, J. M., Kannberg, L. D., Mahaffey, J. A., and Watson, D. G. 1976b. Evaluation of Haddam Neck (Connecticut Yankee) Nuclear Power Plant, environmental impact prediction, based on monitoring programs. BNWL-2151/NRC-1. Richland, WA: Battelle, Pacific Northwest Laboratories.

Gore, K. L., Thomas, J. M., Kannberg, L. D., and Watson, D. G. 1977. Evaluation of Millstone Nuclear Power Plant, environmental impact prediction, based on monitoring programs. BNWL-2152/NRC-1. Richland, WA: Battelle, Pacific Northwest Laboratories.

McKenzie, D. H., Kannberg, L. D., Gore, K. L., Arnold, E. M., and Watson, D. G. 1977. Design and analysis of aquatic monitoring programs at nuclear power plants. PNL-2423. Richland, WA: Battelle, Pacific Northwest Laboratories.

Murarka, I. P. 1976. An evaluation of environmental data relating to selected nuclear power plant sites. The Nine Mile Point Nuclear Power Station Site. ANL/EIS-7. Argonne, IL: Argonne National Laboratoryies

Murarka, I. P., Policastro, A., Daniels, E. W., Ferrante, J. G., and Vaslow, F. 1976a. An evaluation of environmental data relating to selected nuclear power plant sites: The Zion Nuclear Power Station site. ANL-EIS-5. Argonne, IL: Argonne National Laboratory.

Murarka, I. P., Ferrante, J. G., Daniels, E. W., and Pentecost, E. E. 1976b. An evaluation of environmental data relating to selected nuclear power plant sites: Prairie Island Nuclear Generating Plant Site. ANL-EIS-6. Argonne, IL: Argonne National Laboratory.

NUS Corporation. 1978. Commercial nuclear power plants, edition no. 10. Rockville, Maryland.

Scheffe, H. 1959. The analysis of variance. New York: Wiley.

Southern California Edison Company. 1977. San Onofre Nuclear Generating Station Unit 1, environmental technical specifications annual operating report, biological data supplement - 1976. Rosemead, CA.

Southern California Edison Company. 1978. San Onofre Nuclear Generating Station Unit 1, environmental technical specifications annual operating report, Vol. 2, biological data - 1977. Rosemead, CA.

Tiku, M. L. 1972. More tables of the power of the F-test. J. Am. Stat. Assoc. 67:709-710.

SIMULATION MODEL EVALUATION

SIMULATION MODEL EVALUATION

INTRODUCTION

Simulation models have potential application to the analysis of impacts of nuclear power plants on aquatic ecosystems. The research we report in this chapter focused on evaluation of representations of processes controlling the dynamics of consumers (zooplankton and fish). This work, part of a collaborative effort with Dr. Gordon Swartzman of the University of Washington, is designed to evaluate the application of existing models to impact analysis.

Models were selected for the review based on their potential applicability to impact analysis and on the availability of clear documentation supporting them. The models included in our review represent a wide range of complexity and resolution. They were built to satisfy different objectives, ranging from synthesis of information to management of commercial fisheries. While some focus on a single species, others are multiple-species models with an elaborate fish age structure. In spite of this great diversity, however, the models share many similarities. The dynamics of modeled components are described by sets of differential equations representing critical processes (e.g., consumption, respiration and metabolism, growth, fecundity, and mortality). These rate equations are functions dependent on environmental conditions and the values of principle model variables (e.g., biomass, numbers of individuals, age and weight of an individual).

Similarities in equation form permit generation of hybrid models combining features of many of the existing models, and we have developed and implemented a simulator which permits such hybridization with minimal reprograming effort. In order to make full use of this powerful tool and to guard against misuse, a detailed guide for its use is required. PNL is compiling such a guide. This process notebook will include a process-by-process description of all representations, translation of each equation into a standard notation, critical evaluation of supporting rationale, typical parameter values for the equations, a subjective rating of parameter "variance," and recommendations regarding the range of applicability of each representation. In addition, this process notebook will include a history of the development of process representations, notes to the user, and compatibility schemes that define allowable combinations of representations. With these tools a user may select representations appropriate to his needs and to the data base available to him.

Final selection of the "best" model for a particular need will involve careful definition of objectives and a tradeoff between higher resolution and increased requirements for data on which to base parameter estimates. Initially we plan to test the hybrid model synthesizer with data for Lake Keowee, South Carolina, which is used to cool a nuclear power station, and to examine model sensitivity to parameter values.

PNL's primary role during this reporting period has been to evaluate process representations and their supporting rationale and to assess parameter estimates and their "variance." Our objectives have been to describe the

representations, to examine their range of applicability and develop guidelines for their use. An overview of the process representations and their historical development has been completed and appears in this chapter. A more thorough analysis is being conducted for inclusion in the process notebook to be published in the near future.

CONSUMPTION

Consumption is defined as the quantity of prey eaten during a given period of time by a class of predators. It is a critical consideration in describing ecosystem dynamics. It encompasses determination of available energy in prey consumed and identification of prey items taken, both of which are key elements in describing energy transfer between trophic levels and defining mortality of prey items due to their being eaten. In general the models reviewed represented ration (the quantity of prey eaten by one predator during a given period of time) as a power function of the predator's body weight. Several of the models also included an effect of temperature and some representations were functions of prey density or of selection of specific prey items by the predator.

Relating ration to body weight may be historically traced to a growth model proposed by Pütter (1920). He assumed that the rate of food intake (absorption from the gut) is directly proportional to the surface area of the gut. Under the further assumption that growth is isometric (i.e., all body parts grow in linear dimension at the same rate), surface area and volume of different body parts are related by a 2/3 power function. Pütter therefore modeled food intake as $hw^{2/3}$, h being a proportionality constant and w representing body weight. Von Bertalanffy (1938) extended Pütter's work to develop a general model of fish growth.

Ursin (1967) generalized the weight-ration relationship to hw^m and discussed methods for estimating m. These led to several estimates of m, all <2/3, and indicated that the value may increase with fish size. Thus, it seems that growth is not precisely isometric, and that use of Pütter's model may lead to an overestimation of food absorption for larger fish. Although estimates of m contain an unknown bias or lack precision because of experimental difficulties, Ursin claimed that m may be set to 2/3 without introducing an unacceptable error. In order to derive a representation of the ration consumed per individual, Ursin (1967) assumed feeding level to be a constant fraction of the maximum possible absorption from the gut.

Andersen and Ursin (1977) and Beyer (1967) suggested nearly identical consumption representations based on Ursin's formulation (1967), with the addition of a selectivity factor. Total food available to a predator was represented by the sum of the biomass of each potential prey item weighted by suitability coefficients. The suitability coefficients represent the probability that a given potential prey item will be included in the food available to the predator. Both of the models used size preference (the relative probability that a given size of prey item will be included in the diet) to weight suitability. Size preference was represented by a log-normal function based on Ursin's finding (1973, 1974) that prey twice the preferred size were equally attractive as those half the preferred size. Andersen and Ursin (1977) also weighted prey biomass with a vulnerability factor, since different prey of equal size may be differentially susceptible to capture and ingestion. They weighted available biomass by the fraction of the prey which was pelagic or demersal to arrive at two stocks of available food.

Ration in the Andersen and Ursin (1977) model is represented as a modification of the equation presented by Ursin (1967). Consumption is based on search rate, probability of encounter of prey and the fraction of encountered prey consumed. The feeding level (f_i) was thus derived as

$$f_i = \frac{\phi i}{\phi i + Qi} \; ; \quad Qi = \frac{V}{q_i w_i^{\,r}}$$

where

the subscript, i, denotes the i^{th} predator
ϕi = weighted available food (weighted by suitability, vulnerability and position in the water column)
V = volume of water
w_i = body weight
q_i and r are coefficients.

Thus, the half-saturation constant for feeding is $1/q_i w_i^{\,r}$ and the formulation corresponds to a Michealis-Menton rate equation. Andersen and Ursin (1977) placed an upper bound on feeding level while the Beyer (1976) did not.

Warren and Davis (1967) utilized Ivlev's balanced equation for distribution of the energy contained in consumed food. This energy must equal the sum of energy used for growth, waste products, heat and work. Ivlev's equation was modified slightly by assuming that the rates of energy use were all proportional to body weight raised to a power to make it more biologically meaningful. For the equation to balance, the powers of the weight relationships must all be equal. Warren and Davis (1967) briefly reviewed works which empirically determined the power for metabolic rate. Winberg (1956) critically reviewed experimental procedures reported in a large number of articles and found that, for a wide variety of fish species, the power should be 0.8. This value concurs with other findings cited by Warren and Davis.

Kerr (1971b), considering a similar balanced energy equation, substituted relationships for each of the equation terms and solved the resulting equation for consumption. His consumption equation represents energy used for total metabolism less standard metabolism, leaving energy available for foraging and specific dynamic action. This result was divided by energy cost per prey item for foraging plus specific dynamic action to arrive at the number of items of prey in the ration, which was multiplied by prey weight to determine consumption. Kerr (1971a) substituted the relationships examined by Winberg (1956) and by Paloheimo and Dickie (1966) for total weight and standard metabolism. Thus, ration became a function of body weight raised to a power. Kerr (1971a) selected a power of 0.85 after Winberg (1956), Brett (1965) and Job (1955).

The energy cost of foraging in Kerr's model is formulated as the energetic cost of swimming based on the work of Fry (1957), who showed swimming cost to be proportional to weight times the square of swimming speed. Swimming speed

was taken to be linearly related to body length, and body length was a power function of body weight (Ricker, 1932). The mean distance swum between prey items was dependent on prey density and the distance at which a prey item was perceived. Specific dynamic action was assumed to be linearly related to consumption.

Jørgensen (1976) used two different equations for feeding level, both of which he claimed were fit to feeding tables available from Ewos, a Swedish firm. In his model, both of these relationships were expressed as functions of body weight raised to a power. No rationale for selecting the relationship used was indicated, other than an empirical fit to the feeding tables. Food not used must be subtracted from the feeding level to determine ration. Thus consumption was a function of feeding level, body weight and temperature. Rationale for the representation was not given, except that the temperature relationship was derived from data reviewed by Speece (1973).

Kitchell, Stewart and Weininger (1977) formulated a maximum consumption rate as a power function of body weight. This rate was adjusted for temperature effects. The power function, which reflects the relationship of stomach volume and digestive rate to body weight, was taken from Elliot (1976b), who fit the function to feeding data. The temperature relationship was taken from O'Neill et al. (1972) and follows an exponential rise with temperature up to the optimum temperature. Above the optimum, the consumption rate quickly falls, reaching zero at the maximum temperature for feeding.

Eggers (1975) found the set of selectivity indices to maximize net energy intake, which he based on Holling's disc equation (1959). Net energy was defined as the energy content of consumed prey minus the energy cost of pursuit and handling, divided by 1 plus handling time. Consumption was defined as the product of prey density, encounter rate, selectivity coefficient, successful capture rate and energy content per prey item, summed for all available prey types and divided by 1 plus handling time. Handling time increases with season and with hunger. Hunger is the ratio of stomach content (a time-dependent variable with a first derivative equal to the ration less gut evacuation) to stomach size. Stomach size is a function of body size, temperature and stomach content. The representation of encounter rate was derived from a model of prey sighting and predator swim speed. Sighting distance depended on the fourth power of prey length and light intensity, and swimming speed was a function of body length and season. During schooling, which occurs in the summer when light levels are within threshold values, the encounter rate was adjusted for visual overlap and prey density adjusted to account for predation by the leading portion of the school.

Steele and Frost (1977) developed a formulation of consumption based on a theoretical analysis of copepod filtering mechanics. The area available for filtering was determined by assuming a particular fan geometry of the setae. The size of setae and the angle between them was assumed to be proportional to body length raised to a power between 1 and 2. The difference between the costs of filtering water and metabolism, and assimilated energy, is growth. After deriving filtering costs and defining standard metabolism, Steele and

Frost found filtering flow velocity to optimize growth. If optimum growth was less than the maximum growth rate, the animals were assumed to select the corresponding optimum filtering velocity, from which consumption was computed. If the maximum growth rate was less than the optimum, the filtering flow velocity was reduced accordingly.

Scavia, Eadie and Robertson (1976) modeled zooplankton grazing to include a preference factor for each potential predator-prey pair. Consumption was linearly proportional to biomass of zooplankton. A modification of the preference mechanism used by Andersen and Ursin (1977) and Beyer (1976) allowed for introduction of a minimum (threshold) prey level to stimulate feeding. The threshold was partitioned among the prey groups according to preference. Weighted prey biomass and half-saturation constants were corrected for the effect of inclusion of the threshold term. Effects of temperature are modeled in a manner nearly identical to that of Kitchell, Stewart and Weininger (1977). A parameter value specified the slope of the temperature coefficient below the optimum temperature, and the coefficient rapidly dropped off at temperatures above the optimum.

In summary, nearly all of the models reviewed which included consumption by fish related it to a power of body weight to account for effects of absorbtive surface area and digestive rate. The exception is the model proposed by Patten et al. (1975), in which consumption was linearly related to the initial biomass of fish and thus fails to account for changes in population size of individual weight during the simulation run. One of the two models of zooplankton consumption considered it related to a power function of length. The other model assumed a linear relationship with biomass.

Temperature effects on consumption are modeled in a variety of ways when they are included. Jørgensen (1976) allowed the wasted food coefficient to decrease with increasing temperature, thus increasing consumption as temperature rose. This treatment is unrealistic over an extended temperature range because consumption declines at a temperature above the physiological optimum. The formulation used by Patten et al. (1975) is a logistic curve, approaching a horizontal asymptote as temperature rises. Kitchell, Stewart and Weininger (1977) and Scavia, Eadie and Robertson (1976) used very similar equations to describe the temperature effect. These provided a more realistic decrease in consumption rate at high temperatures. Thornton and Lessem (1978), also proposed a realistic formulation consisting of the product of two logistic equations. Eggers (1975) included the effect of temperature in his formulation of digestion and evacuation rate. His equation was unbounded and must be used carefully to avoid unrealistic effects at high temperatures.

Where included, selectivity of prey is either described by prey size using a log-normal distribution (Steele and Frost, 1977; Andersen and Ursin, 1977; Beyer, 1976) or by species-preference weighting factors (Eggers, 1975; Patten et al., 1975; Scavia, Eadie and Robertson, 1976), or by vulnerability weighting factors (Andersen and Ursin, 1977). All of these approaches appear to be supported by available information, and a combination of them, such as Andersen and Ursin (1977) employ, appears to be the most realistic formulation unless preference weighting factors are separately specified for different sizes of prey within a particular prey species.

ASSIMILATION

Assimilation represents the portion of ingested food available for metabolism and growth. Winberg (1956) defined "physiologically useful energy" (i.e., assimilation) as ration minus egestion and excretion. Ursin (1967) cited evidence that the proportion of ingested food absorbed decreases as the feeding level increases. The assimilation factor (β) was defined as

$$\beta = 1 - e^{-h_2/f}$$

where

h_2 is a constant
f = feeding level.

Thus, for extremely low feeding levels, nearly all the ingested food is absorbed. Urine production and specific dynamic action are combined in a single term which is a constant proportion of ingested food.

Andersen and Ursin (1977) defined assimilation similarly, but utilized a constant proportion of ingested food to characterize egestion. Excretion was defined as a constant fraction of assimilated food plus a power function of body weight representing excretion due to fasting catabolism.

Beyer (1976), Karr (1971a, b), Eggers (1975), Steele and Frost (1977) and Scavia, Eadie and Robertson (1976) assumed that a constant fraction of food ingested is lost to both feces and urine. Warren and Davis (1967) used a power function of weight to describe this combined loss as well as consumption. Thus, assimilation was also considered a constant portion of consumption.

Kitchell, Stewart and Weininger (1977) use formulations developed by Elliot (1976a) to relate egestion (F) and excretion (U) to consumption, temperature and feeding level:

$$F, U = \alpha C T^{\beta} e^{\delta P}$$

where

C = consumption
T = temperature
P = feeding level
α, β and δ are regression coefficients that differ for fecal or urine production.

Jørgensen (1976) defined fecal production as a function of available feed (F), temperature (T), body weight (W) and consumption (F-NUF):

$$\text{assimilation} = (F\text{-}NUF)\ (1\text{-}NDF)$$

where

$$NDF = \begin{cases} \dfrac{WFC \cdot F}{W^{EA}} & \text{if } \dfrac{WFC \cdot F}{W^{EA}} \leq 0.5 \\ 0.5 & \text{elsewhere} \end{cases}$$

$WFC = 4.158 \times 10^{2} \times T^{-0.807}$
NDF = non-digested feed
F = available feed
T = temperature
W = body weight
(F-NUF) = consumption
WFC = wasted food coefficient
EA = appetite exponent.

Similarly, he defined excretion as a temperature-dependent fraction of assimilation:

$$ALC = 0.021\ T^{0.703} \cdot (\text{Assimilation})$$

where ALC = assimilation loss coefficient.

Both factors were corrected for the relative proportions of dry matter in the consumer and in the feed.

Patten et al. (1975) established temperature-dependent fluxes for feces and urine production. In this donor-controlled linear model, the production of feces and urine was a linear function of biomass. The temperature dependency was defined by a multiplier which is a logistic function of temperature.

Only the formulation by Andersen and Ursin (1977) accounts for both the effect of fasting catabolism and variations in consumption. However, the formulation proposed by Ursin (1967) and that of Kitchell, Stewart and Weininger (1977) have an advantage in considering the effects of feeding level. In addition, temperature was considered in their formulation.

METABOLISM AND RESPIRATION

Like consumption, metabolism and respiration are generally modeled as power functions of body weight. These catabolic terms are also strongly dependent on temperature. The energy remaining after catabolism is subtracted from assimilation is available for growth and reproduction. Thus, the dynamics of a population are very strongly dependent on respiration.

Ursin's definition of metabolism (1967) included two catabolic terms: a fasting-related term which was a function of body weight and a feeding-related term which was a linear function of ration. Total catabolism was the sum of the two terms. Excretion-related energy loss was included in the fasting term without being separately defined. The rate of fasting catabolism was assumed to be related to the fish's ability to obtain oxygen. Since oxygen uptake had to be related to surface area of the body and gills, and since the gill surface area is isometrically related to body size, a power function of body weight was used to describe respiratory surface and to approximate the total area with a single term.

Since these terms are both power functions of body weight with similar values, they were approximated by a sum of the terms that was set equal to an intermediate power of body weight. Temperature effects on catabolism were derived from the Michaelis-Menton equation describing enzyme-substrate kinetics and the Arrhenius equation, which relates temperature to activation energy required for an enzyme-mediated reaction. A multiplier for the effect of temperature was expressed as the reciprocal of the sum of two exponential functions of temperature, and was approximated as a simple exponential function of temperature.

The model by Andersen and Ursin (1977) followed the same formulation as that used by Ursin, but omitted temperature effects. Beyer (1976) utilized Putter's growth equation (Pütter, 1920) and thus assumed all catabolic losses to be represented by a linear function of body weight.

Warren and Davis (1967) divided total metabolism into three components: standard metabolism, specific dynamic action (the energy required to process food) and swimming activity cost. Each of these components was assumed to be a power function of body weight with equal exponents. Since they represented consumption as a similar power function of body weight, specific dynamic action and swimming cost are linearly related to ration.

Kerr (1971b) set total metabolism equal to the sum of foraging metabolism, standard metabolism and the internal cost of food utilization (specific dynamic action). The sum was set equal to Winberg's power function of body weight (Winberg, 1956). The metabolic cost of foraging was a function of sighting distance and swimming cost, as defined above. Standard metabolism was defined as a power function of body weight, and specific dynamic action was a linear function of ration.

Kitchell, Stewart and Weininger (1977) multiplied standard metabolism (taken from Winberg, 1956) by a parameter to account for activity, and by a temperature correction factor. The temperature correction was similar to that used for consumption, which had a different set of parameters (see section on consumption). A factor for specific dynamic action that was linearly related to food consumption was then added.

Eggers (1975) considered specific dynamic action, standard metabolism, foraging activity and spontaneous activity terms in defining total respiration. Standard metabolism was characterized after Winberg's definition (1956) as a power function of weight times an exponential temperature correction factor. Activity terms (T_i) were all identically defined as the product of the standard metabolism (T_s) with an exponential function of temperature and swimming speed:

$$T_i = T_s \left| e^{(\alpha_1 - \alpha_2 T)S} - 1 \right|$$

where

α_1 and α_2 are parameters
T = temperature
S = swimming speed.

This formulation was based on Brett's investigations (1964) of the effects of activity and temperature on oxygen consumption by sockeye salmon (Oncorhynchus nerka). The specific dynamic action term is linearly related to assimilated energy. The coefficient of specific dynamic action is dependent on food type, but independent of activity, body weight and temperature, as stated by Kleiber (1961).

Patten et al. (1975) defined metabolism as a linear function of compartment biomass in their linear, donor-controlled model. Fluxes are corrected for temperature using the same logistic function as defined in the consumption discussion, but with a different parameter.

Jørgensen (1976) defined respiration loss as a power function of body weight multiplied by a power of temperature. This function is similar to that formulated by Winberg (1956). Scavia, Eadie and Robertson (1976) defined respiration for zooplankton as a constant maximum rate multiplied by a factor for temperature. This temperature factor is identical to that described for consumption. Steele and Frost (1977) defined respiration (R, below) of phytoplankton cells as proportional to surface area divided in cell carbon. The relationship between cell carbon and volume is not known precisely. Hence, two different extreme values of the formulation were used in the model:

$$R = 0.32\ D^{-0.33}$$
$$R = 1.5\ D^{-1.0}$$

where D is cell diameter.

Respiration of zooplankton was assumed proportional to body surface area. Surface area is proportional to the square of body length under the assumption of isometric growth.

In summary, most of the models represent metabolism and respiration as power functions of body weight. Effects of temperature are modeled with a variety of functions. Some of these functions have a limited range of valid application, as discussed above.

PREDATION MORTALITY

Mortality to a prey group depends on ration taken and on selection of the group by the predators. Thus, for most of the models predation mortality is found by summing the number of mortalities to a given prey item inflicted by each of the predators in the system. For example, Beyer (1976) modeled mortality of a prey group due to predation by each consumer as the predator ration multiplied by the fraction of available food that the particular prey item represents. Available food was defined by weighted values of prey based on suitability coefficients (discussed in the above section on consumption). The total predation mortality of a prey group was found by summing the mortality inflicted by each predator over all of the predator classes. The same formulation was also used by Andersen and Ursin (1977).

The mechanism by which Patten et al. (1975) computed coefficients of flux for consumption is also discussed above. Total predation mortality, in Patten's model, is found by summing the coefficients over all predators on a single prey. Similarly, Scavia, Eadie and Robertson (1976) determined grazing mortality by summing consumption over predators. Their preference-weighting mechanism is also described above.

Steele and Frost (1977) represented predation on zooplankton as an exponential function of prey biomass dependent on time:

$$M = -(H +_{\star} H\, m^{-u})\, e^{Z_o B T^2} / (T_o^2 + T^2)$$

where

M = mortality
B = biomass of predator
T = time
H, $H_{\star}$, u, Z_o and T_o are parameters
m = average weight of prey.

This complex formulation was derived to simulate variation in predation over time and the influence of prey density on predator biomass. Both invertebrate and fish predators were considered, but not modeled dynamically. Therefore, a nonmechanistic relationship that gives empirically reasonable results is used.

FECUNDITY AND RECRUITMENT

Several of the models reviewed include representations of fecundity and subsequent recruitment. Their approach is to assume that a portion of the biomass of mature females is converted to eggs and that a portion of the eggs hatch to produce a new cohort. In one model mature zooplankters are assumed to use energy remaining after respiration for production of nauplii.

Beyer (1976) represented the number of eggs produced by a species by summing the biomass of all mature groups (those exceeding a minimum age and weight), multiplying by a spawn mass coefficient adjusted for the proportion of females in the population and dividing by the "egg weight." Since the model does not consider early life stages, the "egg weight" is grossly overestimated to represent the weight of a recruit. Thus, it is assumed that mature fish spawn a fraction of their body weight at a designated spawning time. All of the spawn is considered recruited unless recruitment is controlled by a Beverton-Holt equation describing the results of compensatory larval mortality:

$$R = \frac{E}{A \cdot E + R_{max}} \quad R_{max}$$

where

R = number of surviving recruits
A = a parameter
E = number of "eggs" prior to compensation
R_{max} = asymptotic maximum number of surviving recruits

Andersen and Ursin (1977) also considered the mass of spawn to be a fraction of body weight of mature (by age only) fish. The total biomass of spawn is adjusted for the proportion of females in the age group. Eggs are assumed to hatch immediately. Their biomass is adjusted for egg loss and respiration as fractions of the egg biomass. Finally, the number of newly hatched larvae is determined by dividing by the weight of one larva. Recruitment is determined by the previously discussed Beverton-Holt mechanism in the reduced model presented for computation. In the full model, mortality of larvae is a function of their numbers over the weight per larva.

$$M = \frac{N}{\hat{R}} \quad \frac{(dw/dt)_{max}}{W}$$

where

M = mortality of larvae
N = larvae numbers
$(dw/dt)_{max}$ = highest possible growth rate (age-specific)
$\hat{R}$ = a parameter approximating the number of one-year-old recruits
W = weight per larva.

Patten et al. (1975) also assumed that spawning is a linear function of body weight, but used linear interpolation of a table of reproductive coefficients to establish time-dependent reproductive rates. One-half of the population was assumed to be female. The eggs spawned are assumed to hatch immediately and to appear as larvae with no mortality. Larval growth and mortality are then modeled in a manner similar to other model components.

Steele and Frost (1977) permitted copepods to grow to a maximum size in their model. After the maximum is reached, additional energy available for growth goes into production of eggs which have a mass equal to that of first-stage nauplii. Development to the feeding stage takes 8 days. During that period, respiration is accounted for by the reduction of nauplii numbers.

REFERENCES

Andersen, K. P., and Ursin, E. 1977. A multispecies extension to the Beverton and Holt theory of fishing, with accounts of phosphorus circulation and primary production. Meddr. Danm. Fisk. -og Havunders 7: 319-435.

Beyer, J. E. 1976. Ecosystems: An operational research approach. Lyngby, Denmark: IMSOR. 315 pp.

Brett, J. R. 1964. The respiratory metabolism and swimming performance of young sockeye salmon. J. Fish. Res. Bd. Canada 21: 1183-1226.

Brett, J. R. 1965. The relationship of size to rate of oxygen consumption and sustained swimming speed of sockeye salmon (Oncorhynchus nerka). J. Fish. Res. Bd. Canada 22: 1491-1501.

Eggers, D. M. 1975. A synthesis of the feeding behavior and growth of juvenile sockeye salmon in the limnetic environment. Ph.D. Thesis, Univ. of Washington.

Elliot, J. M. 1976a. Energy losses in the waste products of brown trout (Salmo trutta L.). J. Anim. Ecol. 45: 561-580.

Elliot, J. M. 1976b. The energetics of feeding, metabolism, and growth of brown trout (Salmo trutta L.) in relation to body weight, water temperature, and ration size. J. Anim. Ecol. 45: 923-948.

Fry, F. E. J. 1957. The aquatic respiration of fish, pp. 1-63. In The Physiology of Fishes, Vol 1. Metabolism, M. E. Brown, ed. New York: Academic Press.

Holling, C. S. 1959. Some characteristics of simple types of predation and parasitism. Can. Entomol. 41: 385-398.

Job, S. V. 1955. The oxygen consumption of Salvelinus fontinalis. Univ. Toronto Biol. Ser. 61, Publ. Ont. Fish. Res. Lab. 73. 39 pp.

Jørgensen, S. E. 1976. A model of fish growth. Ecol. Modeling 2: 303-313.

Kerr, S. R. 1971a. Analysis of laboratory experiments on growth efficiency of fishes. J. Fish. Res. Bd. Canada 28: 801-808.

Kerr, S. R. 1971b. Prediction of fish growth efficiency in nature. J. Fish. Res. Bd. Canada 28: 809-814.

Kitchell, J. F., Stewart, D. J., and Weininger, D. 1977. Applications of a bioenergetics model to yellow perch (Perca flavescens) and walleye (Stizostedion vitrium vitrium). J. Fish. Res. Bd. Canada 34: 1922-1935.

Kleiber, M. 1961. The Fire of Life. New York: Wiley.

Krogius, F. V., Krokhin, E. M., and Menshutkin, V. V. 1969. The pelagic fish community in Lake Dalnee: An experiment in cybernetic modeling. Kotinro: Academy of Science of the USSR.

O'Neill, R. V., Goldstein, R. A., Shugart, N. H., and Mankin, J. B. 1972. Terrestrial ecosystem energy model. Eastern Deciduous Forest Biome--International Biological Program Report 72-19.

Paloheimo, J. E., and Dickie, L. M. 1966. Food and growth of fishes. Pt. II, Effects of food and temperature on the relation between metabolism and body weight. J. Fish. Res. Bd. Canada 23: 869-908.

Parrish, J. D. 1975. Marine trophic interactions by dynamic simulation of fish species. Fish Bull. 73(4): 695-715.

Patten, B. C., Egloff, D. A., and Richardson, T. H., et al. 1975. Total ecosystem model for a cove in Lake Texoma, pp. 205-421. In Systems Analysis and Simulation Ecology, Vol. 3, B.C. Patten, ed. New York: Academic Press.

Pütter, A. 1920. Studien uber physiologische Ahnlichkeit. VI, Wachstumsahnlichkeiten. Pflugers Arch. Gesamte Physiol. Menschen Tiere 180: 298-340.

Ricker, W. E. 1932. Studies of speckled trout in Ontario. Publ. Ont. Fish. Res. Lab. 44: 69-110.

Scavia, D., Eadie, B. J., and Robertson, A. 1976. An ecological model for Lake Ontario model formulation, calibration, and preliminary evaluation. NOAA Tech. Dept. ERL-371-GLERL-12.

Speece, R. E. 1973. Trout metabolism characteristics and the rational design of nitrification facilities for water reuse in hatcheries. Trans. Am. Fish. Soc. 102: 323-334.

Steele, J. H., and Frost, B. W. 1977. The structure of plankton communities Phil. Trans. Royal Soc. London Ser. B 280:485-534.

Thorton, K. W., and Lessem, A. S. 1978. A temperature algorithm for modifying biological rates. Trans. Am. Fish. Soc. 107: 284-287.

Ursin, E. 1967. A mathematical model of some aspects of fish growth, respiration, and mortality. J. Fish. Res. Bd. Canada 24: 2355-2453.

Ursin, E. 1973. On prey size preferences of cod and dab. Meddr. Danm. Fisk. -og Havunders, N. S. 7: 88-98.

Ursin, E. 1974. Search rate and food size preference in two copepods. Intem. Counc. Exp. Sea, C. M. 1974/L:23 (mimeographed).

Von Bertalanffy, L. 1938. A quantitative theory of organic growth. Hum. Biol. 10(2): 181-213.

Warren, C. E., and Davis, G. E. 1967. Laboratory studies on the feeding, bioenergetics, and growth of fish, pp. 175-214. In Biological basis of freshwater fish production, S. D. Gerking, ed. Oxford and Edinburgh: Blackwell Scientific Publications.

Winberg, G. G. 1956. Rate of metabolism and food requirements of fishes. Fish. Res. Bd. Can. Trans Ser. No. 194.

HYDROLOGIC MODELING TASK

HYDROLOGIC MODELING TASK

INTRODUCTION

The hydrologic modeling research conducted during this fiscal year includes preparation of a compendium of models representing the mathematical class commonly applied to nuclear power plant sites, and application of two hydrodynamic models to a specific site. The purpose of compiling information on these models is to provide a reference for input and verification data for model users and designers of monitoring programs. This reference contains descriptions of the basic physical phenomena simulated and of the numerical techniques used in calculating the quantities desired. Data required to operate the model are listed where possible and should be of use to monitoring program designers. The description of the numerical schemes gives information which will influence the spatial layout of the sampling stations. For example, finite element and finite difference modes should have sampling networks arranged in polyhedral and rectangular grids, respectively. The discussion of physical phenomena and numerical schemes will also provide guidance for selection of an appropriate model for a particular application. The present use and verification status of the models are also specified when possible to aid in model type selections.

This year's research also included the application of two well-received hydrodynamic models to a nuclear power plant site. The first aim of these applications was to reveal, at the operational level, considerations for designing monitoring programs to support these models. Second, the effects of the quality, abundance and spatial arrangement of data on the performance of the model were studied. For example, it was found that computational schemes often fail to conserve mass in regions with irregular morphology. This was mitigated by increasing the resolution of the water body discretization which causes an attendant need for more detailed monitoring data.

Criteria used for selection of the site for the model applications were data availability and a water body geometry which could tax the performance of the models. The Surry Nuclear Power Plant (Figure 3.1) on the James River in Virginia met the criteria as a model testing site. Velocity and tidal elevation data from field surveys conducted in 1974 by the Virginia Institute of Marine Science were used to operate the models.

The models chosen for application were a finite difference hydrodynamic model (Leendertse, 1967) and Research Management Associates' finite element hydrodynamic models RMA-I and II (Norton et al., 1973). The Leendertse model is well established and useful for nuclear power plants sited on estuaries or tidally influenced rivers. The RMA model is applicable to the same types of water bodies. A comparison of the influence of monitoring data quality on the performance of a finite difference and a finite element model is easier to relate to model structure than a comparison of two models of the same type.

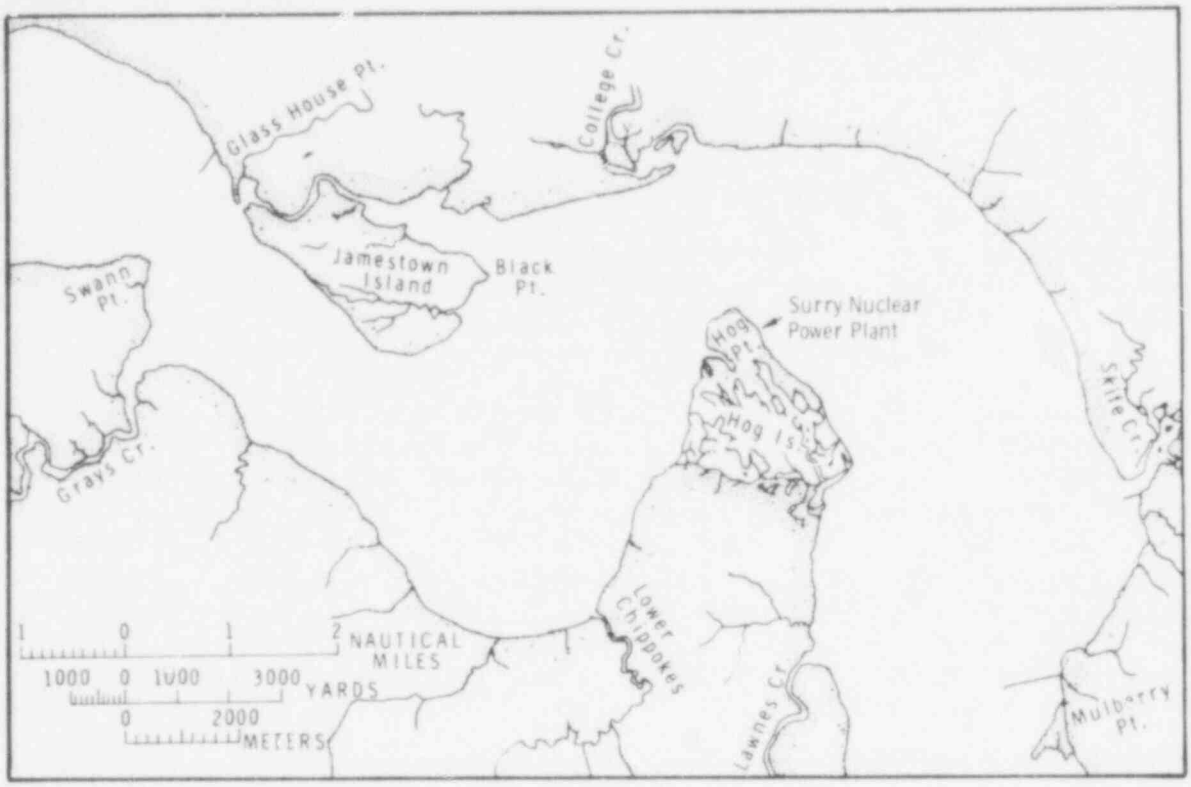

FIGURE 3.1. Vicinity of the Surry Nuclear Power Plant Used in this Study

COMPENDIUM OF MATHEMATICAL MODELS

The discussions of the mathematical models are grouped as follows:

1) General hydrodynamic and hydrothermal models
2) Hydrodynamic/water quality models
3) Integral thermal plume models
4) Constituent/sediment transport models.

The first group includes models giving numerical solutions to the general momentum and continuity equation and those also giving a thermal energy balance. The second group consists of models which solve a general or restricted form of the hydrodynamic equations and some form of the advection/diffusion equations for constituent transport. The third is a selection of integral thermal plume models for surface and submerged plume predictions. The final group contains two transport models which do not have hydrodynamic components and must use field data or hydrodynamic model output for velocity inputs.

GENERAL HYDRODYNAMIC AND HYDROTHERMAL MODELS

The discussions in this section are concerned with general hydrodynamic and hydrothermal models. The two- and three-dimensional finite difference codes of Leendertse are discussed first, followed by reviews of the stream function vorticity code VECTRA, and the finite element hydrothermal model RMA-II.

Leendertse's Two-Dimensional Model (1967)

The two-dimensional nonsteady motion of waves in estuaries and coastal seas is simulated by the Leendertse model. The model was developed under the sponsorship of the Department of the Air Force at the Rand Corporation. It was originally intended to simulate waves generated by nuclear explosions and is presently used to study many varied types of unsteady hydrodynamic situations. The model is well known for its success in estuarine simulations. The equations governing long-wave motion in their vertically integrated form are the basis of the model. To account for viscosity, shear stress terms are derived from the vertical eddy viscosity in the equations representing wind friction at the free surface and bottom friction. Wind stress is usually assigned a constant value. Bottom shear stress (τ_b) is proportional to the square of the velocity and can be written in one dimension as

$$\tau_b = \rho C^{-2} V|V|$$

where

ρ = density of the fluid
C = Chezy coefficient
g = gravitational acceleration.
V = velocity

Introduction of this bottom-stress term into the vertically averaged two-dimensional equations of motion results in

$$\frac{\partial U}{\partial t} + U\frac{\partial U}{\partial x} + V\frac{\partial U}{\partial y} - fV + g\frac{\zeta}{\partial x} + g\frac{U(U^2 + V^2)^{1/2}}{C^2(h + \zeta)} = F_{(x)}$$

$$\frac{\partial V}{\partial t} + U\frac{\partial V}{\partial x} + V\frac{\partial V}{\partial y} + fU + g\frac{\partial \zeta}{\partial y} + g\frac{V(U^2 + V^2)^{1/2}}{C^2(h + \zeta)} = F_{(y)}$$

where

U = vertically averaged x component of velocity
V = vertically averaged y component of velocity
f = Coriolis parameter
g = gravitational acceleration
ζ = water surface elevation
C = Chezy coefficient
h = distance between reference plane and bottom
t = time

and $F_{(x)}$ and $F_{(y)}$ are the forcing functions of the wind and barometric pressure in the x and y directions, respectively.

The boundary condition for the free surface is

$$w(\zeta) = \frac{\partial \zeta}{\partial t} + u\frac{\partial \zeta}{\partial x} + v\frac{\partial \zeta}{\partial y}$$

and at the bottom,

$$w(-h) + u\frac{\partial h}{\partial x} + v\frac{\partial h}{\partial y} = 0$$

where

u, v = x and y velocity components
h = distance between reference plane and bottom.

The conservation of mass equation is similarly vertically integrated.

The solution scheme is a finite difference method using a space-staggered grid in which the velocities and water levels are computed at staggered locations. Figure 3.2, taken from Leendertse (1967), shows this grid. In designing a monitoring program to support this model, the space-staggered scheme should be borne in mind when trying to match verification monitoring stations with locations where model calculations are performed.

To run the model, initial velocities and water levels must be specified (constant values are usually assigned). As boundary conditions, water levels must be specified at every half time step on open water boundaries. At freshwater inflows, discharges can also be specified. This program has been successfully applied (Sissenwine, Hess and Saila, 1974) and can be considered verified.

Model of Leendertse, Alexander and Liu (1973)

A quasi-three-dimensional model for estuaries and oceanic regions was developed by Leendertse, Alexander and Liu (1973) using numerical procedures similar to those developed for Leendertse's two-dimensional model described above. The model simulates three-dimensional variable density flow and salinity transport with a vertically layered computational structure.

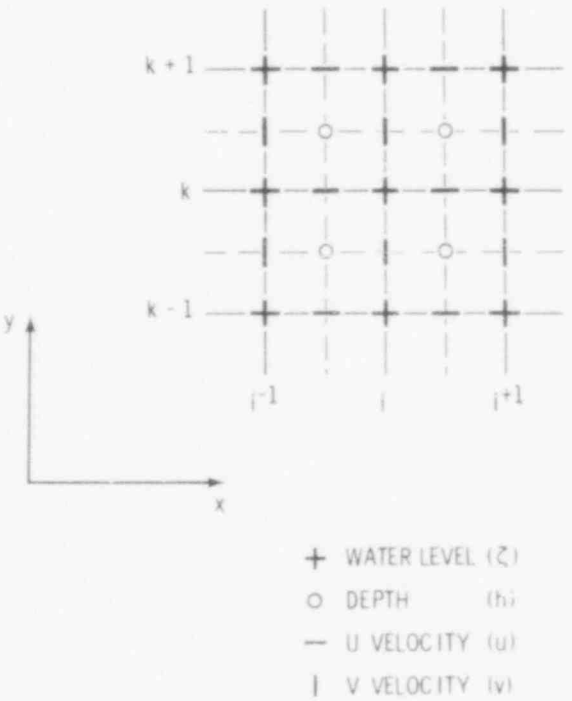

FIGURE 3.2. Space-Staggered Scheme

Figure 3.3, taken from Leendertse, Alexander and Liu (1973), shows a typical layout of the vertical grid. The horizontal grid is similar to the Leendertse two-dimensional model. The k^{th} layer has thickness h_k. The vertical arrangement of computational points is space-staggered in a fashion similar to the horizontal grid. Monitoring program designers should keep this in mind when matching monitoring stations with computation points.

The three-dimensional governing equations for mass and momentum, which are straightforward three-dimensional generalizations of those in the two-dimensional model, are integrated over the k^{th} layer for k = 0, 1, 2,..., b where b is the bottom layer. Conservation of salinity and temperature equations are also included in the model.

The boundary conditions which must be specified with monitoring data are

- water levels at open boundaries (at every half time step)
- boundary temperatures and salinities
- boundary velocity gradients.

Initial velocity, temperature and salinity distributions must also be specified.

The model has been applied to Chesapeake Bay with good results. A discussion of this application can be found in Leendertse, Alexander and Liu (1973). This discussion offers an operational guide to users who are unfamiliar with the model. Linear stability criteria, which are useful in obtaining stable calculations even for nonlinear equations, are also provided by Leendertse, Alexander and Liu (1975).

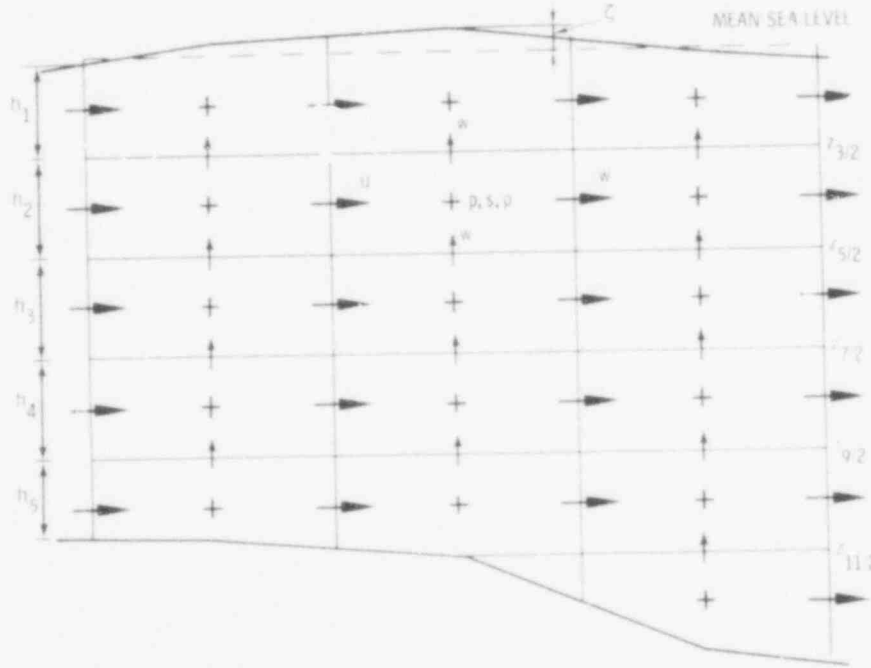

FIGURE 3.3. Location of Variables on the Vertical Grid
u = longitudinal velocity component
w = vertical velocity component
ρ = density of water
p = pressure
s = salinity
$Z_{K+1/2}$ = interference between k^{th} and $k+1^{st}$ layers

Vorticity Energy Code for Transport Analysis (VECTRA)[1]

A finite difference model was developed at PNL to numerically simulate a broad range of two-dimensional flow and heat transfer problems (Trent, 1973). The computation scheme is a finite difference approximation of the viscous, incompressible Navier-Stokes equations (given in vorticity-stream function form) and the First Law of Thermodynamics.

The code uses different numerical algorithms to solve transient and steady-state problems. The code is flexible and its capabilities include

- Cartesian or cylindrical coordinates
- user-specified geometry
- temperature-dependent transport properties
- multiply-connected flow regions in the solid
- transient or steady-state calculations
- user-specified hydrodynamic and thermal boundary conditions. Thermal boundaries can be constant-temperature, radiative, convective or insulated. Hydrodynamic boundary velocities can be of the no-slip, free-slip, specified or calculated type.

All these options can be implemented from the code input, therefore requiring a large amount of input data.

In addition to program control parameters, the input data includes characterization of the region to be modeled, including location of nodes, types of cells (boundary, internal), interconnectivity of regions and physical characteristics such as thermal conductivity, density and diffusivity. The initial ambient and inflow conditions such as velocity, pressure, temperature, eddy viscosity for each cell, and the Prandl number must also be specified. Boundary conditions of velocity and temperature must also be given. The user may also specify the relaxation parameters for the numerical solution. The output can be printed tables and/or computer plots of velocity and temperature distributions in the region.

One important feature of the model is that the momentum may or may not be coupled to the energy equation by buoyancy, depending on the physical problem and the desires of the user. Because of the flexibility of the code, the applications are not limited to thermal plume transport. The VECTRA code calculations have been compared with experimental and analytical results. The model has also been applied to predict the thermal plume transport from the South Bay Power Plant, San Diego and the airborne thermal plume from the dry cooling towers at Wyodak Power Plant in Wyoming (Onishi, 1976; Onishi and Trent, 1976).

---

[1] The version discussed below is substantially improved from the version reported in Trent (1973).

RMA - Finite Element Model (Norton, King and Orlob, 1973)

This two-dimensional hydrodynamic and transport model was developed by W. R. Norton and I. P. King of Water Resources Engineers, Inc. (Norton, King and Orlob, 1973). The model starts with the typical continuity relationship, equations of momentum in the x, y, and z directions, and the convection-diffusion equation with wind stress, bottom stress and Coriolis effects included in the momentum equations. The model equations are solved numerically using the finite element method with quadratic elements. The finite element formulation was based on Galerkin's method of weighted residuals.

Before the system can be stimulated, it must be approximated by an appropriate finite element network. Proper network layout is essential. The network should include major characteristics of the region, but must have as few corners as possible. The preprocessor RMA-I can be used to represent the network and to calculate various element properties. The coordinates of the element corner nodes, the depth at the nodes, the turbulent exchange coefficients and Chezy coefficients for each element must be specified as input to RMA-II.

The input requirements also include average latitude of the water body, average water surface elevation and factors for scaling the x and y coordinates. These scaling factors can be used to convert the coordinate position given in the input to the true coordinates. All boundary conditions must be specified. These may include velocity values, head values or a specification that flow may only occur parallel to the boundary. Velocity values must be specified at the upstream edge and head values at the downstream edge. If wind stress is included in the formulation, then wind data must also be supplied. If a dynamic solution is desired, then dynamic boundary conditions and length of simulation must also be given. An option exists for restarting the dynamic simulation from the previous output. These data can be stored at the end of the dynamic simulation if specified by the user.

The input for this option consists of nodal numbers along lines across the flow. The output consists of velocity, depth and head values at each node. In addition, an option exists for checking mass conservation along predetermined points in the system. The output compares computed valuables for x and y velocity and mass flux with the input data to determine mass conservation.

The RMA model has mostly been applied to dynamic water quality predictions such as those for St. Pablo Bay and Suisun Bay (King and Norton, 1978) in California and the Snake River in Washington (Norton, King and Orlob, 1973). Steady-state analysis of a thermal discharge to Johnsonville Reservoir for a Tennessee Valley Authority power plant was also performed (Orlob, King and Norton, 1975).

HYDRODYNAMIC/WATER QUALITY MODELS

The models of Leendertse (1970) and Dailey and Harleman (1972) and the Battelle model EXPLORE-I (Battelle, 1974) each have both hydrodynamic and

water quality components. In Leendertse's model, the hydrodynamic treatment is quite general for a two-dimensional code and is essentially the same as the hydrodynamic component of Leendertse's two-dimensional model (i.e., Leendertse, 1967). The water quality equations in Leendertse (1970) are general advection-diffusion equations. The model of Dailey and Harleman has essentially the same level of generality as Leendertse's except for being one-dimensional. The EXPLORE-I model has a simplified two-dimensional treatment of the hydrodynamics and a lumped parameter (no spatial variation) version of water quality dynamics.

Leendertse (1970)

Leendertse has generalized his two-dimensional model (Leendertse, 1967) to simulate the transport of constituents by two-dimensional (horizontal-longitudinal) advection and diffusion. This model (Leendertse, 1970) is applicable to well-mixed estuaries and coastal seas. For such water bodies, the mass balance equation for an arbituary substance A with a vertically averaged mass concentration P is

$$\frac{\partial(HP)}{\partial t} + \frac{\partial(HUP)}{\partial x} + \frac{\partial(HVP)}{\partial y} - R = \frac{\partial\left(HD_x \frac{\partial P}{\partial x}\right)}{\partial x} + \frac{\left(HD_y \frac{\partial P}{\partial y}\right)}{\partial y}$$

where

$$P = \frac{1}{H}\int_{-h}^{\zeta} A\,dz, \qquad H = h + \zeta$$

D_x, D_y are dispersion coefficients
R includes local addition of substances and the rate of production of the substance in a water column with unit dimension
P = vertically averaged mass concentration
A = mass density of substance A
h = undisturbed water depth
ζ = water surface elevation
U = vertical averaged x component of velocity
V = vertical averaged y component of velocity
Z = vertical coordinate.

The solution scheme for these transport equations is a finite difference method very much like that used in the two-dimensional model. The hydrodynamic boundary and initial conditions to be specified by monitoring data are also the same as in the two-dimensional model.

In addition to water levels on the open boundaries needed to drive the hydrodynamic portion of the model, constituent concentrations (and sometimes

concentration gradients) are also required on open boundaries for the water quality model.

This model was applied successfully at Jamaica Bay, New York (Leendertse, 1970), where it predicted the coliform distribution in the bay caused by storm runoff (Leendertse, 1970). To give an indication of the monitoring data used in this application, the following input data were required to operate the model:

1) Water levels and mass densities at the mouth of the bay
2) Discharges at the location of the outfalls of treatment plants and the combined sewer overflows
3) Mass densities associated with these discharges.

Dailey and Harleman (1972)

The most sophisticated one-dimensional hydrodynamic and water quality model reviewed was that of Dailey and Harleman (1972). This model incorporates a solution of the dynamic one-dimensional (longitudinal) momentum and full advection-diffusion equations. These governing equations are solved along a network of branched and looped one-dimensional channels using the finite element method.

The advection-diffusion equation is solved in the form

$$\frac{\partial}{\partial t}(Ac) + \frac{\partial}{\partial x}(Qc) = \frac{\partial}{\partial x}\left(AE\frac{\partial c}{\partial x}\right) + \left(\frac{r_i}{\rho} + \frac{r_e}{\rho}\right) A$$

where

c = concentration of constituent
A = channel cross-sectional area
Q = tidal discharge
E = longitudinal dispersion coefficient in tidal time
ρ = density of water
r_i = time rate of internal addition of mass per unit volume by generation of substance within the fluid
r_e = time rate of external addition of mass per unit volume by generation of substance within the fluid
t = time.

The constituents treated by this equation are salinity, temperature, biochemical oxygen demand (BOD) and dissolved oxygen (DO). The reaction terms, r_i and r_e, depend upon the constituent considered. They are zero for conservative substances. The nonconservative constituents are often modeled with first order kinetics.

Tidal motions are given by the following longitudinal momentum equation with a hydrostatic pressure contribution.

$$\frac{\partial}{\partial t}(AU) + \frac{\partial}{\partial x}(QU) = -Ag\left(\frac{\partial z}{\partial x} + \frac{U|U|}{C_z^2 R_h}\right)$$

where

Q = discharge
A = cross-sectional area
U = cross-sectional average velocity = Q/A
g = acceleration of gravity
C_z = Chezy coefficient
R_h = hydraulic radius
t = time.

In the finite element method employed, linear variation of the equation terms over the elements are preferred over higher polynominal variations in the interest of simplicity and physical interpretability.

The boundary and initial conditions are of the hydraulic and constituent types. The initial conditions of both types are commonly estimated roughly and the simulation is started far enough in advance that the starting transient has disappeared. Values of initial velocities, constituent concentrations and water levels must be assigned. Hydraulic boundary conditions are

- water levels as a function of time on the ocean boundary
- zero discharge assignment at the head of tide
- fresh water inflow entered as a lateral inflow.

The constituent boundary conditions are specified as boundary concentrations, dispersive and advective mass flux. A user's guide should be consulted for recommended representations of these fluxes.

It should be noted that no Coriolis or channel curvature effects are accounted for in this model. Nonprismatic channel effects may be included, however.

The model has yielded useful results in applications at Cork Harbor, Ireland and the James River in Virginia (Daily and Harleman, 1972). The present model is an improvement of earlier models of Lee and Harleman (1969) and Thatcher and Harleman (1972).

EXPLORE-I (1974)

The EXPLORE-I model (Battelle, 1974) is a one-dimensional hydraulic and water quality model in a network system of channels and junctions characterizing the geometry of the water body. Thus, the two-dimensional character of a water body can be simulated even though the model equations are one-dimensional.

The EXPLORE-I hydraulic simulation program uses a modified form of the Saint-Venant equations to model the two-dimensional flow in an estuary or the one-dimensional flow in a river system. The system to be simulated is geometrically represented by a computational grid network. Using a simple routing concept, the flow in the system is prescribed along paths designated by channels connected by junctions. Each junction is characterized by its surface area, water surface elevation, bottom elevation and the actual (x,y) coordinates. Surface areas are computed from those polygons formed by the perpendicular bisectors of channels in the network. Water flows between these junctions through rectangular channels connecting them. Each channel is described by length, width, Manning coefficient and average bottom elevation at the midpoint. Figure 3.4 illustrates the channel-junction configuration.

In the numerical solution scheme, the Saint-Venant equations are not solved simultaneously for all points in the water system. Instead, the equation of motion is solved for each of the channels in the system on the basis of present values of the junction heads.

Momentum is described by

$$\frac{\partial V}{\partial t} = - V\frac{\partial V}{\partial x} - g\frac{\partial H}{\partial x} - gS_f + gS_w$$

where

V = velocity
H = water surface elevation measured from the datum plane

S_w = wind stress = $\frac{K}{d}\ \frac{\rho a}{g\rho_w}\ U^2 \cos X$

S_f = resistance slope
K = dimensionless coefficient with a value of 0.0026
d = depth of flow
$\rho a, \rho$ = air and water densities
U = wind velocity
X = angle between the wind direction and its axis of the channel
g = gravitational acceleration
t = time.

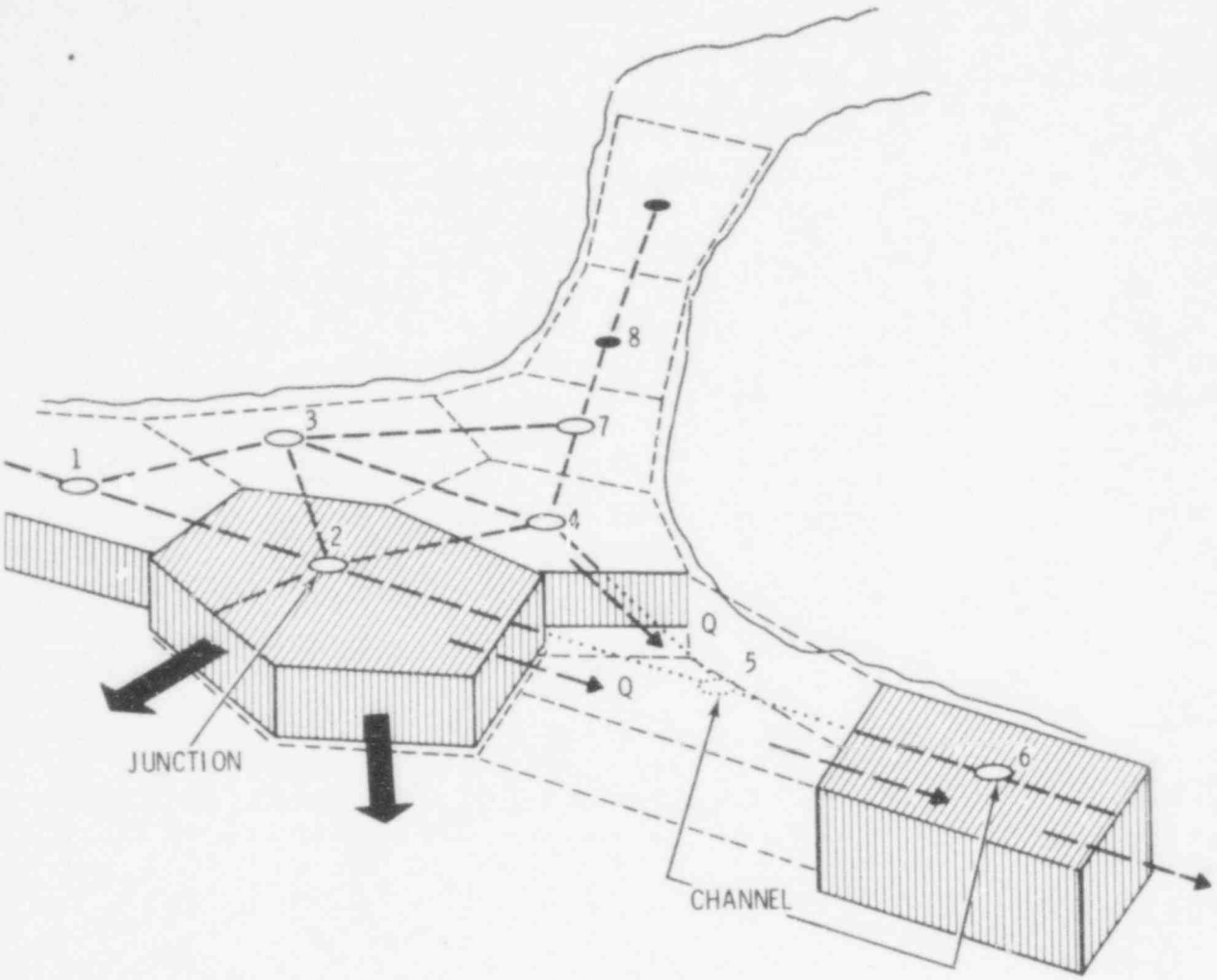

FIGURE 3.4. Channel-Junction Definition for Computational Mesh

The velocity and flow in each of the channels is thus determined. The equation of continuity is solved at each of the junctions on the basis of predicted flows in each of the channels.

Continuity is described by

$$A_{sj} \frac{\partial H_j}{\partial t} = \sum_{i=1}^{k} Q_i + Q_j^{im} - Q_j^{ex} - Q_j^{ev}$$

where

A_{sj} = surface area associated with the junction j
H_j = water surface elevation in the jth channel
Q_i = flow of a connecting channel
$Q_j^{im}, Q_j^{ex}, Q_j^{ev}$ = water import, export and evaporation rates at the junction
k = number of channels connected to the jth junction
t = time.

The numerical integration technique employed in the hydraulic model uses a space- and time-staggered scheme based on a simple Runge-Kutta approximation. The constituents simulated in the water quality model are as follows:

1) Benthic oxygen demand
2) Sedimentary phosphorus
3) Soluble phosphorus
4) Organic phosphorus
5) Carbonaceous BOD
6) Nitrogenous BOD
7) Refractory organic carbon
8) Total organic carbon
9) Ammonia nitrogen
10) Nitrite nitrogen
11) Nitrate nitrogen
12) Organic nitrogen
13) Toxic compounds
14) Phytoplankton
15) Zooplankton
16) Dissolved oxygen.

The hydraulic code of EXPLORE-I requires that channel roughness, which can vary from channel to channel, be entered as Manning's "n" value. Initial values of velocity must be specified for each channel; they are usually set equal to zero. Constant inflows or outflows can be specified at each node while time-varying inflows or outflows can be entered separately as a set of

discharges and times. The water quality code requires initial constituent concentrations at all nodes and boundary concentrations at boundary nodes. EXPLORE-I has been successfully applied at the James River, Virginia and Grays Harbor, Washington (Onishi and Wise, 1978; Battelle, 1974).

INTEGRAL THERMAL PLUME MODELS

The thermal plume models discussed below use the integral analysis modeling approach. The integral analysis is a macroscopic solution of the flow and temperature field. The precise shape of the lateral and vertical velocity and temperature profile are assumed. Assumptions on the mixing of ambient fluid into the jet and on the pressure field determine the entrainment function and drag formulations. Another common assumption made in modeling the jet regime by the integral method is that inertial forces dominate the buoyancy forces within the jet; therefore, density-induced pressure gradients can be neglected.

The principal difficulty with the integral technique is that the physical processes must be simulated artificially in the context of the presumed jet structure. This produces model parameters such as entrainment parameters and drag coefficients that may not be physically measurable. The Shirazi-Davis model (1974) avoids this problem by deriving the parameters from fitting the model to data. Nevertheless, the data sources are generally inadequate.

Stolzenbach-Harleman Integral Model (1971)

The Stolzenbach and Harleman model (1971) was developed from three-dimensional, time-averaged equations yielding mass, momentum and energy conservation for a turbulent, incompressible fluid. The model produces the near-field temperature distribution for surface discharges of heated water into lakes.

As with all integral models, this model addresses only the narrow zone of heated water along the jet trajectory; any flow outside this zone is ignored. Ambient currents interact with the plume primarily through deflection or bending of the plume. The model solution is based primarily on nonbuoyant jet theory with some modification of the coefficients such as the vertical entrainment and lateral spreading velocity to include buoyant effects. If buoyant effects on the ambient currents are too large, then some of the basic assumptions of the model are invalid and this model should not be used.

The near field is divided into four regions in which the basic model equations are solved. Three of these regions represent the zone of flow establishment where the velocity and temperature profiles are assumed to be uniform and have not mixed across the entire jet width. Boundary conditions are prescribed for these regions to arrive at a proper interface velocity and temperature for the fully mixed region or established zone (the fourth region).

The basic solution technique is to assume profiles for the lateral and vertical velocity, temperature distributions in each of the four regions and

boundary conditions on the outer edges of the four regions. The assumed temperature and velocity profiles are called similarity functions. The equations are then integrated perpendicular to the discharge centerline to eliminate turbulent terms. After integration, the equations are scaled by various dimensionless parameters and small terms eliminated. The original equations have thus been reduced to a series of simultaneous one-dimensional ordinary differential equations which are solved numerically by using a fourth order Runge-Kutta routine. The solution gives the centerline temperature and velocity distribution of the plume. Temperature and velocity at other points in the plume can be found from the appropriate similarity functions for that region.

In those cases having a cross-flow in the ambient water body, a plume-bending equation and a new set of coordinates centered on the axis of the plume are employed. The plume-bending equation is formulated only for bending due to "entrainment" by the cross-flow and does not include external forces such as wind acting on the surface or drag of ambient current.

The input data required to run the program consist of the dimensionless quantities used in scaling the integrated equations. These are 1) initial densimetric Froude number, 2) aspect ratio between the length and height of the rectangular open channel through which the plume is discharged, 3) surface heat loss parameters, 4) a series of parameters to specify termination criteria and error criteria and 5) the vector of cross-flow velocities.

Although this model has been applied to predicting the thermal plume resulting from operation of the Pilgrim Nuclear Power Plant in Massachusetts, the restrictions on the use of the model resulting from satisfaction of the many model assumptions make the model of limited value in real-world applications (Dunn et al., 1975). These limitations include 1) rectangular channel outfall structure, 2) infinite water boundaries in all directions, 3) homogeneous, uniform and steady-state ambient and outfall conditions, 4) absence of wind momentum imparted to the plume and 5) cross-flow velocity of less than 10% of the outfall velocity. Also, Dunn et al. (1975), in examining various thermal plume models, discovered that for many combinations of Froude number and ambient cross-flow velocities, singularities in the solution technique occur. Jet width and temperature predictions do not match, and the length of the stable region (zone of flow establishment) is predicted to be much longer than experimental evidence suggests. They recommended that this model not be used where the various model assumptions are not met, and that even for those few cases where the model assumptions may be approximated, anomalies in the solutions should be examined.

Prych Integral Model (1972)

The Prych three-dimensional model (1972) is based on the same conceptual framework as the Stolzenbach-Harleman integral model discussed previously. This model, however, represents an increased effort to include phenomena considered alien to jet diffusion in the integral equations. Among these phenomena is the addition of the effects of ambient turbulence in the mass flux equations. The momentum flux equation includes buoyant forces, shear forces

between ambient and jet fluids, drag forces caused by any cross-flow and entrainment of ambient momentum. The heat flux equation includes surface heat loss. The formulation of the similarity functions for temperature and velocity uses exponential functions to describe the lateral and vertical decay instead of the polynomial functions used by Stolzenbach and Harleman (1971). The solution to the model equations yields explicit formulations for the derivatives of the dependent variables in contrast to the set of equations developed for the Stolzenbach and Harleman model. In that case, the derivatives must be derived numerically by solving the set of simultaneous equations.

Treatment of the zone of flow establishment is substantially different from treatment in the Stolzenbach-Harleman Integral Model. The velocity and temperature values at the end of this zone provide the initial conditions for the established zone. In the Stolzenbach-Harleman model this zone was divided into three regions. The temperature and velocity distributions were derived for each region from the equation solutions. Prych treats this zone as a control volume and solves the mass, momentum and energy balance for the conditions at the interface with the established zone. No distribution of temperature or velocity within this zone is considered. Dunn et al. (1975) felt that the formulation was inadequate because 1) numerous assumptions are questionable and based on little or no data, such as the amount of dilution and the amount of lateral spreading in this zone and 2) the flow establishment length is based on nonbuoyant jet theory and is, therefore, inadequate.

The required input to the model is

1) basic ambient and outfall parameters
2) E_o--entrainment coefficient for 2-D uniform-density jet flow
3) E_h--multiplier for horizontal ambient turbulent diffusion coefficient
4) E_v--multiplier for vertical ambient turbulent diffusion coefficient
5) K--heat transfer coefficient
6) C_D--Empirical drag coefficient
7) C_F--coefficient of interfacial shear.

Output consists of the centerline velocity and temperature distribution in the established zone. From the output, the velocity and temperature at any point in the plume can be calculated based on the similarity functions.

The output from this model has been compared with two sets of data (Dunn, Policastro and Paddock, 1975). The first set consisted of two hydraulic model experiments carried out by Stolzenbach and Harleman (1971) for a rectangular heated jet into a deep basin, and the second set of data was for the hydraulic model for Oskarshamnsverket. In neither case did the comparison indicate agreement. Centerline temperature decay predictions were good, but plume width and thickness predictions were not correct.

A comparison of various thermal plume models by Dunn, Policastro and Paddock (1975) indicate that although this model is an improvement over the

Stolzenbach and Harleman model, its applicability is limited, especially with regard to the zone of flow establishment calculations.

Shirazi-Davis Integral Model (1974)

Shirazi and Davis (1974) assimilated all available laboratory and field data and used it to modify and calibrate the Prych integral model. The model formulations were modified slightly, notably in the buoyant spreading, making the model more sensitive to the key model parameters and thus easier to fit to the data. Shirazi and Davis also calibrated the modified Prych model.

Shirazi (1973a,b) discussed the various applicable laboratory and field data available at that time. The data was insufficiently refined to determine explicitly the trend of plume changes with each parameter. Furthermore, the data appeared inconsistent and widely varying. This diversity among the data and the absence of information on such factors as turbulence levels generally inhibited the development of a universal correlation. Correlation parameters were determined by multivariable regression analysis for individual data sets and for various combinations of data. The range in correlation parameters wa very large and a consistent procedure for combining data sets was not found.

Shirazi and Davis made two major changes and three additions to Prych's model. The basic assumption that spreading of the plume caused by buoyancy can be analyzed by considering the notion of a density wedge was retained. However, the velocity of the wedge was changed to

$$c = c_1 \sqrt{\frac{\rho}{\rho_o} g d} \qquad \frac{H}{B}$$

from

$$c = c_1 \sqrt{\frac{P}{\rho_o} g d}$$

where

c = celerity of spreading wedge
c_1 = numerical constant (1.01)
ρ = local density
ρ_o = discharge density
g = gravitational acceleration
d = characteristic depth of plume
H = characteristic depth of jet
B = local width of jet
P = kinematic pressure.

The rationale for this change came from an analysis by Koh and Fan (1970). The formulation of the zone of flow establishment length was modified to indicate densimetric Froude number effects. The formula for this length is now

$$S_1 = 5.4\ H_o\ (A^2/F_o)^{1/3}$$

where

S_1 = zone of flow establishment length
H_o = depth of discharge channel
A = aspect ratio
F_o = initial densimetric Froude number.

This change was based on a number of experiments carried out by EPA's Pacific Northwest Environmental Research Laboratory (Shirazi and Davis, 1974). Shirazi and Davis also improved the algorithm for integrating isotherm areas and added time-temperature calculations to determine the temperature history that an organism would encounter while passing the plant cooling system. To bypass the singularities that occur in the solution technique, an extrapolation method was developed. This extrapolation technique must be used with caution since it is not based on conservation laws and probably does not satisfy them.

The model contains four undetermined coefficients. These are the entrainment coefficient E_o, turbulent exchange coefficients E_h and E_v and a coefficient occurring in the bouyant layer spreading function, XKI. Each of these parameters was determined by fitting the model to various sets of data. Difficulties arose with this method because of the lack of data, and the wide variation in what data there were. Also, since the parameters of the model were fitted one at a time, the interactions of parameters with one another were not considered.

To operate the program very few input data are required since many of the parameters are computed internally as mentioned above. The characteristics of the discharge, including temperature, angle, channel structure volume and the ambient water body characteristics such as water temperature and velocity must be given.

Model predictions using the calibrated parameters were compared with different data sources. Both centerline temperature decay and width predictions appear to be in agreement. Thus, the model has in effect been validated for those cases. Shirazi and Davis (1974) then proceeded to compile a workbook of the model predictions which would permit the user to make calculations of centerline temperature and plume width without actually running the program. For this reason, this model has received wide application, including numerous applications to power plants.

CONSTITUENT/SEDIMENT TRANSPORT MODELS

The following pure transport models do not calculate the flow field which provides the mechanism for advective transport of constituents. Both models require velocity data as input. These data must be supplied by an associated monitoring program, or as the output of a suitable hydrodynamic model. The first model discussed in this section is a finite element transport model (FETRA--Onishi, 1977b) which simulates the movement of particulate sediments as well as dissolved constituents represented by the usual advection-diffusion equations. This model is suitable for simulating the transport of sediment-bound radionuclides and other hazardous contaminants. The second model is the Discrete Parcel Random Walk (DPRW--Ahlstrom et al., 1977) based upon the random walk nature of the diffusion process. The numerical scheme appeals to this fact and does not deal directly with the governing differential equations.

Finite Element Transport (FETRA) Model (Onishi, 1977a, b)

The most advanced model for the simulation of radionuclide transport in estuaries and coastal areas is the FETRA model of Onishi (1977a, b). The FETRA code is a transient (and steady), two-dimensional, sediment-contaminant transport model utilizing the finite element computation method with the Galerkin weighted residual technique. The model has general convection-diffusion equations with decay and sink/source terms with appropriate boundary conditions. It consists of three submodels joined to include the mechanisms of sediment-contaminant interaction. The submodels are a sediment transport model, a dissolved contaminant transport model and a particulate contaminant (contaminants absorbed by sediment) transport model. Transport of sediment and particulate contaminant is simulated for each sediment size within each sediment type. The modeling procedure for FETRA involves simulating the transport of sediments. The results are then utilized to simulate dissolved and particulate contaminants by including interaction with the sediments. Finally, changes in river and clean bed conditions are calculated. These include river and ocean bottom elevation change, distributions of each sediment component in the bed and distribution of contaminants in the bed. The input data needed to operate the FETRA code are as follows:

1) The velocities at computation points for each time step
2) Concentration and/or concentration gradients
3) Initial concentrations
4) Erodability coefficients
5) Size fractions of suspended sediment
6) Critical shear stress for scouring and deposition
7) Sediment fall velocity
8) Density of sand, silt and clay.

In the implementation of the finite element method, triangular elements are used with six nodes associated with each element. Quadratic approximations are made within each element. Velocity data are input only for the corner nodes.

The model was applied to the James River estuary to determine the longitudinal movement of sediment and migration of the pesticide, Kepone, in both dissolved and particulate forms, under unsteady estuary flow conditions (Onishi, 1977a; Onishi and Wise, 1978). Sediment transport modeling was conducted for cohesive and noncohesive sediments and for organic matter. Computer analysis of sediment, dissolved and particulate Kepone distributions agreed with field data, confirming the validity of the model. The model also calculated the scour and deposition of sediment and Kepone in the James River.

Discrete Parcel Random Walk (DPRW) Transport Model, Coastal Effluents Version (Ahlstrom et al., 1977)

The DPRW transport model was developed at Battelle, Pacific Northwest Laboratories to simulate the transport of radionuclides in groundwaters. Experimentation with several numerical methods of addressing temporal and spatial resolution and transport simulation problems led to the selection of the DPRW method. This method has significant advantages over traditional finite element and finite difference numerical techniques for certain applications. In the DPRW approach, an initial distribution of point masses is allowed to be advected with the specified flow field and allowed to follow random walk approximations of the diffusion process. The DPRW computational scheme is absolutely stable in time and completely mass-conservative. This means that there are no time step restrictions per se, or fictitious mass gains or losses. The accuracy of the method has been shown to increase as the square of the number of particles simulated. Therefore, it is very expensive to obtain highly accurate results.

The coastal effluent version of the code was developed to model the transport of chemical, thermal and biologic effluents in surface waters. It can simulate the transport of 24 separate constituents, each having its own characteristics. The transport is not tied to any grid. However, velocity data are interpolated from values on a nonuniform rectangular grid. The boundaries of the simulated region may be much more complex than the velocity grid. It should be understood that the flow field is still only resolved on the rectangular grid and does not necessarily represent the detailed boundaries of the transport simulation.

The method is particularly well suited for passive transport of conservative constituents where incremental differences in concentration are to be evaluated. In this case, the complete history of each particle may be computed and recorded as being independent of other particles. If, on the other hand, interactions depend on the entire ensemble, then all particles must be traced to a given time plane before proceeding to the next time.

The model may be operated in a one-, two- or three-dimensional (vertically layered) manner. Vertical layer thicknesses are laterally constant unless the bottom is encountered and then bottom contours are followed. Bathymetric information for the entire water body is, therefore, input to the model. Each layer may be different in characteristic depth. Up to nine vertical layers are

permitted. The parcels simulating effluent masses may be dispersed horizontally and vertically. Dispersion coefficients, analagous to those determined from mean free path considerations in gases, are required in each dimension and may be functions of position. Settling and buoyancy velocities can also be input for the parcels. Dispersion coefficients can also be a function of velocity in all three directions.

Sources and sinks are entered as particles per unit time. A source velocity field may be entered and may be superimposed over any other velocity field input. As with all transport models, the velocity field must be available to drive the advective portion of the transport. It may be input at all grid points or a superposition of basic currents (assumed the same everywhere but varying in time). Discharge or wind-induced flows can also be employed. An initial distribution of constituent concentration can be input. This concentration is immediately converted to a distribution of mass parcels for subsequent calculations. Four types of boundary conditions are available. The parcel may either be reflected, destroyed, immobilized or partially immobilized. These conditions imply the characteristics of the boundary and of the constituent. A reflecting boundary causes a totally suspended passive constituent or parcel to bounce back into the water after encountering a solid boundary. A destructive boundary is a flow boundary where the constituent leaves the system. An immobile boundary is one in which the constituent remains attached to and impacts the boundary. A partially immobile boundary is one which both reflects and immobilizes in different degrees as specified by the user.

Surface exchange coefficients can function as input for each constituent. Wind speed effects can also be used to influence transport of surface contaminants.

The results of simulation necessarily have considerable variance. Variance is a natural and unavoidable characteristic of modeling and several smoothing techniques are available for its reduction.

The code has been verified primarily by comparison to analytical solutions. Because the numerical technique is direct, no other comparative tests are appropriate except comparison with field data. Model results were compared with infrared overflight data for the San Onofre Generating Station Unit One thermal plume (Ahlstrom et al., 1977). Field data for November 15, 1972 was used as calibration (Ahlstrom et al., 1977). Excellent agreement was obtained. Data gathered by a different contractor nearly four years later (August 4, 1976) was compared to model predictions with no adjustment to the model. Satisfactory agreement was obtained. The model was subsequently used to predict the nutrient and suspended particulate distributions in the region of the outfall.

Although density of the parcels may be treated in the model, there can be no coupling between the hydrodynamics and the effluent constituents. The model does treat nonlinear reactions between constituents, but the speed of the simulation is adversely affected.

The simulation technique is not restricted in time step, although the resolution of movement by the flow field essentially limits the time step. Simulation of advective transport beyond more than one or two flow field grid points during a single time step compromises the value of an accurate flow field. The model can serve equally well in near-field and far-field applications. However, because the model does not provide for coupling to the hydrodynamics, it will be most applicable in the far field.

MODEL APPLICATIONS

As indicated earlier, Leendertse's and RMA's models suggest ways of collecting data to guarantee adequate model performance for monitoring program designs. The effects of data quality and abundance on model performance are sometimes subtle and there can be no substitute for actual model applications for detecting them. One of the most evident and important model performance parameters which can be influenced by the regional discretization and corresponding data collection plan is mass conservation through the computational scheme.

Because of the need to represent the water body by a discrete number of computational points and to restrict computation methods to satisfy certain boundary values, the governing equations (now in discretized form) cannot always be satisfied throughout the water body. The errors incurred by not completely satisfying the governing equations may not be serious, depending on the application. If the application is such that the flow-field is of more or less qualitative value, then such errors are of little concern, provided they are within about 15% of the true value. If the flow field is to be used to drive a transport-type model (contaminant, salt, energy, water quality, sediment, or any other model which essentially solves the advection-diffusion equations of continuity), then the computational accuracy of the model is far more critical. An error of 10 to 15% in satisfaction of flow field continuity can have disastrous effects when trying to model pollutant transport and fate. It is not difficult to imagine what might happen to pollutant concentrations when 20% of the mass is lost in the locale of a pollutant discharge, particularly when the mass loss is continuous. Mass is not always lost by the computational scheme, however. Mass is almost always gained back at another location in the water body, further confounding the transport simulation.

APPLICATION OF THE LEENDERTSE MODEL

In this section the two-dimensional model of Leendertse (1967) was applied to the vicinity of the Surry Nuclear Power Plant on the James River in Virginia. The aim of this application was to elucidate some of the design requirements of a supporting monitoring program sufficient to insure adequate model performance. The aspect of performance which was most evidently affected by data quality and levels of resolution was the computational conservation of mass by the numerical scheme (SMASH Program). Five simulations (Table 3.1) were run to study conservation of mass of the SMASH Program. Depths, Chezy coefficients, channel geometry and cell size were varied in these five cases for comparative purposes. In the following paragraphs, comparisons between Cases I and II, Cases II and III, and Cases IV and V are made.

Cases I and II

Channel geometry, number of half time steps, initial water surface elevation and upper and lower boundary water level table values were set the same

TABLE 3.1. Summary of Cases

Case	Depth	Chezy Coefficients	Channel Geometry	
			Cell size, Meters	Grid
I	variable	variable	726	31 x 31
II	constant	constant	726	31 x 31
III	constant	constant	slightly different from above	
IV	constant	constant	363	30 x 50
V	constant	constant	726	15 x 25

for Cases I and II. The water depths and Chezy coefficients differed in the two cases. Case I water depths were determined by superimposing the 31 x 31 grid over a U.S. Coast and Geodetic Survey bathymetric chart and estimating the mean depth of each cell. Case II water depths were set at 6 m for all cells. This water depth is the approximate mean depth of the James River Estuary in the area of simulation. Chezy coefficients for Case I were calculated for each cell based on the following formulation:

$$C = \frac{r^{1/6}}{n}$$

where

C = Chezy coefficient
r = hydraulic radius
n = Manning roughness factor, set at 0.027.

Chezy coefficients for Case II were set at 50 for all cells.

Mass conservation calculations for Cases I and II were performed by computing cross-section discharges at a number of sections, then comparing them to the discharge at the upstream end of the simulation area. Since these two cases were run under steady-state conditions, the discharge at each section should be the same as that at the upstream section. Figure 3.5 is based on mass conservation calculations for Cases I and II. Discharges for 42 sections were calculated and compared to the discharge of Section 2. Percentages less than 100 caused a loss of mass and, conversely, percentages greater than 100 caused a gain in mass.

In Case I, in which the depth and Chezy coefficient were variable, there was a general loss of mass (average 7Δ). The greatest losses in mass occurred

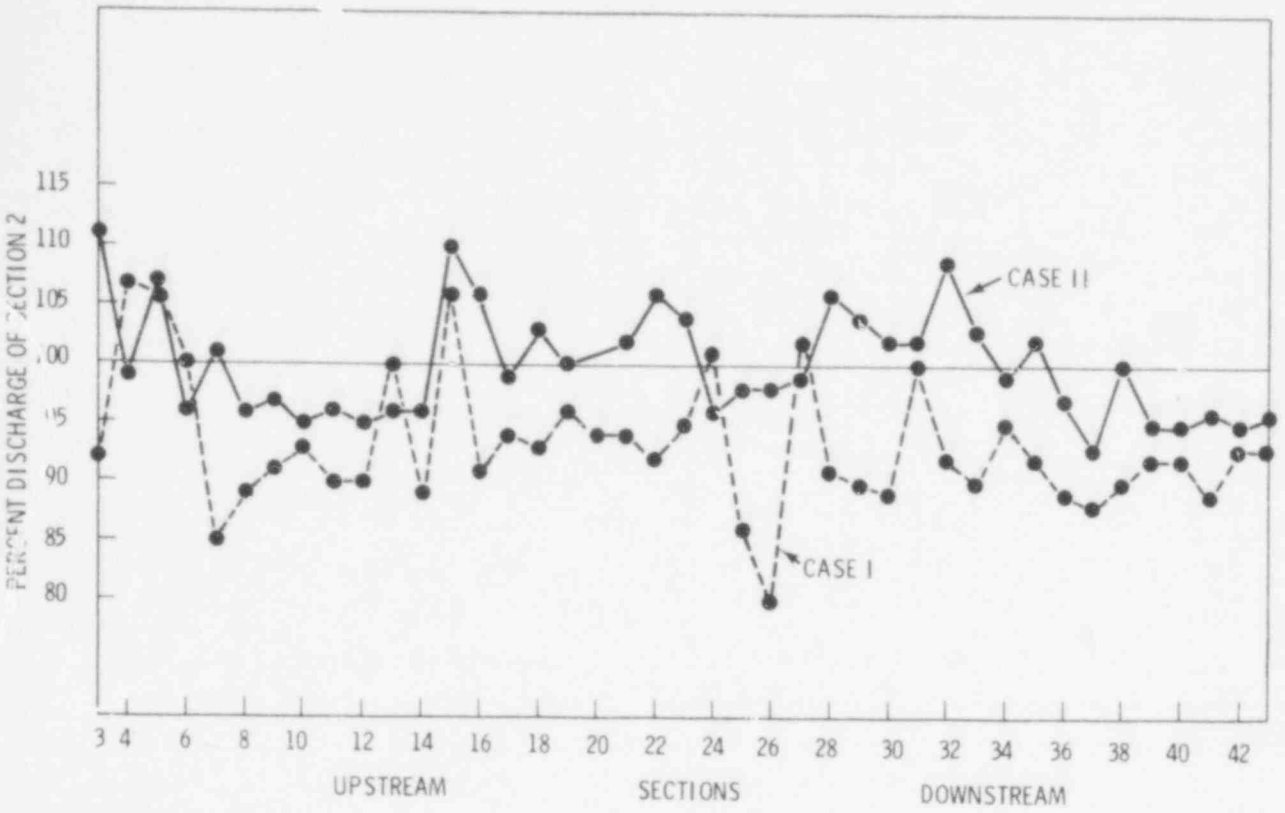

FIGURE 3.5. Leendertse's Model Simulations, Cases I and II

in sections where there was a large variation in depth across the section. Maximum losses (over 15%) of mass occurred at Sections 6 and 25.

In Case II, in which the depth and Chezy coefficient were constant, the loss or gain of mass varied less from section to section than in Case I. There was no average loss or gain in mass, although individual sections show losses or gains in mass of as much as 10%.

Cases II and III

Cases II and III are identical except that the geometry was changed slightly in Case III. The shaded cells in Figure 3.6 were changed from land cells to water cells in Case III to evaluate the change in conservation of mass with a slight change in geometry. As a result, the discharge throughout the simulated area increased as shown in Figure 3.7. A 3% increase in water surface area in Case III increased the discharge on an average of 14% over that of Case II. An increase in water surface area has a tendency to smooth it the water surface slope, as shown in Figure 3.8. The head (increase in water elevation over the mean depth) at the upper end of the simulation area, Sections 3 through 20, was significantly larger for Case III than Case II,

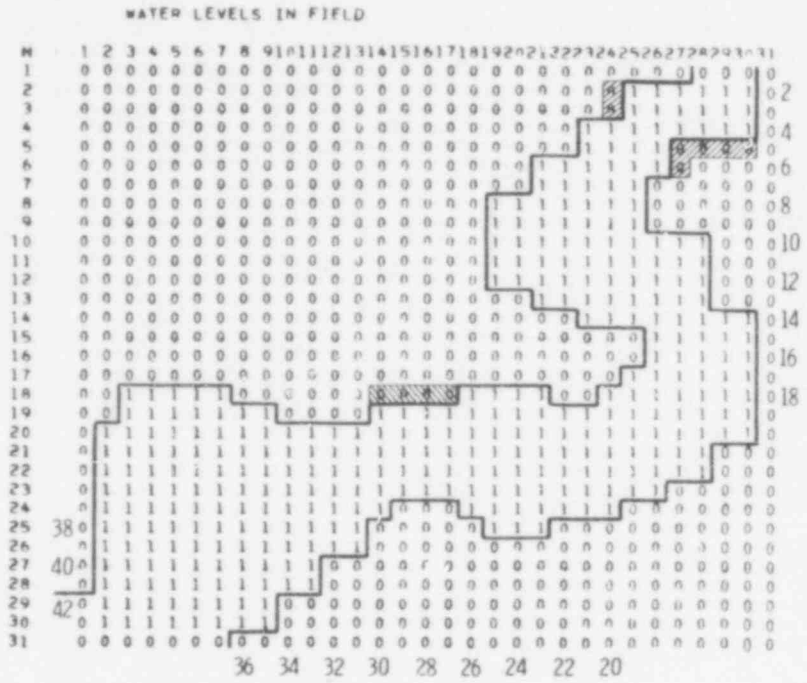

FIGURE 3.6. Computational Grid for Leendertse's Model Simulations, Case III

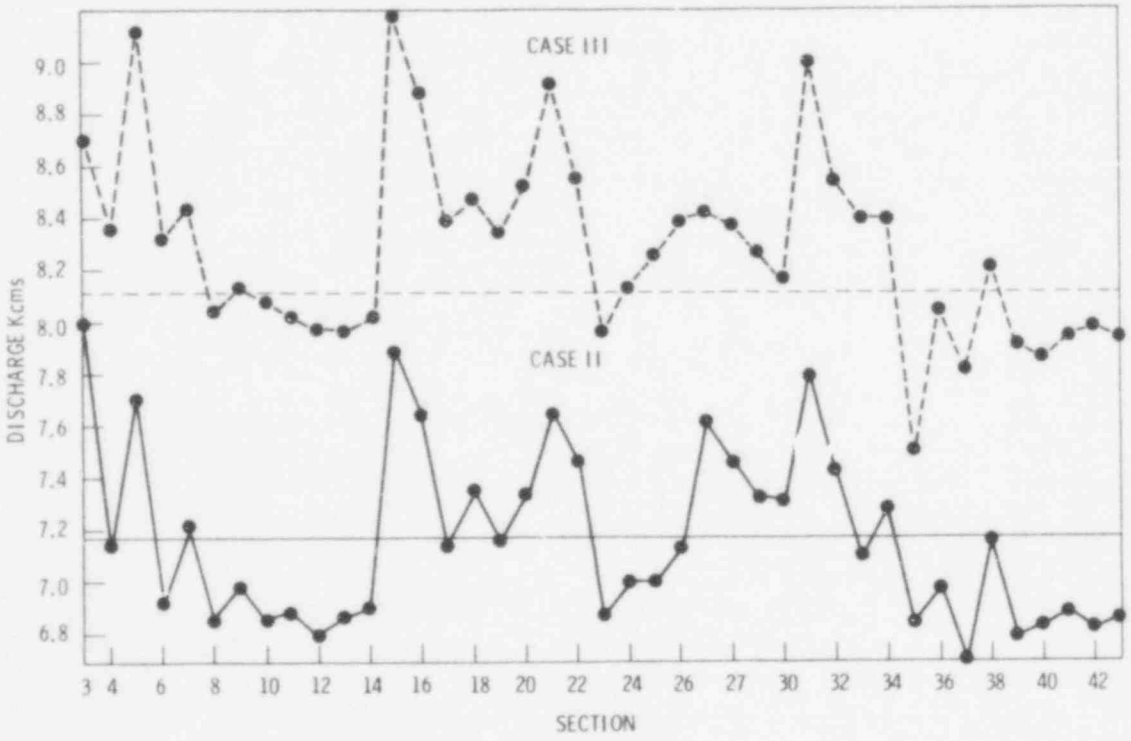

FIGURE 3.7. Leendertse's Model Simulations, Cases II and III

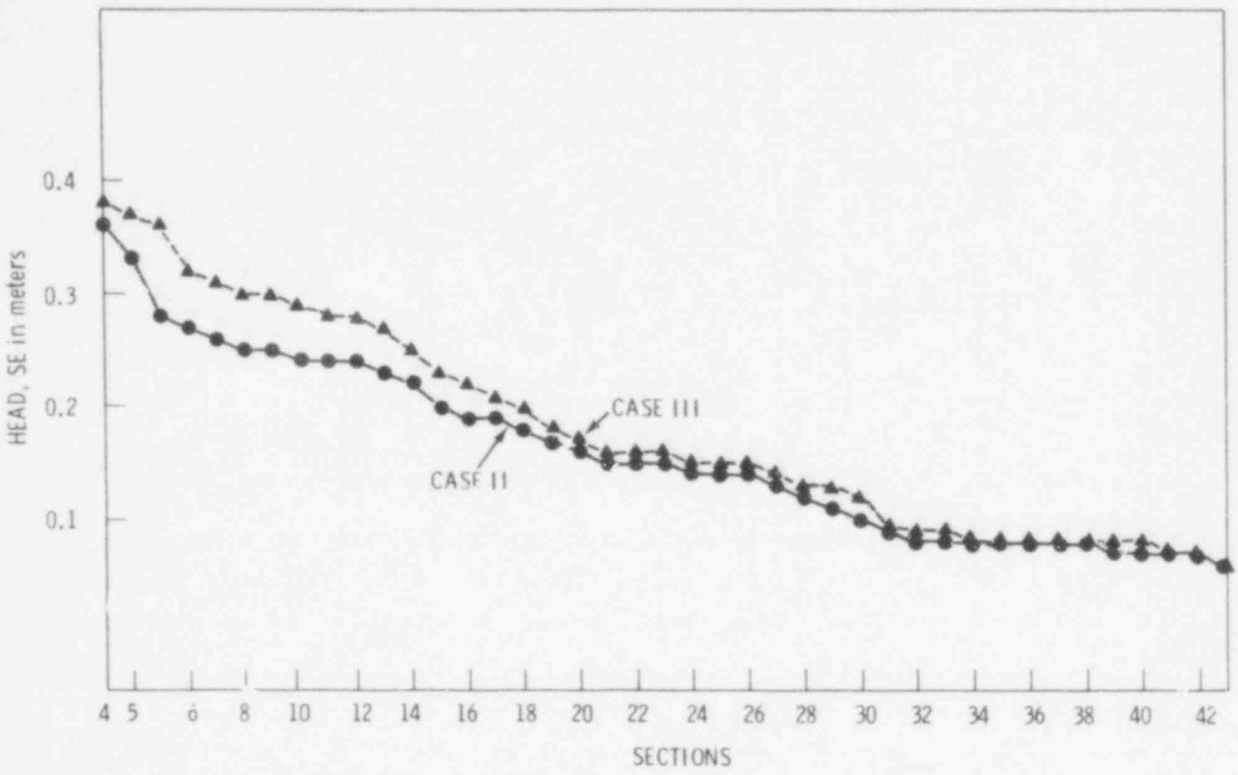

FIGURE 3.8. Water Levels for Leendertse's Model Simulations, Cases II and III

indicating that the narrowness of the channel near Section 4 of Case II was hindering the flow. By increasing the width from two to three cells, the restriction was partially removed.

Figure 3.9 compares mass conservation of Cases II and III. The two curves are very similar except that the Case III curve is offset upward as a result of an increase in the total discharge. In both cases, the discharges through downstream sections were within 90% of the discharge through the upper open boundary.

Cases IV and V

Cases IV and V evaluate the effect of changes in cell size on conservation of mass. These cases are run under identical conditions except for the cell size. Case IV cell size is 363 m and Case V cell size is 762 m, twice that of Case IV. The water surface, geometry, upper and lower boundary

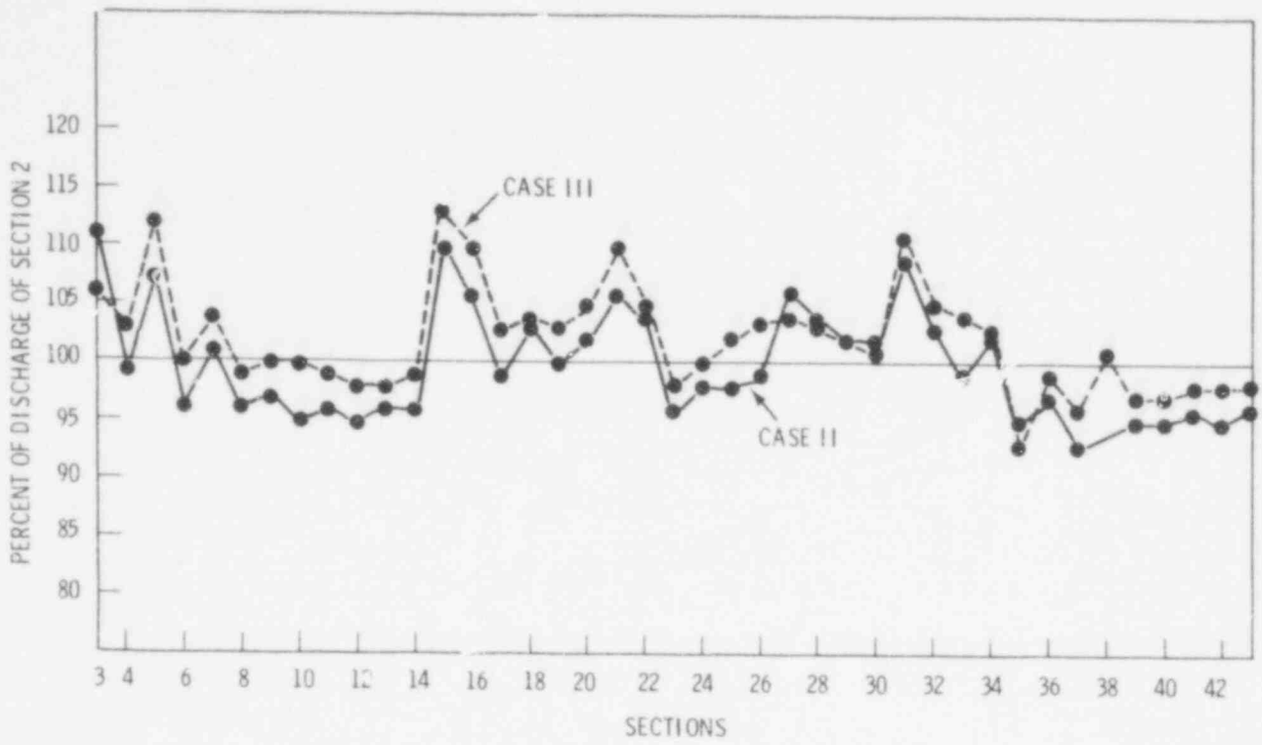

FIGURE 3.9. Mass Conservation in Leendertse's Model Simulations, Cases II and III

surface elevations, depths and Chezy coefficients are identical. Figures 3.10 and 3.11 show the grid setup for Cases IV and V, respectively.

Figure 3.12 is a comparison of discharges through comparable sections for Cases IV and V. Although the water surface area of the two cases is identical, Case IV has a significantly larger or smaller discharge as a result of the finer grid network. The discharges through sections are also less variable with the finer grid network (Case IV).

Comparison of conservation of mass of Cases IV and V is shown in Figure 3.13. In Case IV there is an overall gain in mass. Section 15 had the largest gain in mass of 9%. Case V is somewhat more variable with a maximum gain in mass of 11% and a maximum loss of 6%.

Summary of Conservation of Mass Tests

Comparisons of Cases I through V show that the SMASH Program is sensitive to changes in depths, geometry and cell size. Generally, less mass is conserved with large fluctuations in depth and with constructions of complex geometry in the flow channel. Conservation of mass improves with a finer grid

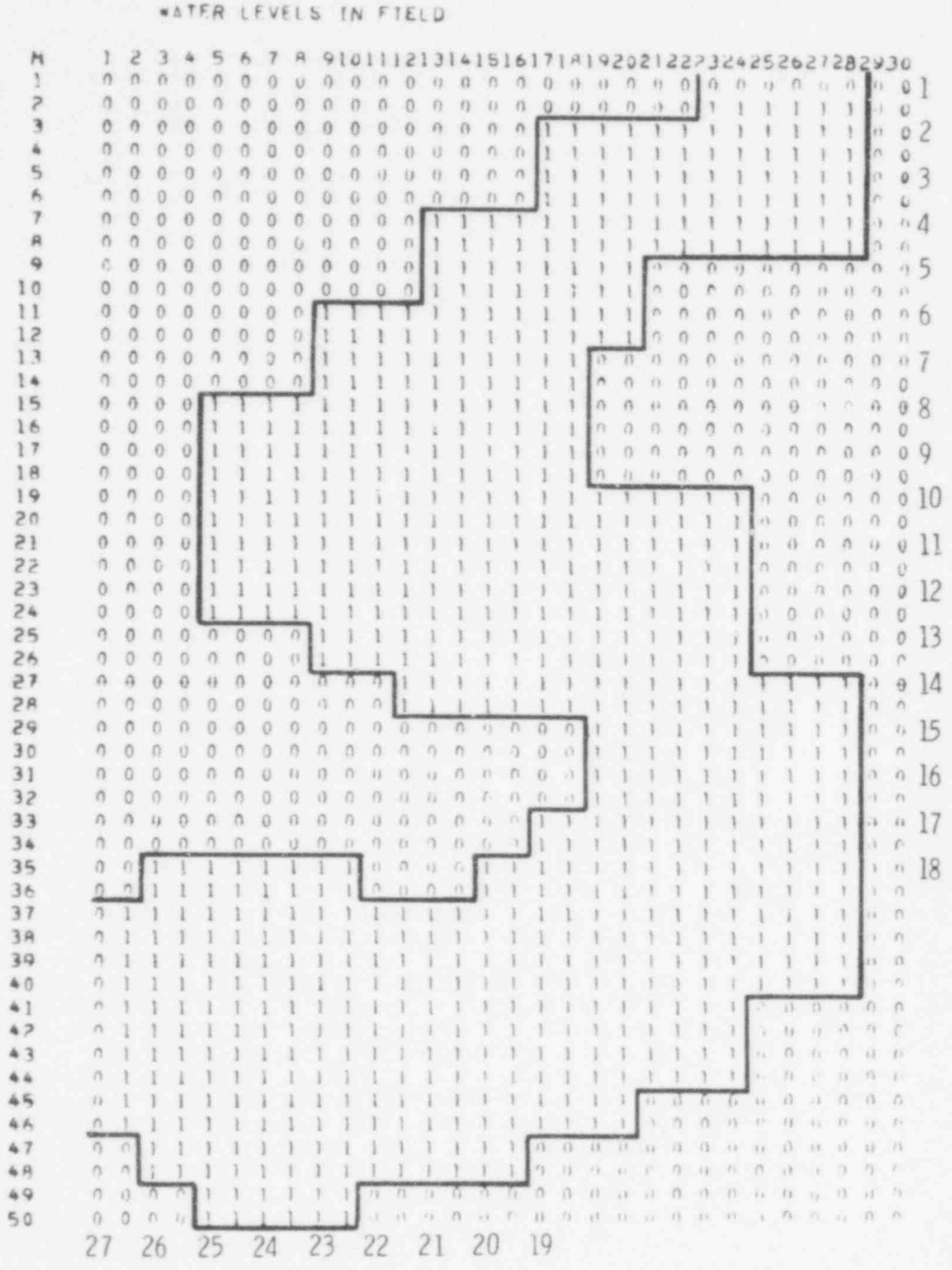

FIGURE 3.10. Computational Grid for Leendertse's Model Simulations, Case IV

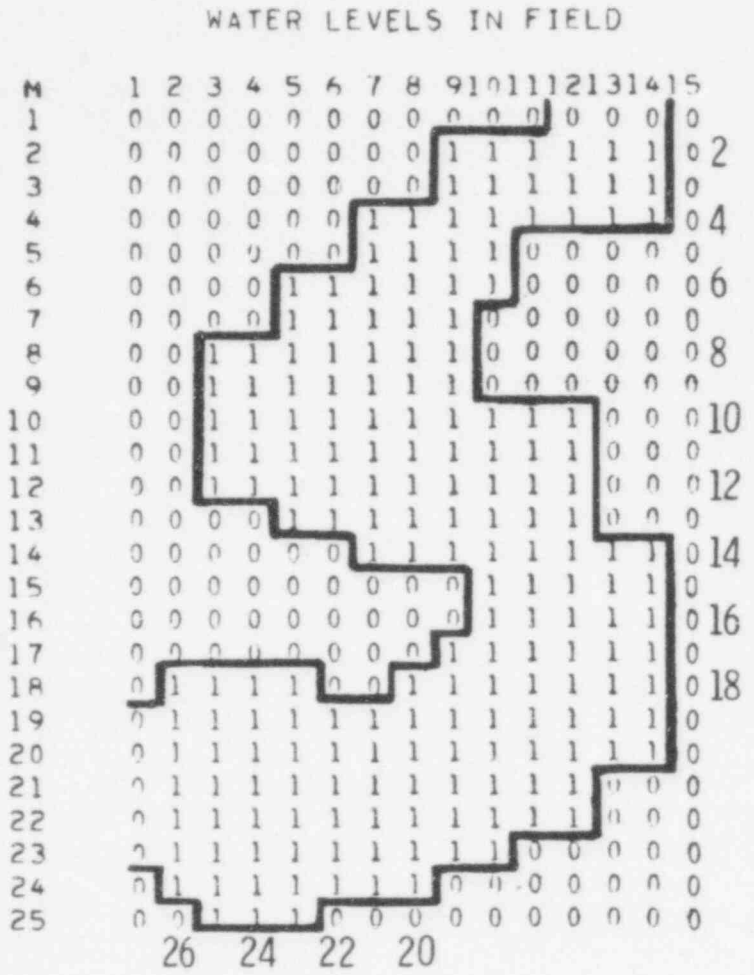

FIGURE 3.11. Computational Grid for Leendertse's Model Simulations, Case V

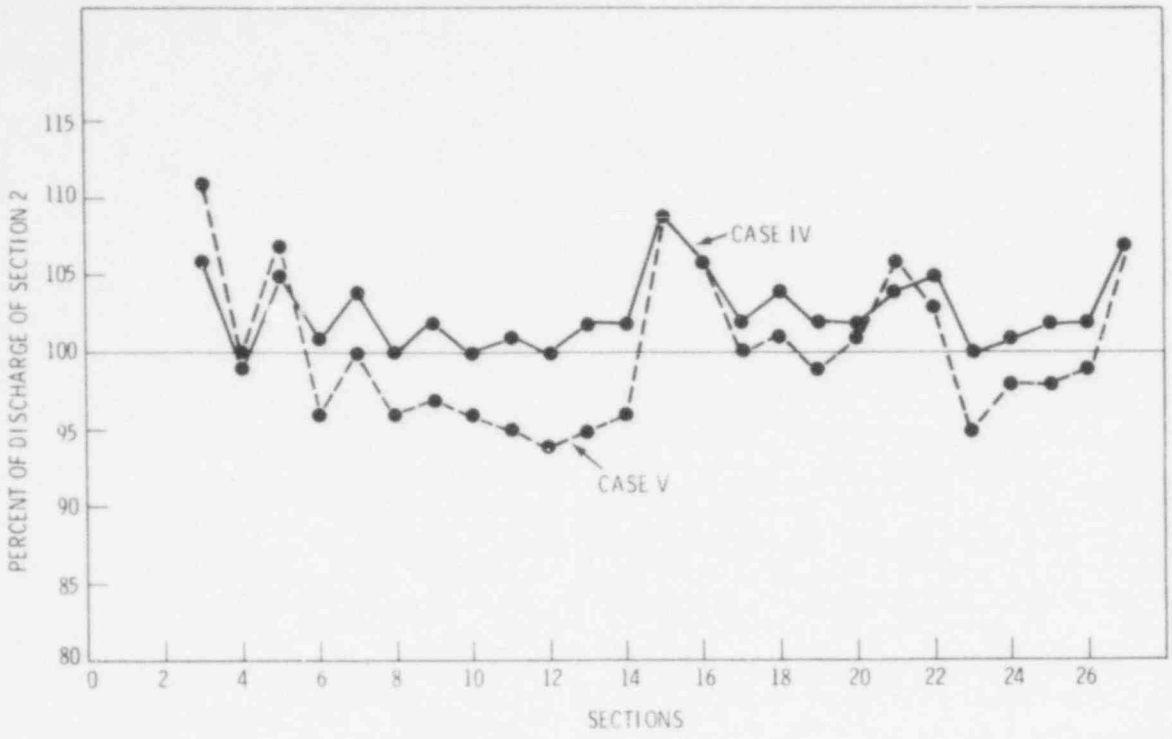

FIGURE 3.12. Discharges for Leendertse's Model Simulations, Cases IV and V

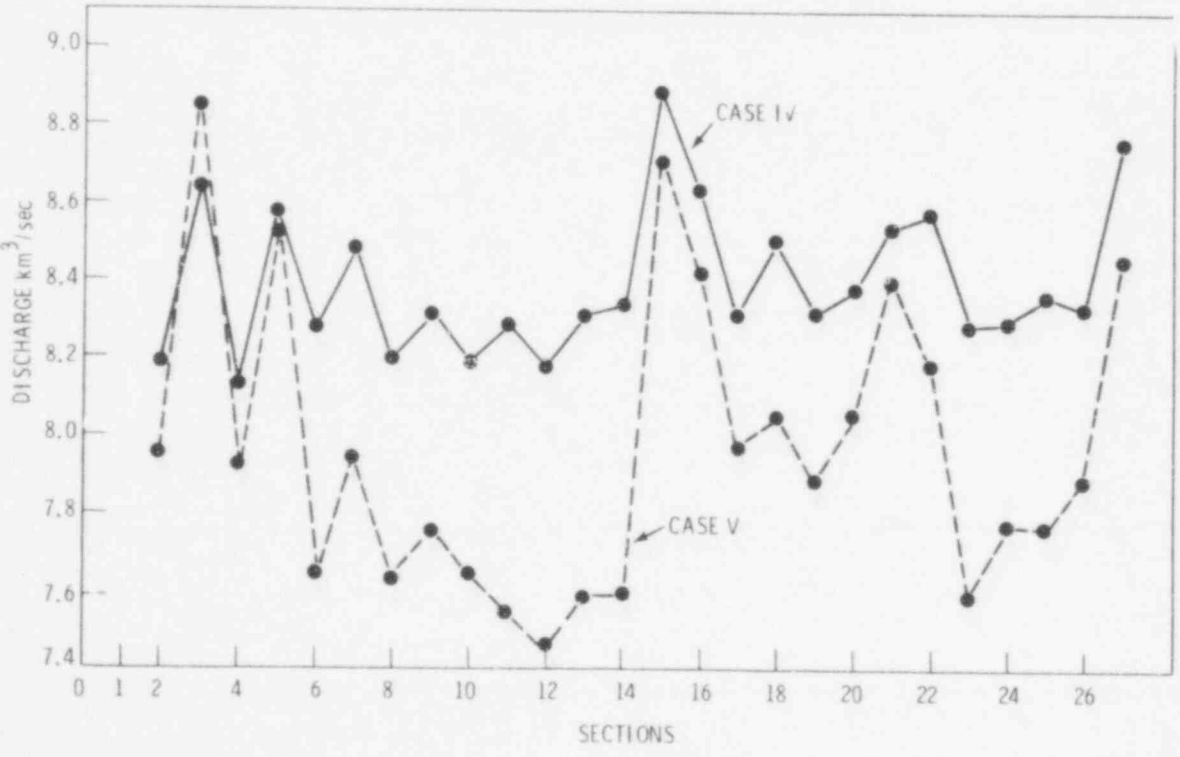

FIGURE 3.13. Conservation of Mass in Leendertse's Model Simulations, Cases IV and V

network. This refinement creates the need for additional computation grid points and their attendant data which must be considered by the monitoring program designer.

APPLICATION OF RMA MODEL

Five simulations were run for the RMA model under steady-state conditions and one simulation was run under variable conditions:

Run 1. Constant depth, constant Chezy coefficient
Run 2. First adjustment of depths to get better conservation of mass
Run 3. Second adjustment of depths to get better conservation of mass
Run 4. Same as Run 3 but changed downstream head to 23 cm from 7 cm
Run 5. Same as Run 3 but multiplied upstream velocities by 2
Run 6. Variable depths, variable Chezy, based on results of Run 3.

These six simulations do not correspond to the simulations for the Leendertse model. The simulations examined the influence of depth, velocity and head on the conservation of mass. The finite element network for the simulations is shown in Figure 3.14 and the positions of the continuity check lines are shown on Figure 3.15. The simulation results are expressed at these continuity check lines. The upstream velocity values were taken from the Leendertse simulation Case III and the downstream head values were taken from field data.

Constant Depth and Depth Adjustments (Runs 1, 2, and 3)

For the first three runs, the boundary conditions, Chezy coefficient and dispersion coefficients were kept constant. The discharge for each of these runs was 129,000 cfs which is approximately one-half of the discharge predicted by the Leendertse model. The reason for this discrepancy is not known. The percent conservation of mass is shown in Figure 3.16. For each of the depth adjustments, a new depth was computed which made the discharge for that line equal to the inflow discharge. This depth was then used as input across that section. The depths are given in Table 3.2, and Figure 3.16 shows the results of the simulations. Note that conservation of mass improves a little each time. Additional simulations not reported here have resulted in even better continuity at some points. However, the discontinuity between Lines 4 and 5 remained significant. These lines lie on either side of the sharp bend at Hog Island in the James River and probably illustrate the model's difficulty in solving for the velocity on this section. Further element refinement would probably yield better simulation results and mass conservation there.

Boundary Conditions Variation

The results of Run 3 were compared to the results obtained from the same input conditions with only the downstream head values changed (Run 4). These results are shown in Figure 3.17. The increase in downstream head caused the mass to increase significantly at Line 9. Slight increases also occurred for

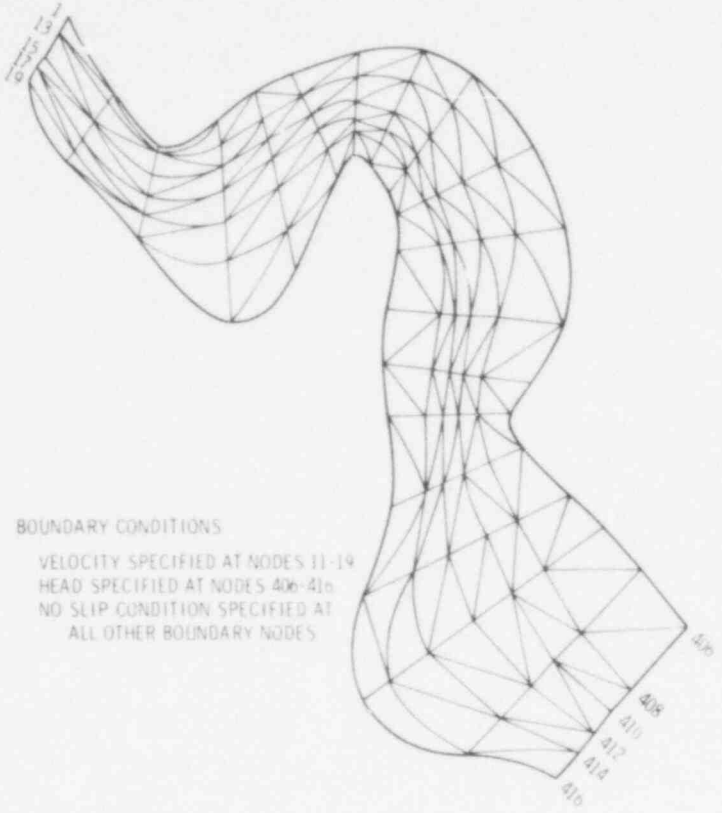

FIGURE 3.14. Regional Discretization for RMA model

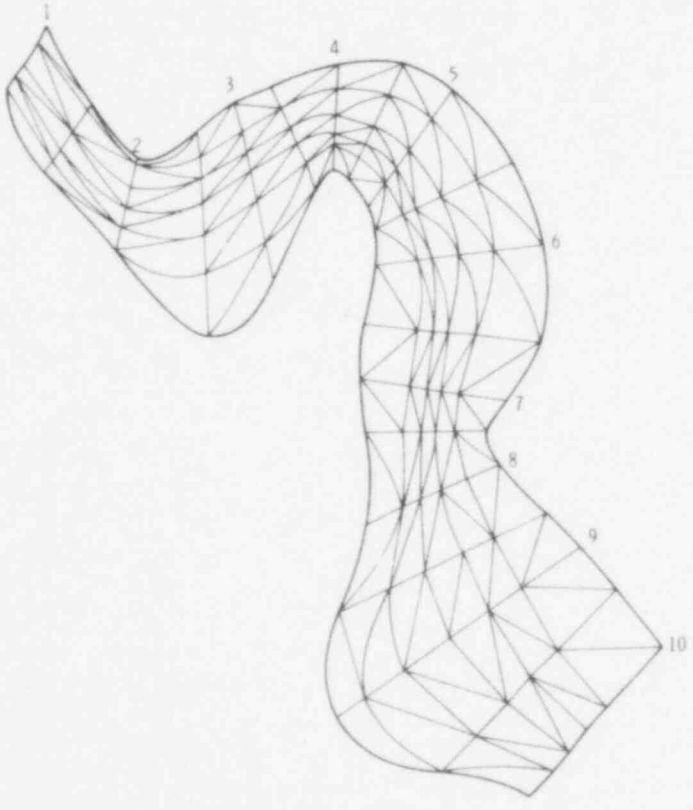

FIGURE 3.15. Finite Element Subdivision of Surry Vicinity

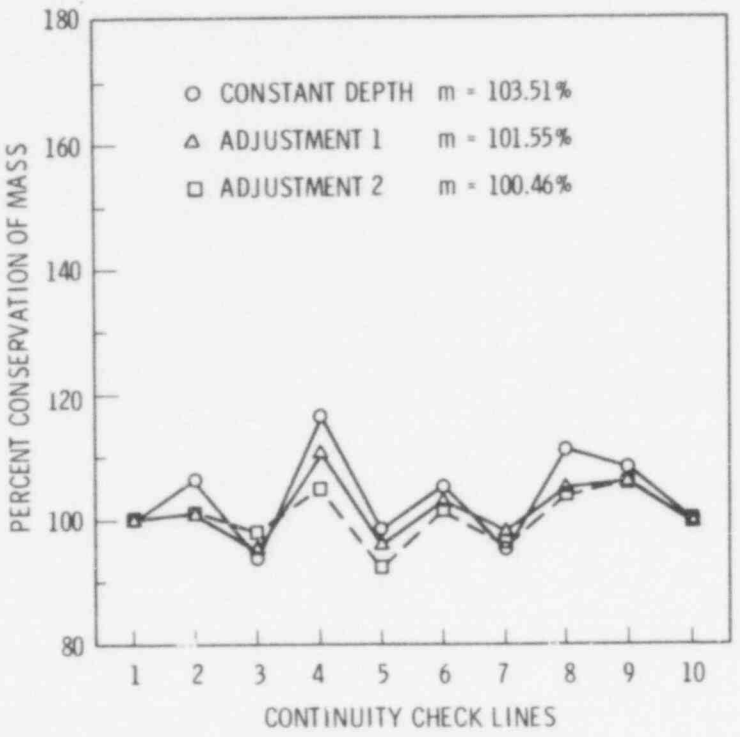

FIGURE 3.16. Mass Conservation Characteristics for RMA Runs 1 Through 3

TABLE 3.2. Depths in Meters for RMA Runs 1 Through 4

Check Lines	Constant Depth	Adjustment 1	Adjustment 2
1	6.89	6.89	6.89
2	6.89	6.21	6.21
3	6.89	7.90	8.22
4	6.89	5.88	5.31
5	6.89	7.29	7.35
6	6.89	6.68	6.52
7	6.89	7.38	7.24
8	6.89	6.10	6.06
9	6.89	6.62	6.58
10	6.89	6.89	6.89

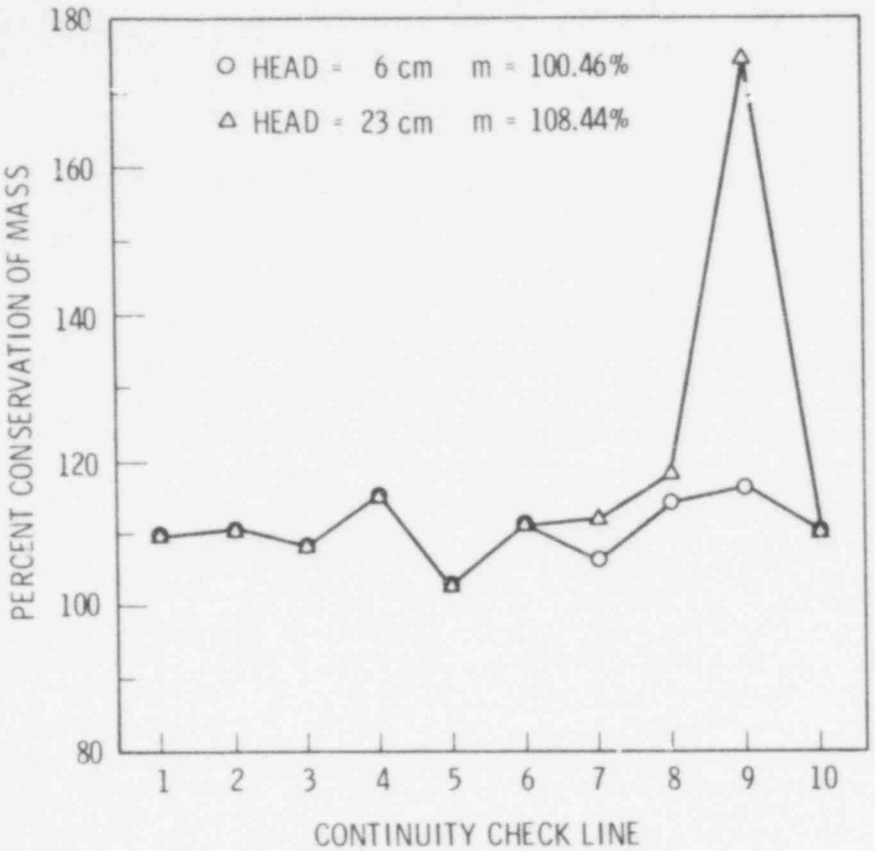

FIGURE 3.17. Mass Conservation Characteristics for RMA Run 4

adjacent upstream lines. Although the increase in head is exaggerated, smaller increases in head would result in similar mass increases, although comparably smaller in magnitude.

Likewise, the results of Run 3 were compared to those in which the upstream input velocity was doubled (Run 5). Discharge and velocity values were doubled, changing the percent mass conservation for all of the nodes (Table 3.3).

Variable Section Depth

The results of Run 3 were used as a guide for choosing the mean depth for the cross-section used in Run 6. These were close to actual depths, although sometimes they represented the average depth of an area around the node. The comparison is shown in Figure 3.18. The increases in mass at nearly all the lines suggest that the depths used may be too large.

TABLE 3.3. Comparison of Percent Conservation of Mass for Different Velocity Boundary Conditions

Check Lines	Run 3	Run 5[a]
1	100.0	100.0
2	101.0	99.7
3	98.0	103.6
4	105.1	103.1
5	92.4	93.9
6	101.5	102.6
7	96.3	97.4
8	104.2	103.7
9	106.1	104.8
10	100.0	100.0

(a) Input upstream velocities twice that of Run 3

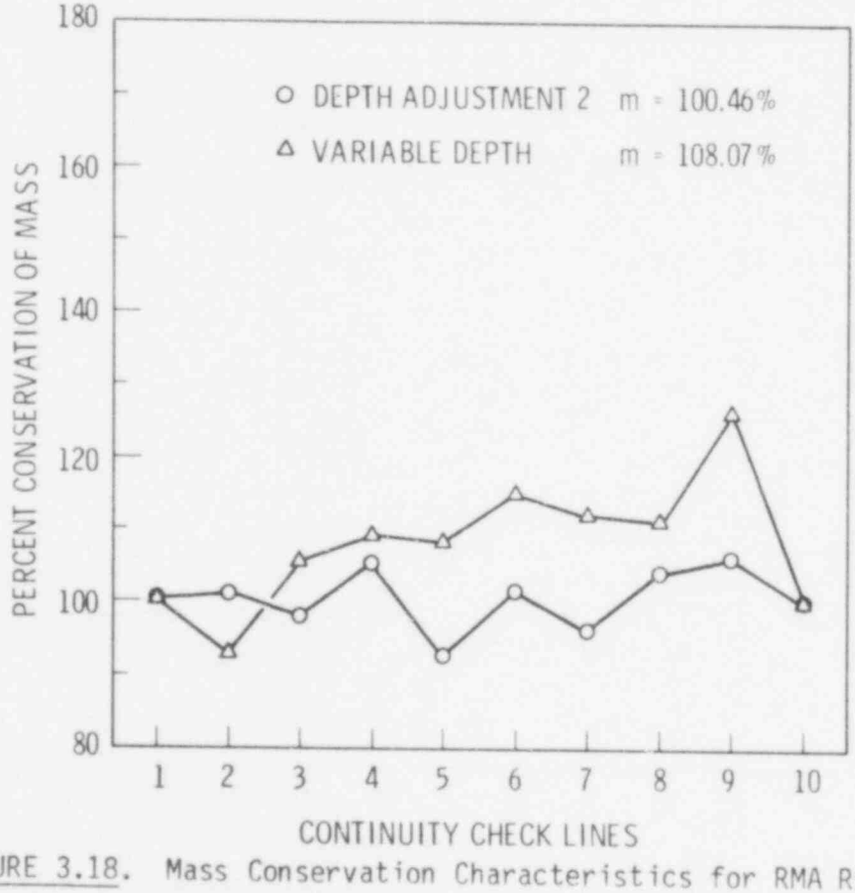

FIGURE 3.18. Mass Conservation Characteristics for RMA Run 6

Conclusions

Results suggest that reasonably accurate mass conservation can be maintained without choosing unrealistic depths for model input, except in regions with very irregular geometrics. It was noted that changes in head value at the lower boundaries result in changes in the mass at the nearest downstream sections but have little influence on upstream sections. Changes in upstream velocity values have a slight influence on mass conservation in all sections of the river. From the viewpoint of a monitoring program designer, these findings indicate that slight inaccuracies of boundary data have little influence on mass conservation and that accurate bathymetry data are necessary for conservation of mass through the model calculations.

REFERENCES

Ahlstrom, S. W., Foote, H. P., Arnett, R. C., Cole, C. R., and Serne, R. J. 1977. Multicomponent mass transport model: Theory and numerical implementation (Discrete Parcel Random Walk version). BNWL-2127. Richland, WA: Battelle, Pacific Northwest Laboratories.

Battelle, Pacific Northwest Laboratories. 1974. Development of a mathematical water quality model for Grays Harbor and the Chehalis River, Washington. Report 211B01360. Richland, WA: Battelle, Pacific Northwest Laboratories.

Daily, J. E., and Harleman, D. R. F. 1972. Numerical model for the prediction of transient water quality in estuary networks. Report 158. Cambridge, MA: Massachusetts Institute for Technology.

Dunn, W. E., Policastro, A. J., and Paddock, R. A. 1975. Water Resources Research Program. Pt. 1, Surface thermal plumes: Evaluation of mathematical models for the near and complete field. ANL/WR-75-3. Argonne, IL: Argonne National Laboratory.

Harleman, D. R. F., and Lee, C. H. 1969. The computation of tides and currents in estuaries and canals. Technical Bulletin No. 16. Committee on Tidal Hydraulics, U.S. Army Corps of Engineers.

King, I. P., and Norton, W. R. 1978. Recent applications of RMA's finite element models for two-dimensional hydrodynamics and water quality. In Proceedings of the second international conference on finite elements in water resources. London: Pentech Press.

Koh, R., and Fan, L. 1970. Mathematical models for the prediction of temperature distributions resulting from the discharge of heated water into large bodies of water. U.S. EPA Water Pollution Control Research Series Report 16130DWO 10/70. Tetra Tech, Inc.

Leendertse, J. J. 1967. Aspects of a computational model for long period water wave propagation. RM-5294-PR. Santa Monica, CA: Rand.

Leendertse, J. J. 1970. A water quality simulation model for well-mixed estuaries and coastal seas: Principles of computation, Vol. I. RM-6230-RC. Santa Monica, CA: Rand.

Leendertse, J. J., Alexander, R. A., and Liu, S. K. 1973. A three-dimensional model for estuaries and coastal seas: Principles of computation, Vol. I. R-1417-OWPR. Santa Monica, CA: Rand.

Norton, W. R., King, I. P., and Orlob, G. T. 1973. A finite element model for Lower Granite Reservoir. DACW68-71-C-0047. Prepared for Walla Walla District by the U.S. Army Corps of Engineers, Walla Walla, WA.

Norton, W. R., and King, I. P. 1977. Operating instructions for computer program RMA-2: A two-dimensional finite element program for problems in horizontal free surface hydromechanics. Walnut Creek, CA: Water Resources Engineers, Inc.

Onishi, Y. 1976. Assessment of the impact of the proposed wildlife reserve island in south San Diego Bay on the South Bay Power Plant. Richland, WA: Battelle, Pacific Northwest Laboratories.

Onishi, Y., and Trent, D. S. 1976. Mathematical and experimental investigation on dispersion and recirculation of plumes from dry cooling towers at Wyodak Power Plant in Wyoming. BNWL-1982. Richland, WA: Battelle, Pacific Northwest Laboratories.

Onishi, Y. 1977a. Finite element models for sediment and contaminant transport in surface waters--transport of sediments and radionuclides in the Clinch River. BNWL-2227. Richland, WA: Battelle, Pacific Northwest Laboratories.

Onishi, Y. 1977b. Mathematical simulation of sediment and radionuclide transport in the Columbia River. BNWL-2228. Richland, WA: Pacific Northwest Laboratories.

Onishi, Y., and Wise, S. E. 1978. Mathematical simulation of transport of sediment and kepone in the James River estuary. PNL-2731. Richland, WA: Pacific Northwest Laboratory.

Orlob, G. T., King, I. P., and Norton, W. R. 1975. Mathematical simulation of thermal discharges from Johnsonville Steam Plant. Report to the Tennessee Valley Authority.

Prych, E. 1972. A warm water effluent analyzed as a buoyant surface jet. Report No. 21. Stockholm: Swedish Meteorological and Hydrological Institute.

Shirazi, M. 1973a. A critical review of laboratory and some field experimental data on surface jet discharge of heated water. Pacific Northwest Environmental Research Laboratory Working Paper No. 4. Corvallis, OR: U.S. EPA.

Shirazi, M. 1973b. Some results from experimental data on surface jet discharge of heated water. Paper presented at the First World Conference on Water Resources, September 1973, in Chicago, IL.

Shirazi, M., and Davis, L. 1974. Workbook of thermal plume prediction. Vol. 2, Surface discharge. Pacific Northwest Environmental Research Laboratory Report EPA-R2-72-005b, Corvallis, OR: Pacific Northwest Environmental Research Laboratory.

Sissenwine, M. P., Hess, K. W., and Saila, S. B. 1974. Interim report on evaluating the effect of power plant entrainment on populations near Millstone Point, Connectiucut. MES-NUSCO Report No. 3. Kingston, RI: Graduate School of Oceanography, University of Rhode Island.

Stolzenbach, K. D., and Harleman, D. R. F. 1971. An analytical and experimental investigation of surface discharges of heated water. Water Pollution Control Research Series, Report No. 16130 DJU 02/71. Cambridge, MA: Ralph M. Parsons Laboratory for Water Resources and Hydrodynamics, Massachusetts Institute of Technology.

Thatcher, M. L., and Harleman, D. R. F. 1972. A mathematical model for the prediction of unsteady salinity intrusion in estuaries. Report No. 144. Cambridge, MA: Ralph M. Parsons Laboratory for water resources and Hydrodynamics, Massachusetts Institute of Technology.

Trent, D. S. 1973. A numerical model for two-dimensional hydrodynamic and energy transport. U.S. Atomic Energy Commission Report BNWL-1803, NRC-1. Richland, WA. Battelle, Pacific Northwest Laboratories.

NUREG/CR-0631
PNL-2891

DISTRIBUTION

No. of Copies

OFFSITE

A. A. Churm
DOE Patent Division
9800 S. Cass Avenue
Argonne, IL 60439

210 U.S. Nuclear Regulatory Commission
Division of Technical Information and Document Control
7920 Norfolk Avenue
Bethesda, MD 20014

(Basic Distribution Under RE)

25 National Technical Information Service

2 DOE Technical Information Center

10 U.S. Nuclear Regulatory Commission
Environmental Specialists Branch
Bethesda, MD 20014

No. of Copies

ONSITE

50 Pacific Northwest Laboratory

E. M. Arnold (4)
K. S. Baker (4)
D. H. Fickeisen (4)
R. F. Foster
D. H. McKenzie (20)
T. L. Page
J. R. Skalski (4)
J. A. Strand
J. M. Thomas
B. E. Vaughan (2)
D. G. Watson
Technical Information (5)
Publishing Coordination (2)

NRC FORM 335 (7-77)

U.S. NUCLEAR REGULATORY COMMISSION

BIBLIOGRAPHIC DATA SHEET

1. REPORT NUMBER (Assigned by DDC): NUREG/CR-0631

4. TITLE AND SUBTITLE (Add Volume No., if appropriate): Quantitative Assessment of Aquatic Impacts of Power Plants

2. (Leave blank)

3. RECIPIENT'S ACCESSION NO.

7. AUTHOR(S): D. H. McKenzie, E. M. Arnold, J. R. Skalski, D. H. Fickeisen, K. S. Baker

5. DATE REPORT COMPLETED: MONTH July, YEAR 1979

9. PERFORMING ORGANIZATION NAME AND MAILING ADDRESS (Include Zip Code): Pacific Northwest Laboratory, Richland, Washington 99352

DATE REPORT ISSUED: MONTH August, YEAR 1979

6. (Leave blank)

8. (Leave blank)

12. SPONSORING ORGANIZATION NAME AND MAILING ADDRESS (Include Zip Code): U.S. Nuclear Regulatory Commission, Washington, D. C. 20555

10. PROJECT/TASK/WORK UNIT NO.

11. CONTRACT NO.: EY-76-C-06-1830

13. TYPE OF REPORT: Annual Report

PERIOD COVERED (Inclusive dates): July 1979

15. SUPPLEMENTARY NOTES

14. (Leave blank)

16. ABSTRACT (200 words or less)

This report is part of a continuing study of the design and analysis of aquatic environmental monitoring programs for assessing the impacts caused by nuclear power plants. The efforts of this year's study were divided into ecological monitoring, simulation model evaluation and hydrologic modeling.

Analysis of ecological monitoring data from three nuclear power plants confirmed the generic applicability of a control-treatment pairing (CTP) design suggested by McKenzie et al. (1977). Simulation models of aquatic ecosystems were reviewed and evaluated. A process notebook was compiled and each model equation was translated into a standardized notation. Individual model testing and evaluation was started. The Aquatic Generalized Environmental Impact Simulator (AGEIS) was also developed at the University of Washington. A compendium of models commonly applied to nuclear power plants was assembled and two well-received hydrodynamic models were applied to data from the Surry Nuclear Power Plant. Conclusions indicated that slight inaccuracies of boundary data have little effect on mass conservation, but for model calculations, accurate bathymetry data are necessary for conservation of mass. The results of this year's work should provide valuable reference information for model users and monitoring program designers.

17. KEY WORDS AND DOCUMENT ANALYSIS

17a. DESCRIPTORS

Environmental monitoring
ecological monitoring
hydrologic modeling
ecosystems
hydrodynamic
bathymetry data

17b. IDENTIFIERS/OPEN-ENDED TERMS

18. AVAILABILITY STATEMENT: Unlimited

19. SECURITY CLASS (This report): Unclassified

21. NO. OF PAGES

20. SECURITY CLASS (This page)

22. PRICE: $

NRC FORM 335 (7-77)

025 070

UNITED STATES
NUCLEAR REGULATORY COMMISSION
WASHINGTON, D. C. 20555

OFFICIAL BUSINESS
PENALTY FOR PRIVATE USE, $300

POSTAGE AND FEES PAID
U.S. NUCLEAR REGULATORY
COMMISSION

925 071